MS – RAND – CPP – PROG0407

Report describing the performance of the improved procedure using MOSES 2 to predict river flows. Summary analysis of the hydrological drivers of recent flooding events in the UK

R.G. Jones[1], V.A. Bell[2], A.L. Kay[2], S. J. Dadson[2] and H. N. Davies[2]

[1]Hadley Centre
and
[2]CEH, Wallingford

Contract Deliverable reference number: 15.06.05

File: M/DoE/2/9

Delivered from authors:	Signature	Richard Jones	Date 31.03.2006
Scientific content approved by Activity Manager:	Signature	Simon Brown	Date 31.03.2006
Approved by HdCPP against customer requirements	Signature	Vicky Pope	Date 31/03/06
Sent to Defra:	Signature	Linda Livingston	Date: 31/03/06

Version Number: 1.0

Number of Pages:

Security Classification: Unclassified

Key outcomes/non-technical summary

Part 1: Coupling the G2G routing model with MOSES 2: performance over the UK and Europe

Previous work by CEH Wallingford under a CPP sub-contract has developed an initial system to predict changes in flooding for the UK. This system provides a grid-based methodology in the form of a grid-to-grid model for translating regional climate model (RCM) meteorological variables, such as rainfall and evaporation, into estimates of river flow and fluvial outflow to the sea. The relevance of using a grid-based methodology as opposed to one based on river catchments is that it allows the modelling to be applied to all river networks in a region rather than just specific catchments. The initial development work used a simple runoff-production scheme, providing reasonable runoff estimates to allow testing of the routing component which transforms the runoff into river flow. This year the routing scheme called the Grid-to-Grid model or G2G has been linked to the Met Office land-surface scheme MOSES. MOSES is an integral part of the RCM into which the G2G model will be embedded. The combined MOSES-G2G model now provides a stand-alone platform to support research into broad-scale runoff-production and routing schemes. This supports the development and testing of a system for off-line assessment of the response of river flows over a whole region to changing meteorological drivers and the integration of this system as a component of the RCM. The latter then allows both the online calculation of the response of rivers flows and the use of this RCM as part of a coupled atmosphere-ocean RCM (which requires freshwater input into the regional ocean component).

The combined model is currently configured for use at two grid-resolutions: (i) on the UK National Grid used by the Met Office Nimrod nowcasting scheme with MOSES operating at a 5km resolution and 1km Grid-to-Grid routing, (ii) on the European RCM domain with both MOSES and G2G operating at a 25km resolution. Initially this required a set of hand-corrected flow-directions at the resolution of each domain (25 and 1km respectively). This gave reasonable river networks and catchment areas but was time-consuming thus alternative methods for deriving river networks from higher resolution Digital Terrain Model (DTM) data were explored. New flow directions have now been developed for the G2G at both spatial scales, and have lead to improved accuracy in catchment area. Only a limited amount of hand-correction to overcome any residual errors is then required to obtain the final derived flow directions. This is consistent with the PRECIS system (the new RCM with the G2G model embedded will become PRECIS V2) which already allows users to change easily other aspects of the land-surface specification such as its height and vegetation.

Initial results indicate that the new MOSES-G2G model is performing moderately well, as modelled and observed flow from a number of catchments show reasonable agreement. For the detailed work of the UK, analysis using the standard configuration of MOSES indicated changes in MOSES parameters which improved performance in some catchments. In others, the treatment of soil hydrology in MOSES appears too crude and improvements in performance will require further work. Future work will also look at different methods of runoff production within MOSES and assess their impact on model performance. As expected, the performance of the new model over Europe at coarse resolution is not so good though reasonable results are being produced for some large catchments. This assessment is based on the comparison of the observed flow history in catchments with that simulated using RCM drivers but does not invalidate the use of the model for providing freshwater input into a regional ocean model (which this system will be applied to for the derivation of marine scenarios for UKCIP08).

Part 2: Modelling recent flow history in selected UK catchments

One outcome of the validation of the MOSES-G2G model over the UK and Europe driven by RCM data is that it is insufficiently accurate to reproduce the detailed evolution of specific observed peak flow events. As a result, the work on assessing the hydrological drivers of recent UK flooding events was undertaken with a catchment-based modelling approach. Specifically, data from a 25km RCM driven by observed boundary conditions for 1985-2001 was input to a catchment rainfall-runoff model to estimate flows and flood frequencies in British catchments.

The flood frequencies derived using RCM input data were generally under-estimated; only one catchment (of 16) shows significant over-estimation, with 13 showing significant under-estimation. This is relatively consistent with under-estimation in annual average rainfall, and explains why the under-estimation tends to be worse for larger catchments, due to the cumulative effect of spatial integration of rainfall errors. Applying a (catchment-specific) correction factor for errors in annual average rainfall improves the performance significantly, although it pushes some catchments into a significant over-estimation of flood frequency.

The general under-estimation of flows is particularly evident in the flood peaks of Autumn/Winter 2000, even after the application of the correction factor. This is probably because of the sustained nature of the rainfall that caused those floods, and the cumulative effect of rainfall deficiencies on antecedent conditions. This implies that even with the use of more detailed and specific catchment models, driving them with RCM data does not allow all the relevant details of specific flooding events (size or ranking of peak) to be captured. In contrast, when using observed rainfall for these catchments, many of the flood peaks were captured. This implies that understanding the hydrological drivers of these events may be achieved by analysis of the detailed meteorology as simulated by the RCM associated with the sequences of the observed precipitation which lead to the events.

Associated publications

Bell, V.A., Kay, A.L., Jones, R.G. and Moore, R.J., 2006. Development of a high resolution grid-based river flow model for use with regional climate model output. *Hydrology and Earth System Sciences,* (in press).

Kay, A.L., Reynard, N.S. and Jones, R.G. (2006). RCM rainfall for UK flood frequency estimation. I. Method and validation. Journal of Hydrology, 318, 151-162.

Kay, A.L., Jones, R.G. and Reynard, N.S. (2006). RCM rainfall for UK flood frequency estimation. II. Climate change results. Journal of Hydrology, 318, 163-172.

Press interest

None

Part 1: Coupling the G2G routing model with MOSES 2: performance over the UK and Europe

INTRODUCTION

This report describes recent progress on a grid-based model developed to quantify flow at any location across a wide area of interest at a variable grid resolution, driven by Regional Climate Model (RCM) data. The aims of this report are (i) to summarise progress during the period March 2005 to January 2006 and (ii) to outline ongoing and future work.

An initial system to predict changes in flooding for the UK has now been developed (Bell *et al.* 2004a,b, 2006; Kay *et al.* 2006a,b). This system provides a grid-based methodology for translating RCM meteorological variables, such as rainfall and atmospheric drivers of evaporation, into estimates of river flow and fluvial input to the sea. The new model, the Grid-to-Grid model or 'G2G', has already been tested off-line from the RCM, and evaluated for individual catchments in the UK alongside a catchment-based hydrological model, the parameter-generalised PDM. An initial assessment using 45 years of observed rainfall and flow data showed the potential of the grid-based routing methodology, and enabled trends in peak flows to be investigated. The variability in the results from the two hydrological models also provided insight into the uncertainty in hydrological model predictions based on different climate scenarios.

Implementation of the G2G model into a coupled RCM is already underway at a 25km resolution, and for the European RCM domain. For this resolution and coverage, flow in major rivers can be estimated, providing large-scale estimates of flooding and fluvial input to the sea. The system can be used to investigate changes in flood frequency at a continental scale under current/future rainfall scenarios, and for simulating extreme flood events in the recent past with a view to examining their meteorological drivers.

For more detailed spatial and temporal modelling of river flow and flooding across the UK, a higher resolution modelling system is being developed. A new 1km version of the G2G routing model will form part of a "one-way" coupled RCM for Europe as part of PRECIS – a Regional Climate Modelling system designed to run on a PC. The 1km G2G routing model will provide the capability for process-based hydrological modelling for UK flood prediction and can provide fluvial input to a shelf-seas model for coastal flooding if required. This will in turn support the development of models to predict estuarine flooding resulting from coincident high river and sea levels/storm surges.

OUTLINE OF PROGRESS

2.1 The Workplan

The specific tasks are as follows:

1. Collaboration between CEH Wallingford and Hadley Centre to develop the hydrological component of a coupled RCM for North West Europe. This new model will combine PRECIS, the G2G routing model with MOSES-derived runoff, and the Met Office/POL shelf-seas model.

2. Collaboration between CEH Wallingford and Hadley Centre to implement and further develop the hydrological component of the 25km coupled RCM, which was incorporated into the Unified Model v6.0.

3. Drive the 1km G2G routing model and the parameter-generalised PDM hydrological model with data from a 25km RCM driven by ERA-40 data (available Summer 2005). The analysis will be supplemented by observed rainfall data where appropriate. This will aid an extended analysis of model performance and further validation of RCM rainfall. The simulations for recent UK floods (including Autumn 2000) will be of particular interest.

4. Investigate factors determining model quality and uncertainty which will provide an indication of confidence in model response to climate change.

Progress on the first two tasks is now well underway. A new coupled model has been developed for use with RCMs which combines a spatially distributed grid-based river flow routing model, "Grid-to-Grid", with MOSES-derived land-surface runoff in the form of the Joint UK Land Exchange Scheme (Jules). The new coupled model is currently being evaluated at two scales (i) for the UK, where MOSES is being run at a 5km resolution with 1km G2G routing, and (ii) on the North West European RCM grid, with both MOSES and the G2G run at a 25km resolution. New flow directions have been developed for the G2G at both spatial scales, and have lead to improved accuracy in catchment delineation, thereby reducing errors in modelled river flow arising from incorrect estimation of the area draining to a river.

Both the G2G and the parameter-generalised PDM hydrological model have been run using by data from the 25km European RCM driven by ERA-40 boundary conditions (Task 3). The analysis has progressed further for the PDM as no model development has been required for this component of the work. The results of the PDM analysis are presented in a separate report "Catchment modelling with data from an RCM driven by ERA-40 boundary conditions" (Kay, 2006). The availability this year of ERA-40-driven RCM data, for 1985-2001, has meant that an extended comparison of RCM and observed rainfall for catchment modelling has been possible for a period including the Autumn 2000 floods in the UK.

An investigation into factors determining model quality and uncertainty is underway (task 4) and a draft report has been produced. This component of the work will be finalised in March 2006.

2.2 Model components

2.2.1 MOSES (Jules)

The Met Office Surface Exchange System (MOSES; Cox *et al.*, 1999) is the basis for the Joint UK Land Exchange Scheme (Jules) and provides the facility to diagnose the hydrological state of the surface and soil given time-varying inputs of temperature, wind speed, humidity, shortwave and longwave radiation, and precipitation. Within Jules there are four horizontal soil layers, each with an associated temperature and soil moisture content. Water and heat are assumed to move in the vertical direction only. Estimates of surface and subsurface runoff are calculated as the amount of liquid water leaving a grid square on the land and below ground, respectively. The influence of stomatal resistance of vegetation is also modelled explicitly in order to estimate evapotranspiration from the canopy, and account is taken of the effect of spatially-varying soil properties and land cover. Estimates of grid-square runoff (surface and sub-surface) required by the Grid-to-Grid routing model are available as a byproduct of the soil-moisture model. These gridded runoff values provide estimates of liquid water leaving a grid-square both on the land-surface and below ground, taking into account the effect of spatially-varying soil properties and land-cover.

The version of MOSES (Cox *et al*., 1999) used in the new modelling platform includes two models of soil-water movement (the Brooks-Corey and Van Genuchten models), together with two schemes representing soil heterogeneity within grid-cells: MOSES-PDM and MOSES-LSH. Figure 1 presents a schematic of a MOSES soil-column highlighting model components common to both MOSES-LSH and MOSES-PDM.

MOSES-PDM (Blyth, 2002) assumes a probability distribution of soil water capacity within a grid-square based on the Probability Distributed Model (PDM) for soil moisture within a catchment developed by Moore (1985, 1999). This formulation allows for spatial and temporal variation in the proportion of the grid-square which is assumed to be saturated and producing surface runoff. An alternative mechanism for estimating runoff within grid-cell, MOSES-LSH (Gedney and Cox, 2003), also estimates the proportion of a grid-cell which is saturated and producing surface runoff, but it does so by explicitly modelling the height of the water table and its relation to local topography. In order to achieve this, a fifth deeper water table layer is assumed to lie below the four MOSES soil layers. So far, only the PDM runoff production scheme has been invoked in the new combined model MOSES-G2G, but assessment of LSH with MOSES-G2G is planned, and may prove beneficial, particularly for groundwater dominated catchments.

At the land-surface, MOSES now assumes heterogeneity of land cover within grid-cells (“Tiling”), within which snow and canopy water stores are maintained for each land-surface type. Snowmelt is modelled with an energy-budget model which takes into account solar radiation and heat fluxes at the land-surface.

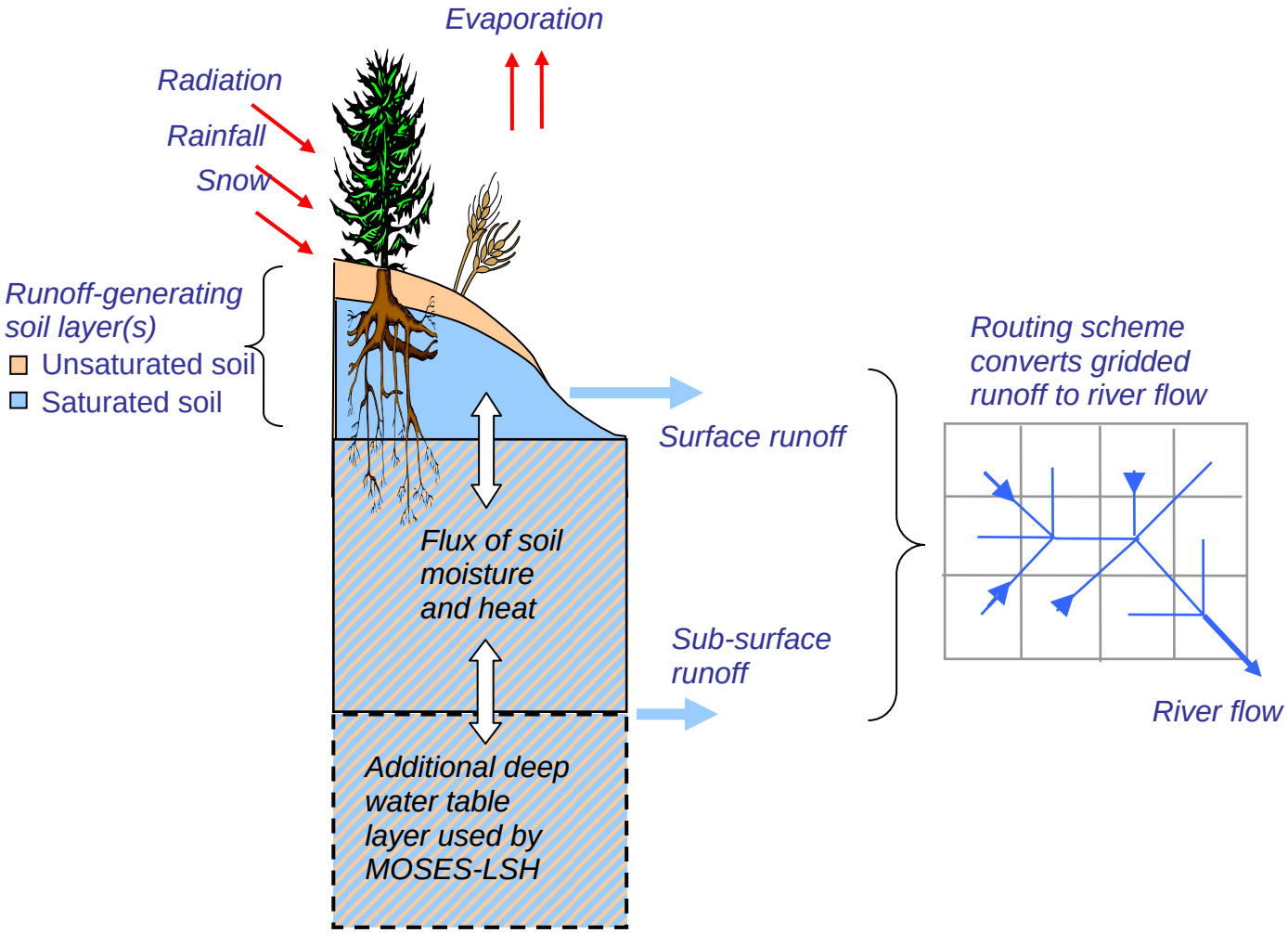

Figure 1 Schematic of a MOSES soil-column highlighting features common to both MOSES-LSH and MOSES-PDM.

Different canopy heights are associated with each vegetation type and allow for interception of rainfall by plant leaves, evaporation and throughfall.

When used within PRECIS, and for more detailed modelling over the UK, the MOSES land-surface scheme will be driven by RCM-derived estimates of atmospheric variables. The gridded surface and sub-surface runoff from MOSES will provide input to the Grid-to-Grid flow routing model to provide an estimate of flow in the rivers to which the grid squares eventually drain.

2.2.3 The Grid-to-Grid Routing model

The Grid-to-Grid routing model (G2G) is configured on a grid to use estimates of runoff provided by a runoff-production, or land-surface, scheme such as MOSES. The Grid-to-Grid model (Bell *et al*., 2004a, 2006) is based on the discrete approximation

to the 1-D kinematic wave equation with lateral inflow. It is assumed that a separate runoff-production model component partitions precipitation and evaporation fluxes into water stored in the soil and canopy, and water is generated as surface and sub-surface runoff. Following the approach of Bell and Moore (1998), kinematic routing is applied separately to sub-surface and surface runoff; the model also allows for different formulations over land and river pathways (initially just a different wave speed). A *return flow* term allows for flow transfers between the sub-surface and surface pathways representing surface/sub-surface flow interactions on hillslopes and in channels. Figure 2 provides a schematic of the model structure.

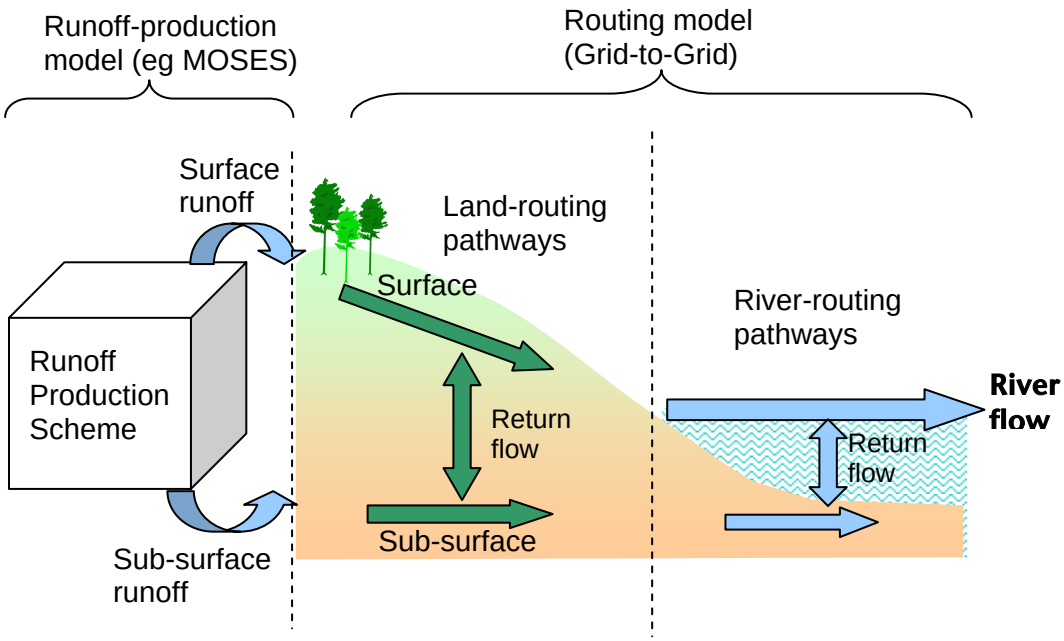

Figure 2 Schematic of the Grid-to-Grid model structure.

Flow routing (or 'runoff routing') models aim to 'route' catchment or grid-cell runoffs through the perceived drainage network, providing estimates of river flow at selected locations (often corresponding to river gauging stations) or on a regular grid.

The network of drainage directions used to route the water from cell to cell is usually determined from Digital Terrain Model (DTM) data at an appropriate resolution.

A key configuration component of flow-routing models is the set of flow directions defining the drainage direction of water from one grid-cell to the next, both on land and in the river. If the flow directions are mis-specified, the catchment area draining to a river will be incorrect, leading to errors in both the water-balance and the estimated river flow. The first version of the Grid-to-Grid flow routing model coupled to the Regional Climate Model for Europe (Bell *et al.*, 2003) used a set of hand-corrected 25km resolution flow-directions. Estimated river networks and catchment areas were considered acceptable following hand-correction. However, some errors remained and the hand-correction process was time consuming, discouraging repeated application to new regions. These limitations prompted investigation of automated

methods such as that described by Fekete *et al.* (2001). The results are presented in Section 2.5 for the 25km European RCM domain.

The Grid-to-Grid routing scheme allows the model user to examine flow and water volumes for any grid-box in the modelled region, and can be extended to estimate the areal extent and depth of flood inundation through the use of DTM data and geomorphological relations (Bell *et al*., 2004c).

2.3 MOSES-G2G

A standalone version of the Met Office Surface Exchange Scheme (MOSES-2) in the form of Jules has now been coupled to the Grid-to-Grid (G2G) routing model. It provides

- Interface to MOSES and G2G ancillary files
- Aggregation of all model parameters (MOSES variants + Grid-to-Grid) to one input file, allowing greater flexibility and control of model features
- Control of model output including automatic generation of files for interactive 2-D display within the GRADS graphical display system.

The combined MOSES-G2G model provides a stand-alone platform to support research into broad-scale runoff-production and routing schemes. The platform is summarised in Figure 3. The coupled model is currently being applied at two scales, 25km across Europe and 1km across the UK. Working at the two spatial scales primarily affects model input and output. Specifically, it relates to regridding of RCM driving data (for UK application), ancillary files for the G2G and MOSES, and changes to the input file relating to new grid size and model time-step.

The model code for the European application is slightly simpler to that developed for the UK as MOSES-G2G is run on the RCM grid and therefore regridding subroutines are not required. New ancillary files for MOSES running at the 25km resolution and domain of PRECIS have been provided by the Met Office. These consist of initial state, soil hydraulic and thermal properties, and soil albedo as listed in Table 1. The files are the standard Met Office ancillaries that were obtained through the International Geosphere-Biosphere Programme (IGBP).

The UK modelling work is being undertaken on the UK National Grid used by the Met Office Nimrod nowcasting scheme. The MOSES component is currently applied at a 5km resolution and the G2G is running on a 1km grid nested within the 5km MOSES grid. Nimrod ancillary files have been used as input to the 5km MOSES.

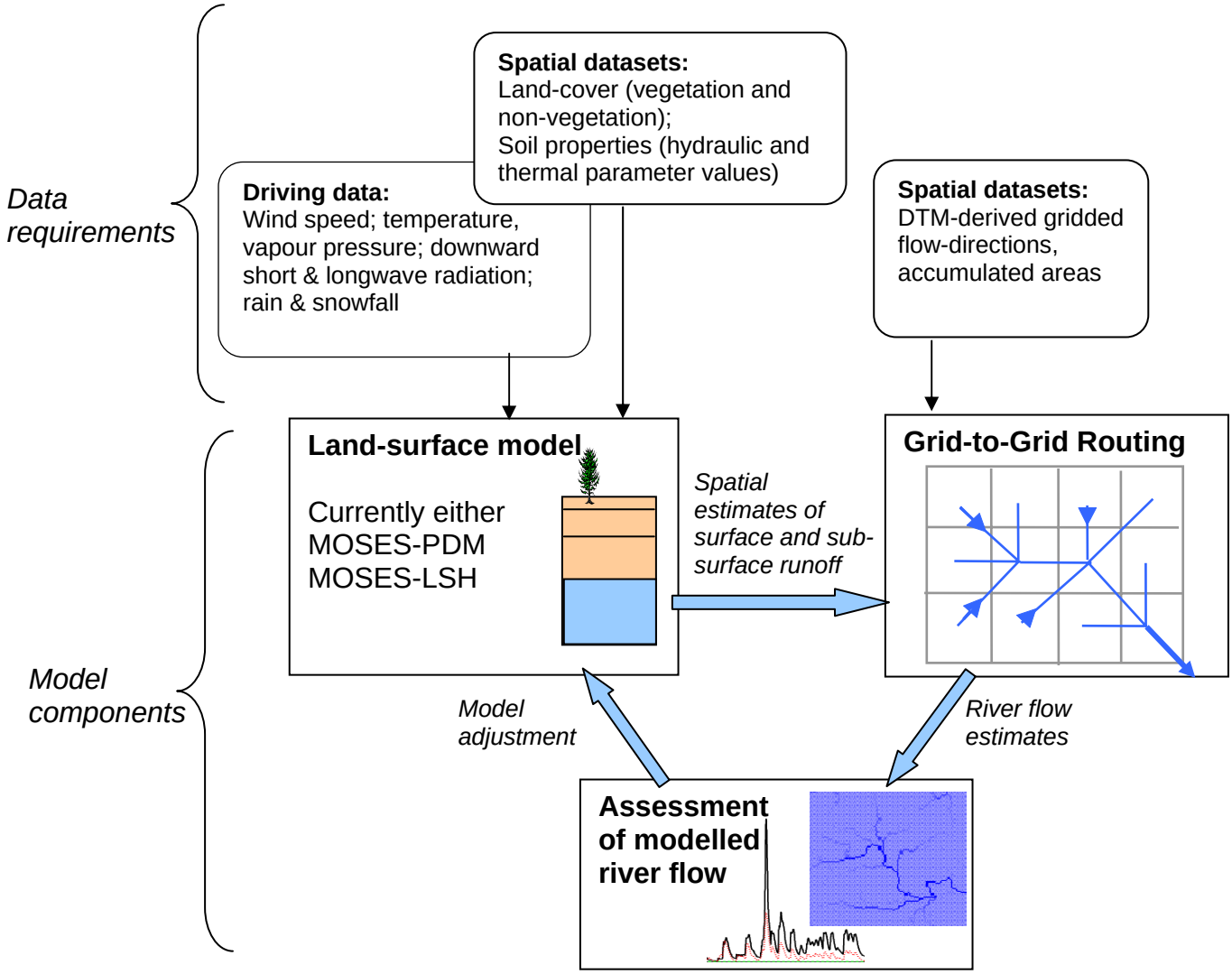

Figure 3. Schematic of the combined MOSES-G2G modelling environment.

Table 1. Ancillary data used in the current assessment.

Data type	Units
Landcover	
Fractional coverage of each surface type, *frac*	–
Amount of water held on canopy, *canopy*	kg m^{-2}
Soil hydraulic and thermal properties	
Clapp-Hornberger exponent, *b*	–
Soil matrix suction at saturation (absolute value), *sathh*	m
Hydraulic conductivity at saturation, *satcon*	kg m^{-2} s^{-1}
Volumetric soil moisture content at saturation, *smvcst*	m^3 m^3
Volumetric soil moisture content at critical point, *smvccl*	m^3 m^3
Volumetric soil moisture content at wilting point, *smvcwt*	m^3 m^3
Dry heat capacity of soil, *hcap*	J m^{-3} K^{-1}
Dry thermal conductivity of soil, *hcon*	W m^{-1} K^{-1}
Soil albedo, *albsoil*	–

2.4 Modifications to MOSES/Jules

Prior to running the Jules–PDM model with embedded G2G river routing, several modifications to the standard scheme structure were made in order to tailor the model's operation to the particular circumstances associated with the current task. These modifications fell into three classes, each of which is described in the following sections: (i) development of gridded scheme; (ii) alteration of soil-freezing and soil moisture transport scheme; and (iii) adjustment of hydrological parameters using observed flow data.

(i) Development of gridded scheme

In its typical application, the Jules–PDM model operates on a single column, with vertical transfers of heat and moisture. For spatially-distributed hydrological modelling, a gridded structure is preferable and so for the present work, Jules–PDM was configured to a rectangular grid of square pixels. A river flow routing component (G2G) was added to represent lateral flow in surface (river flow) and sub-surface (groundwater flow) pathways in the direction of steepest topographic descent. Although the grid resolution in the altered model is adjustable, all results presented here were obtained using a 25km horizontal grid spacing, a value consistent with that of the RCM driving data. The tiled structure of Jules was retained so that sub-grid-scale variations in the thermal and hydraulic properties of soil and vegetation could be represented. Further work is planned in collaboration with the Jules development group to improve the representation of lateral flows of deep groundwater.

(ii) Soil freezing and soil moisture transport

Minor adjustments were made to the Jules–PDM default scheme that accounts for moisture transport through the soil column when that moisture is in a mixture of frozen and unfrozen states. Two separate changes were made. The first change was made to account for the displacement of unfrozen water by that which was frozen. The second consisted of a modification to the default behaviour of Jules–PDM so that excess water generated in any soil layer was routed downwards towards the base of the soil column rather than upwards towards the surface. We judge that this modified behaviour is more appropriate for well-drained land in NW Europe, whereas the default behaviour may be better suited to areas that are permanently or intermittently saturated as a result of frozen soil.

(iii) Adjustment of hydrological parameters

Prior to model runs, a set of hydrological parameters was adjusted in order to obtain optimal model performance over a large region. These parameters determine the volume of runoff (surface and sub-surface) generated by the PDM runoff-production scheme and the kinematic-wave speeds used in the river flow routing component. The parameters are listed in Table 2. In practice values for these parameters were chosen by repeated trial and improvement from within a range of values known to be effective from prior work. An important constraint was that the same parameters be used for all catchments.

Table 2. Runoff generation and flow routing parameters.

Parameter	Typical Value	Units
Runoff production (Jules–PDM)		
Pareto exponent for soil moisture capacity (PDM), *b*	1.000	[–]
Depth over which PDM is applied	0.500	m
Flow routing (G2G)		
Wave speed for surface flow in river pixels	0.5	m s^{-1}
Wave speed for subsurface flow in river pixels	0.5	m s^{-1}
Wave speed for surface flow in land pixels	0.2	m s^{-1}
Wave speed for subsurface flow in land pixels	0.2	m s^{-1}
Return flow fraction (subsurface–surface)	0.001	[–]

2.5 Development of improved G2G river networks

2.5.1 Introduction

A key configuration component of flow-routing models is the set of flow directions defining the drainage direction of water from one grid-cell to the next, both on land and in the river. If the flow directions are mis-specified, the catchment area draining to a river will be incorrect, leading to errors in both the water-balance and the estimated river flow. This year several schemes have been assessed over the UK and Europe, and optimal methods at each scale have been used to derive the ancillary files required by the Grid-to-Grid model

2.5.2 New methods for deriving river networks

The usual method employed to derive flow directions requires gridded elevation data from a DTM (Digital Terrain Model). Unfortunately, the resolution of the DTM can affect the accuracy of the derived river network, particularly when a low resolution DTM fails to detect a narrow river valley, or when the terrain is very flat. There are several ways to improve derived river networks including manual correction using observed river networks as reference. This procedure usually results in an improved set of flow paths, but accuracy is dependent on the patience of the individual undertaking the correction process.

Recently, algorithms have been published which seek to provide an automated method of deriving flow paths for coarse resolution modelling using a higher resolution DTM (e.g. Fekete *et al.* (2001), Olivera *et al.* (2002), Reed (2003)). Methods such as these provide a way forward, but they require an accurate high resolution DTM in order to produce a lower resolution set of flow paths.

Three methods for deriving river networks from DTM data have previously been explored (Bell *et al.* 2005):

1. Mean elevation + hand-correction
2. Minimum elevation

3. Method of Fekete *et al.* (Network Scaling Algorithm (NSA) method)

This year an additional method for deriving river networks has been investigated which has lead to more accurate flow paths over Europe. The Network Tracing Method (NTM) of Olivera and Raina (2003) traces the path of river networks downstream. For a high resolution grid, the NTM identifies the downstream cell for every coarse-grid grid cell that contains a fine-resolution stream. Hence, to obtain a complete coverage of flow directions for an area, a nominal fine-resolution stream has to be present in each coarse resolution grid and the river network has to flow downstream in one direction only. Intersection of the fine resolution network with the coarse resolution grid results in a new network with nodes at the grid cell boundaries.

The NTM also allows the user to adjust the relative numbers of cells for which networks flow through the sides or the corners. This feature is designed to correct a perceived bias in coarse river networks in favour of flow through the sides of grid-cells rather than corners (Olivera *et al.,* 2002). The side:corner ratio measured in digitised observed river networks was calculated to be 59:41, whereas artificial coarse river networks tended to a greater proportion of flow through the sides. The NTM method allows the user to adjust the side:corner ratio via a threshold, λ, which is based on the fine-resolution reach length within a coarse grid cell. If the reach-length is *greater* than the threshold, the cell flows to its immediate downstream cell, while a reach length *less* than the threshold results in flow to a cell further downstream. This procedure gives less weight to grid-cells with short lengths of river and results in a greater proportion of cells with flow through the corner as shown in Figure 4 .

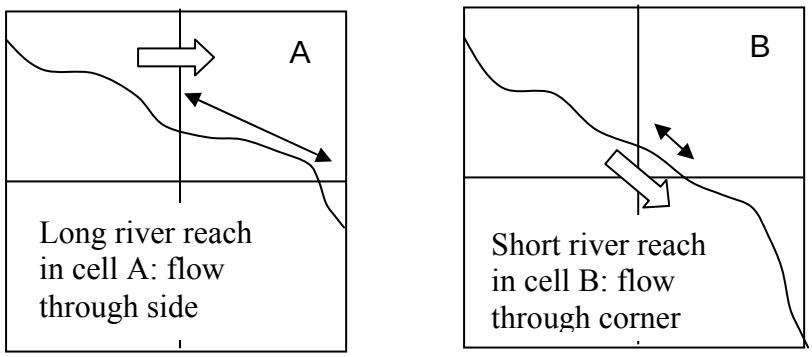

Figure 4. Illustration of the network tracing method used to identify a downstream cell.

The NTM is currently available as an executable file and the input required is an ascii file with columns of record number, length of river section, upstream node number, downstream node number and grid cell identification number. The output is in the form of an ascii file containing flow directions for each grid square.

2.5.3 Results: 25km European scale

At the 25km European scale the NTM method has been compared to the NSA method (Fekete *et al.,* 2001), which had performed well at this scale in a previous comparison (Bell *et al.,* 2005). Derived networks using both methods for two areas of Europe are

shown in Figure 5. The networks from the NTM appear to be better in reproducing the base 1km river network than the previous methods investigated in Bell *et al*. (2005). Problems with rivers crossing catchment boundaries in the lower Rhine and upper Loire which are apparent in the Fekete-derived networks appear to be greatly improved in the NTM-derived networks. The Fekete method also has problems when river networks are close together, such as Norway, as shown in Figure 5(d). Here the NTM has managed to preserve the different river systems whereas the Fekete method has erroneously joined adjacent river networks.

Overall, investigations indicate that the NTM methodology provides an improved method of deriving coarse-scale river networks and flow directions from finer resolution river networks over Europe.

(a) NTM-derived network for central Europe

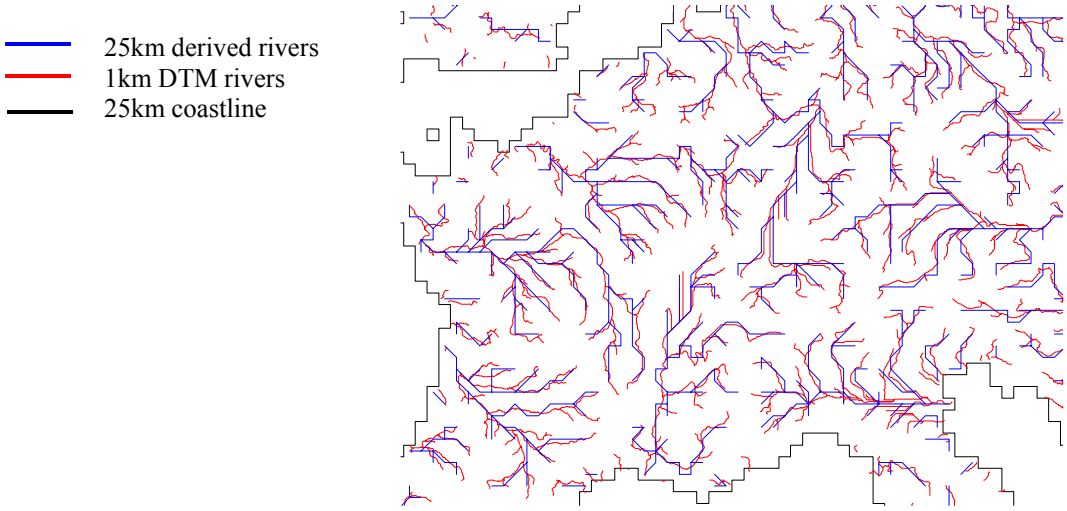

(b) Fekete-derived network for central Europe: problem areas highlighted with circles

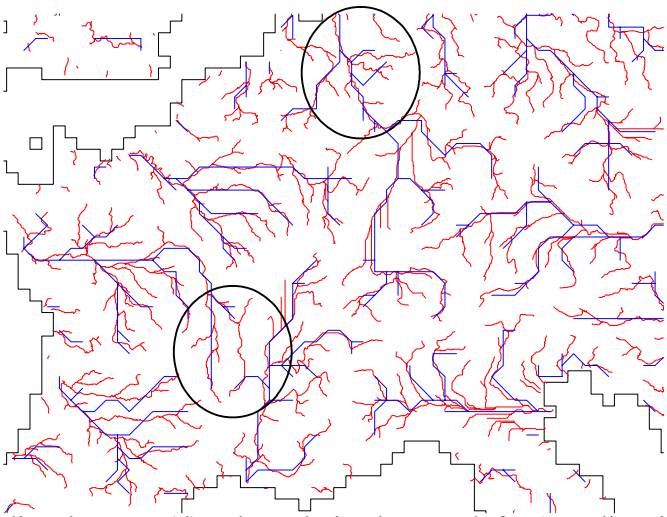

(c) NTM-derived network for Scandinavia

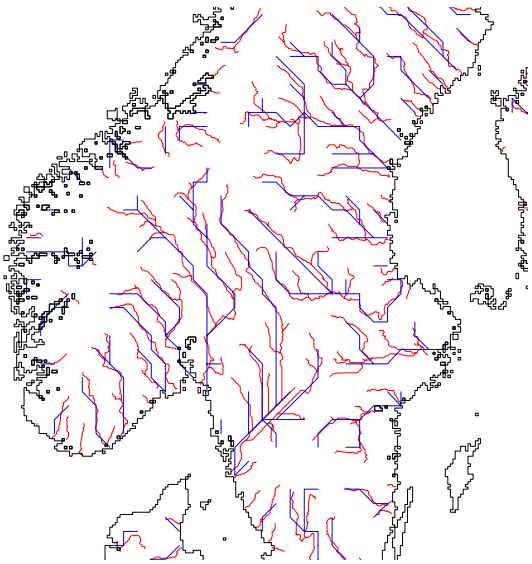

(d) Fekete-derived network for Scandinavia

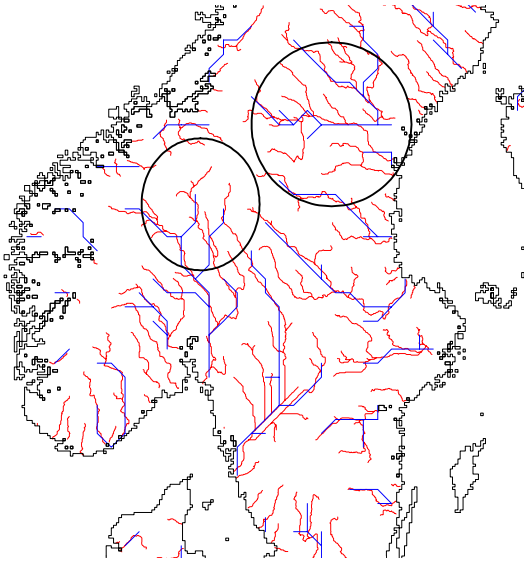

Figure 5. Comparison of DTM-derived European rivers. Coarse–resolution networks at the 25km scale (blue lines) are compared to the base 1km network dataset (red).

As part of the European scale modelling work the CEH and RCM land-sea masks have been “harmonised”. The new land-sea mask and derived river networks are presented in Figure 6. Note that lakes have been treated as ‘land’ in order to derive flow-directions into and out of them. Lakes are assumed to have both river inflows and outflows even though they are probably subject to artificial controls on outflows. The Black Sea and the Sea of Azov are treated as Sea even though they are not linked to the Mediterranean at this grid resolution.

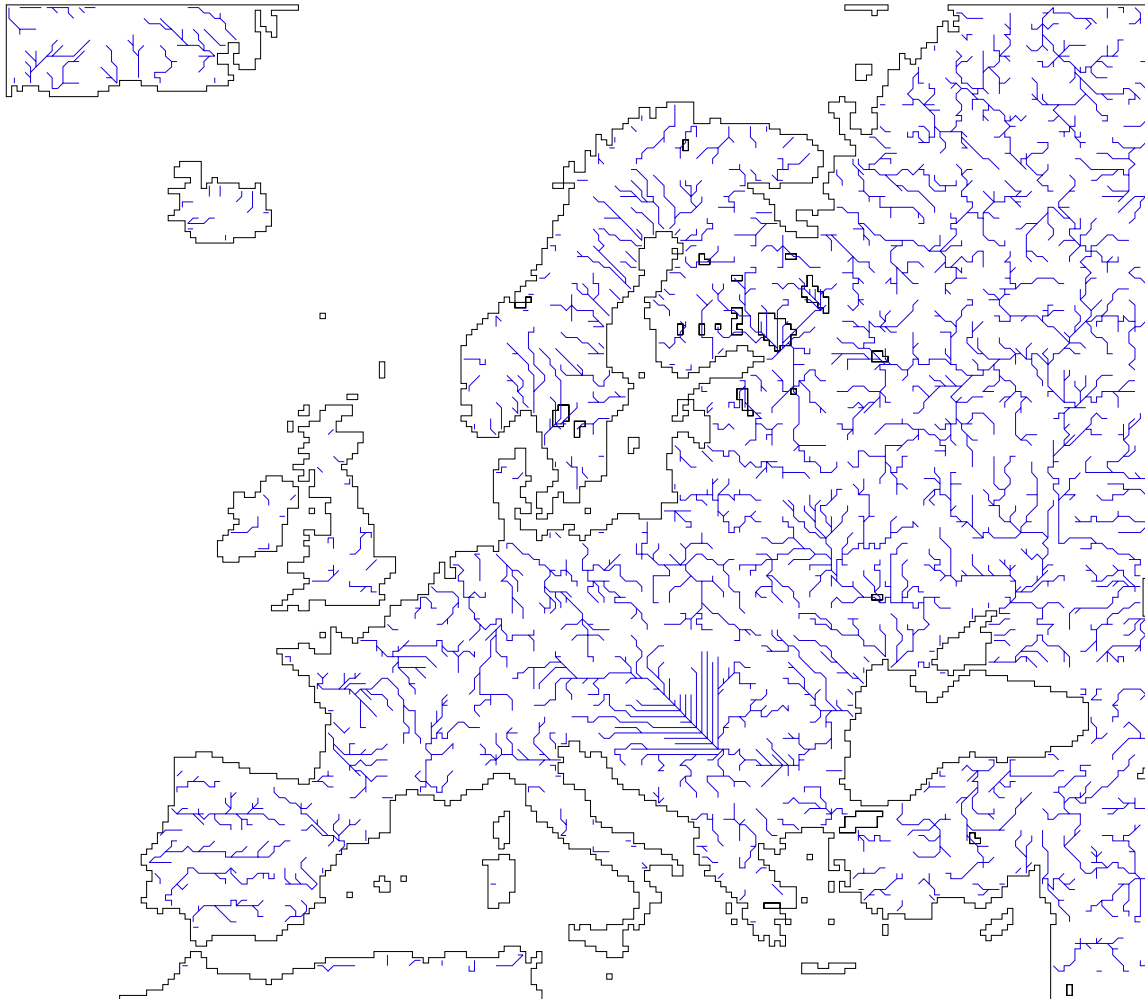

Figure 6. Map of derived river networks and the RCM land-sea mask on the European RCM domain.

In order to determine whether the apparent improvements in network delineation lead to improved estimation of catchment area draining to a river, four major European catchments have been selected for further investigation. DTM-derived catchment areas for the four catchments are presented in Table 3 alongside the true (published) area. The percentage error in the catchment area is shown in brackets.

Table 3. Variation in estimated catchment area using different methods to derive river networks (flow-directions). Best results at a 25km resolution are highlighted in bold typeface.

Site		DTM-derived area (km^2) and error (%)		
	Catchment Area (km^2)	1km DTM	25km Fekete et al method	25km NTM
Thames at Kingston	9948	10452 (5%)	**11875 (13%)**	14375 (27%)
Seine at Paris	43800	45734 (4%)	42500 (7%)	**46875 (2%)**
Labe (Elbe) at Decin	51104	53682 (5%)	48125 (10%)	**56875 (6%)**
Rhine at Lobith	159442	149574 (6%)	176250 (18%)	**150000 (0%)**

For catchments delineated using the 1km DTM the error is measured with respect to the true catchment area. For the 25km DTMs the percentage error is measured with respect to the 1km DTM-derived catchment area because this is the base dataset from which lower resolution networks are derived. (A perfectly accurate 25km river network would not be expected to exceed the 1km base dataset from which it is derived).

The poor performance of the NTM method on the Thames has been investigated in more detail The NTM-derived catchment boundary encloses the Thames river basin more accurately than the Fekete-derived catahment boundary, even though the catchment areas in Table 3 indicate otherwise. This example highlights the problems inherent in using a coarse grid to delineate flow directions for catchments that are small in comparison to the grid-resolution.

Catchment areas derived using the 1km DTM are generally in error by around 5% when compared to observations. Three of the four catchment areas identified at a 25km resolution indicate improved areal estimation when the NTM method is used. A comparison with the detailed river networks indicates that the NTM network–delineation method more accurately estimates catchment areas than the method of Fekete (Davies and Bell, 2005).

2.5.4 Results: 1km UK scale

Clearly errors in the base DTM will affect the quality of the river networks which are derived from it. For the detailed UK modelling work, which is currently being undertaken offline, the original hand-corrected 1km river flow network derived from the 1km Hydro1k base DTM has been replaced by an improved 1km network based on a 50m hydrologically corrected DTM. The CEH Wallingford DTM (Morris and Flavin, 1990) is available at a 50m grid interval and a 0.1m vertical resolution. Ordnance Survey (OS) 1:50000 digitised contours and spot heights, and digitised river networks were used in its derivation.

As part of this analysis, a new 1km land-sea mask was derived from the 50m DTM. The "majority method" was used, whereby if most of the 50m cells within a 1km grid cell are land then the 1km cell is set to land, otherwise it is sea. This method proved successful, except in cases where two rivers entered an estuary in close proximity to each other. If the two rivers joined *before* reaching the sea, erroneously high values of river flow could occur at the coast. This problem was discovered in two places - the

Humber estuary and the Firth of Tay - where hand-correction was required to convert land pixels into sea.

The method chosen for deriving 1km river networks over the UK has been influenced by both accuracy and ease of use. The NTM method was chosen for deriving networks over Europe, as it was found to be the best method of generating 25km flow directions from a 1km resolution grid. But for the 1km UK application, this method has not been used because of excessive processing time at the finer scale. (To run the NTM at the 1km level would require the UK to be split into approximately six regions and incur significant processing time). The NSA method of Fekete used with a 50m DTM was found to provide significant improvement on the previous hand-corrected method (using 1km Hydro1k DTM) and has therefore been chosen to provide the flow-direction ancillary files required by the G2G for the 1km UK work. The resulting 1km derived river network is compared to the 50m detailed river network in Figure 7.

In some places, river meandering present in the 50m river network is not reproduced in the 1km derived river network. This difference is highlighted in Figure 7 which shows river networks for South Wales. Routing flow along river networks which are short in comparison to observed rivers may affect timing of flow peaks, though the error is likely to be small compared to other sources of error.

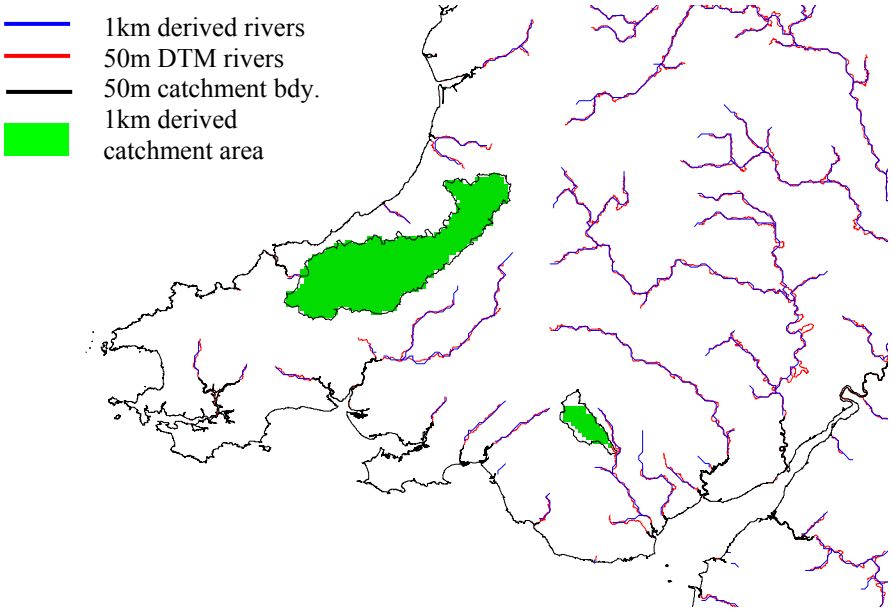

Figure 7. River networks for South Wales highlighting the error in the 1km derived catchment boundary.

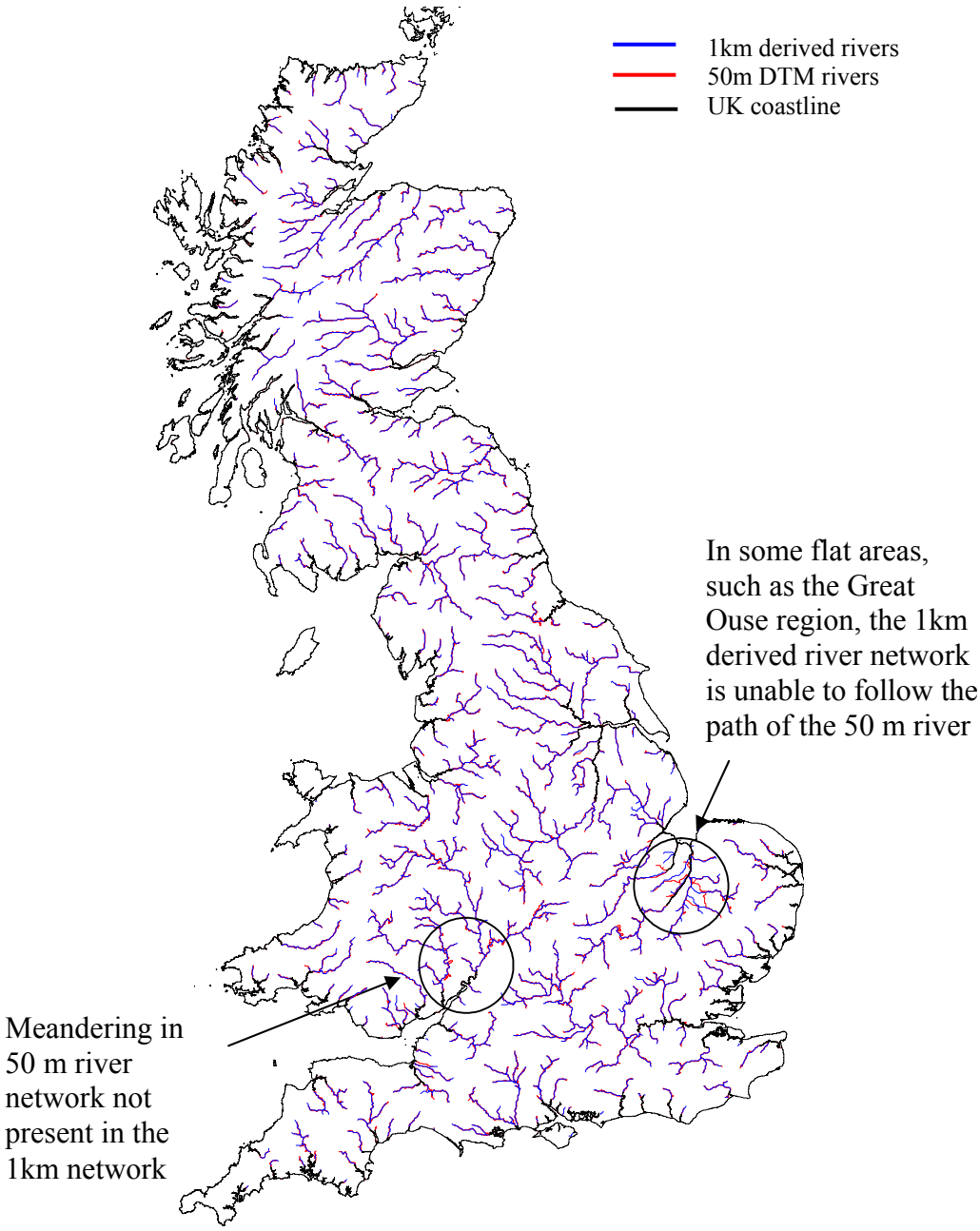

Figure 8. Map of Great Britain showing the NSA-derived 1km river network (blue) overlain by the 50m UKDTM hydrologically-corrected river network (red).

Figure 8 also shows true and 1km network-derived catchment boundaries for two catchments: the Teifi to Glan Teifi and the Cynon to Abercynon. The 1km derived catchment boundary for the Teifi agrees well with the 50m boundary, however the Cynon 1km network-derived boundary is missing an area in the north of the catchment. Further investigation has shown that this problem can occur where the divide between two river valleys is narrow and can lead to parts of a catchment draining into the wrong river. In the Cynon, the north part of the catchment erroneously flows into the Neath

river system leading to a 35% error in the 1km DTM-derived catchment. Figure 9 shows how close the two river systems are, and goes some way to explaining the cause of the high error in the 1km catchment area.

Observed and 1km DTM-derived catchment areas have been compared for 25 catchments across England and Wales. Errors in derived catchment area range in magnitude from 0 to 35%, with a mean error of 5.6%. It is important to try to reduce this error as much as possible as it impacts on the catchment water balance and accuracy of modelled river flow. Ongoing work is evaluating the alternative NTM method, which has proved so successful at the European scale, for selected regions of the UK. Problems associated with the processing time required by this method are also being investigated.

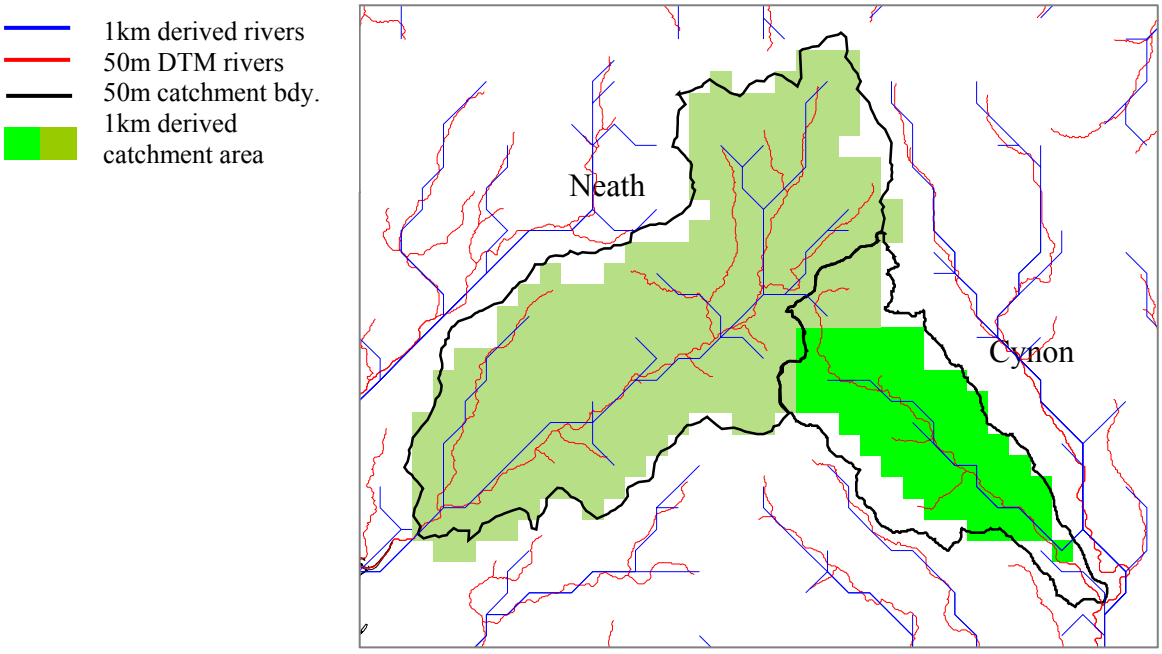

Figure 9. Map of the Cynon and Neath river systems showing how large errors in derived catchment area can arise in steep-sided river valleys.

The accuracy of coarse-scale river networks is heavily dependent on the scale and accuracy of the fine-scale dataset from which they are derived. The 1km fine-scale dataset has provided a good basis for derived 25km networks; however, higher-resolution global DTMs are becoming available. For example, the 90m worldwide DTM grid from the Shuttle Radar Topography Mission (http://srtm.usgs.gov/) and the 5m, 10m and 50m NEXTMap DTM data of the UK (http://www.intermap.com/corporate/nextMap.cfm), may further advance the identification of large scale river networks.

MODEL RESULTS

3.1 European application of MOSES-G2G

For the 25km European application MOSES-G2G is configured to run on the North West European RCM grid, with both MOSES and the G2G run at a 25km resolution. The model is run at an hourly time-step as required by MOSES, but model performance is assessed at a daily time-step. Modelled and observed flow have been compared at a number of locations across Europe. The daily flow data were made available by the FRIEND (Flow Regimes from International Experimental and Network Data) research programme funded by UNESCO.

Eight sites, listed in Table 4, have been used for preliminary model testing and assessment. The sites were chosen because they had a range of catchment drainage areas and observed flow records existed for much of the period covered by the RCM ERA-driven data (1985–2001). A map of the DTM-derived catchments draining to each site is shown in Figure 10. Where a catchment was gauged in multiple locations, the opportunity was taken to compare modelled and observed flows at each of the stations nested within the drainage basin. The catchments used in the initial case studies range in area from *circa* 1,300 km^2 (Loire at Chadrac) to 160,000 km^2 (Rhine at Lobith).

Table 4. NW European catchments used in the initial assessment of MOSES-G2G.

Catchment	River	Station	Area		
ID			observed	DTM-derived	Error
			10^3 km^2	10^3 km^2	%
1699101	Rhine	Lobith	159.4	149.4	-6
1599055	Seine	Paris	43.8	46.3	6
1516019	Seine	Troyes	3.4	4.4	28
1498001	Loire	Montjean	110.0	111.3	1
1498018	Loire	Orleans	37.0	40.6	10
1409016	Loire	Chadrac	1.3	1.3	-5
0417012	Elbe	Decin	51.1	54.4	6
1598003	Maas	Lith	28.8	21.3	-26

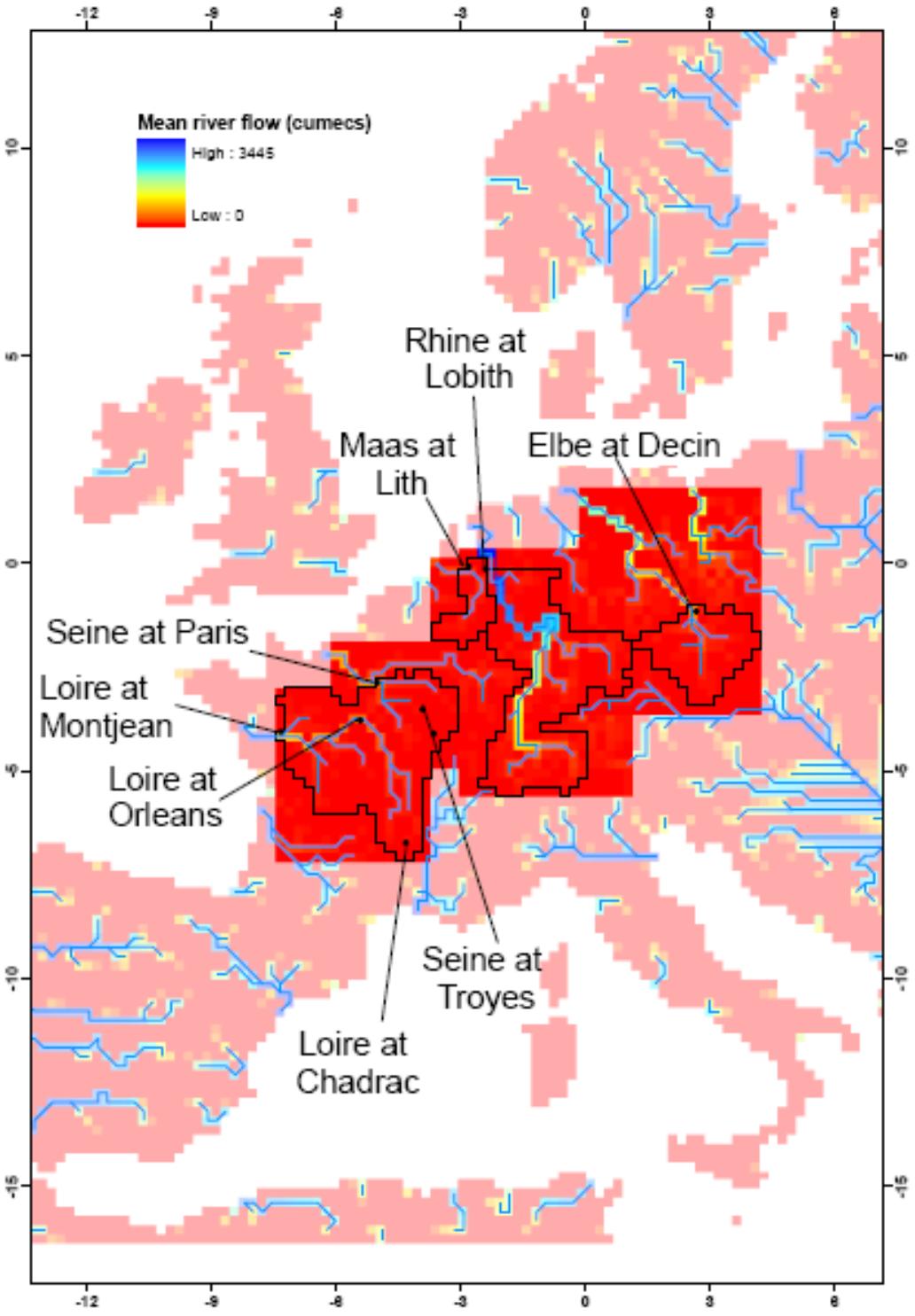

Figure 10. Map of study catchments. Blue lines indicate rivers, black lines delineate catchment boundaries, filled circles mark gauging stations, colour scale indicates drainage area upstream of each grid square, and darker colour scale is used within modelled region.

Table 5 shows goodness-of-fit statistics between observed and modelled flows in each catchment. A number of performance measures have been used to assess model performance: mean discharge over the period of record, the efficiency statistic, R^2, and the Root Mean Square Error, RMSE. In order to summarise the model's success across all the catchments for which it was tested, we have computed an average of the values in the error column of Table 5. This column shows the difference between the means of the modelled and observed discharges over the entire period of comparison. These differences range between +2 and -67%. Since some values in this column are positive, indicating over-prediction, and some are negative indicating under-prediction, we have computed the mean of the absolute differences. This mean is 30%. There appears to be no link between the location or size of the catchment and the discrepancy between water volumes. In the present study, no allowance has been made for artificial abstractions of water and returns. Net abstractions may account for the overestimated model flow in such rivers as the Rhine and Elbe although constraints on abstraction rates for those rivers have yet to be obtained. Significant underestimates of flow by 42% in the Maas and 43% in the Loire at Chadrac may result from the poor correspondence between catchment areas in these rivers. This explanation seems more likely to apply to the findings for the Maas River than the Loire at Chadrac; in the latter case the underestimate may have arisen simply because modelling a catchment with this small drainage area is not possible using Jules–PDM at a 25km resolution, or is beneath the spatial scale at which the ERA–40-driven RCM experiment reproduces natural variability in precipitation. A comparison of RCM and observed rainfall, where possible, may clarify the situation.

Table 5. Preliminary goodness-of-fit indicators between modelled and observed river flow for eight NW European test catchments over the period 1985 -2001.

Catchment	River	Station	Mean discharge				R^2 efficiency	RMSE
			Record length (days)	Observed ($m^3 s^{-1}$)	Modelled ($m^3 s^{-1}$)	Mean % error (%)	[-]	($m^3 s^{-1}$)
1699101	Rhine	Lobith	2918	2194	3297	50	-0.72	1691
1599055	Seine	Paris	2189	273	342	25	-0.69	300
1516019	Seine	Troyes	1822	32	30	-7	-1.61	43
1498001	Loire	Montjean	1459	627	671	7	0.18	711
1498018	Loire	Orleans	2189	223	218	-2	0.13	305
1409016	Loire	Chadrac	1459	11	6	-43	-0.49	16
0417012	Elbe	Decin	1822	329	548	67	-3.53	584
1598003	Maas	Lith	2981	302	175	-42	0.28	257

Of the eight rivers that were modelled here, the best agreement between observed and modelled flows was found for the Maas River, although the mean modelled flow at this location was significantly lower than the mean observed flow for reasons noted above. Good correspondence between modelled and observed flows were also found for the Loire at Montjean and Orleans, and in those locations the modelled discharge

corresponded closely with observed values. The least successful correspondence was noted for the Elbe. This result, taken together with the large overestimate of mean discharge for the Elbe may indicate that abstraction of water affects not only the mean rate of flow for this catchment but also the shape of flood hydrographs.

3.1.3 Results by catchment

Hydrographs of modelled and observed river flows in each of the catchments studied are presented in Figures 11 to 13. Several typical patterns are observed in the shapes of the flood hydrographs in each case. The results from the Rhine indicate that the general form of the hydrograph obtained is correct, although there is evidence that initial peaks are too slow to form and that flow recedes too slowly after each storm. In contrast, the results from the two catchments of the Seine indicate an approximately-correct volume of water discharge but the modelled flood hydrographs form a greater number of high peaks than were observed.

The Loire exhibits what seems to be the correct form for flood hydrographs but there is a suggestion that the RCM precipitation does not correspond well with the precipitation that generated the floods in the observed river record. The lack of correspondence is particularly notable in the smallest of the three hydrometric stations on the Loire at Chadrac. This mismatch is perhaps to be expected if there is a spatial scale at which it is unreasonable to expect the ERA–40-driven RCM to reproduce observed precipitation. For example, the RCM may accurately predict precipitation averaged over a ~100km region but the variability at scales smaller than this may not necessarily match the natural variability. Further work to assess the likelihood of this possibility is described later. In each case, the Elbe and Maas simulations have produced results with more pronounced peaks than are seen in the observed data; in the case of the Elbe, the rate of flow recession is also slower than that observed.

3.1.2 Recommendations for future work at the European scale

The results presented in the previous section indicate that, in general, there are three areas for model improvement: (i) matching average modelled river flows to average observed flows; (ii) matching hydrograph shape between modelled and observed flows; (iii) incorporation of further information on catchment properties such as topography to arrive at more accurate site-specific predictions without compromising the generality of the model. Suggestions for how these goals may be achieved are as follows:

- *Comparison of RCM and observed precipitation*

  One of the main uncertainties associated with the results presented above lies in the attribution of model success or failure to: (a) correct reproduction of observed rainfall by the ERA–40-driven RCM, and (b) appropriate formulation and calibration of the runoff-production and flow-routing schemes in Jules–PDM with G2G. A recommended piece of further research is to undertake a formal comparison of RCM rainfall with observed rainfall. Observed data with which to perform this comparison are more readily available within the UK, but investigation of data availability for parts of Europe is underway.

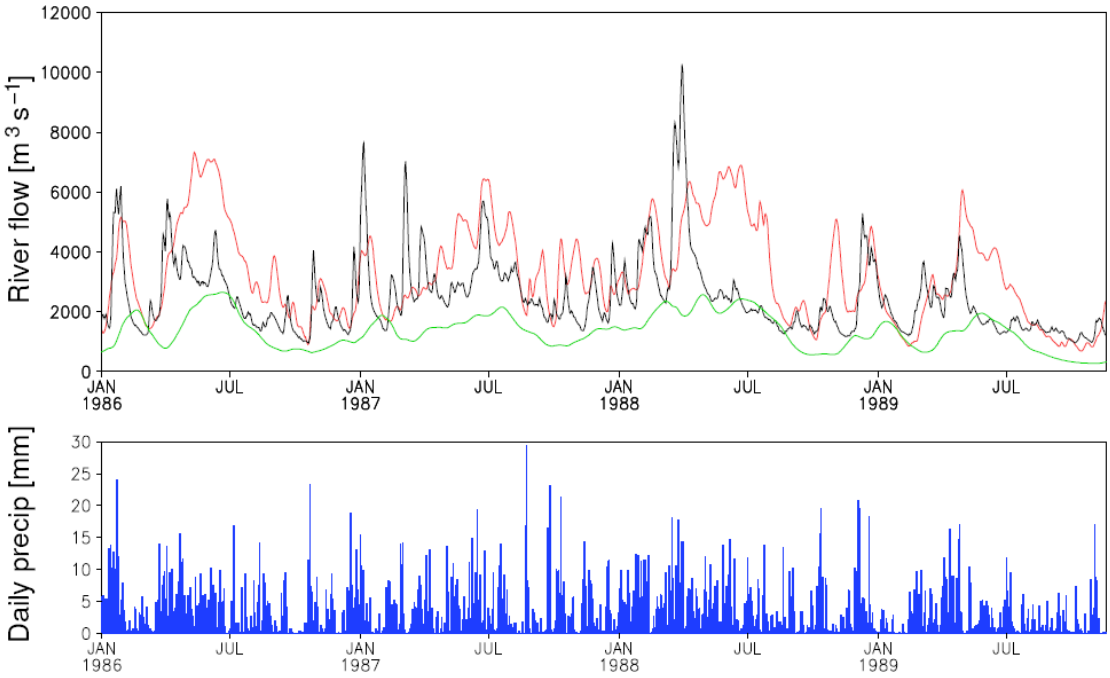

Figure 11. Modelled river flow (red), subsurface flow (blue), observed river flow (black) for the Rhine at Lobith (station 1699101); lower plot: daily catchment precipitation.

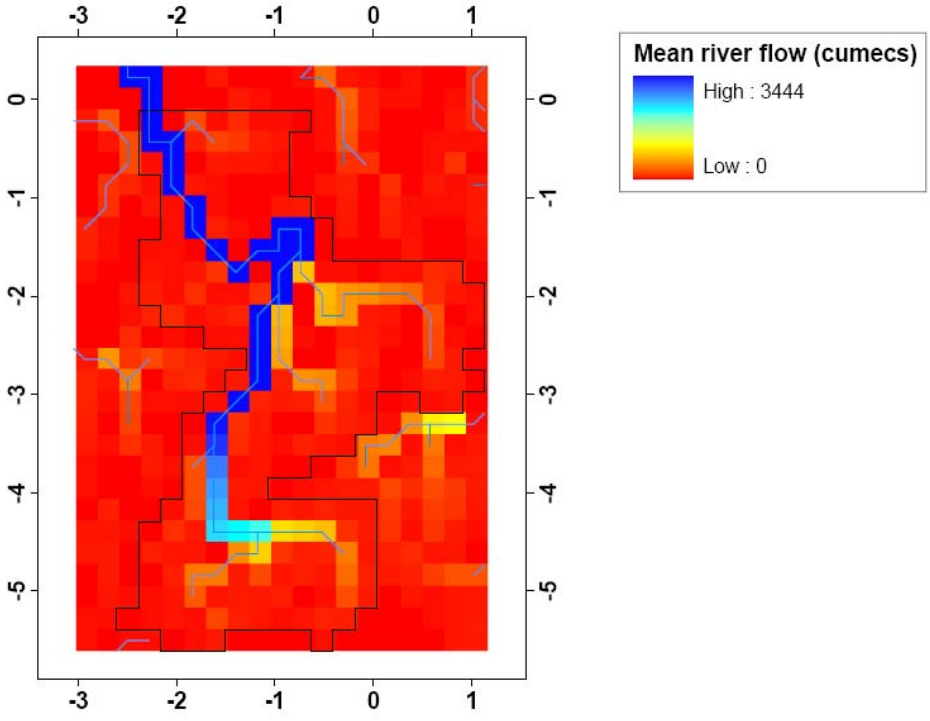

Figure 12. Map showing mean river flow in the Rhine catchment on the 25km gridded model domain. Coordinates are in degrees in the standard RCM rotated latitude-longitude grid. The blue line indicates the river and the black line shows the DTM-derived catchment boundary.

(a) Seine at Paris

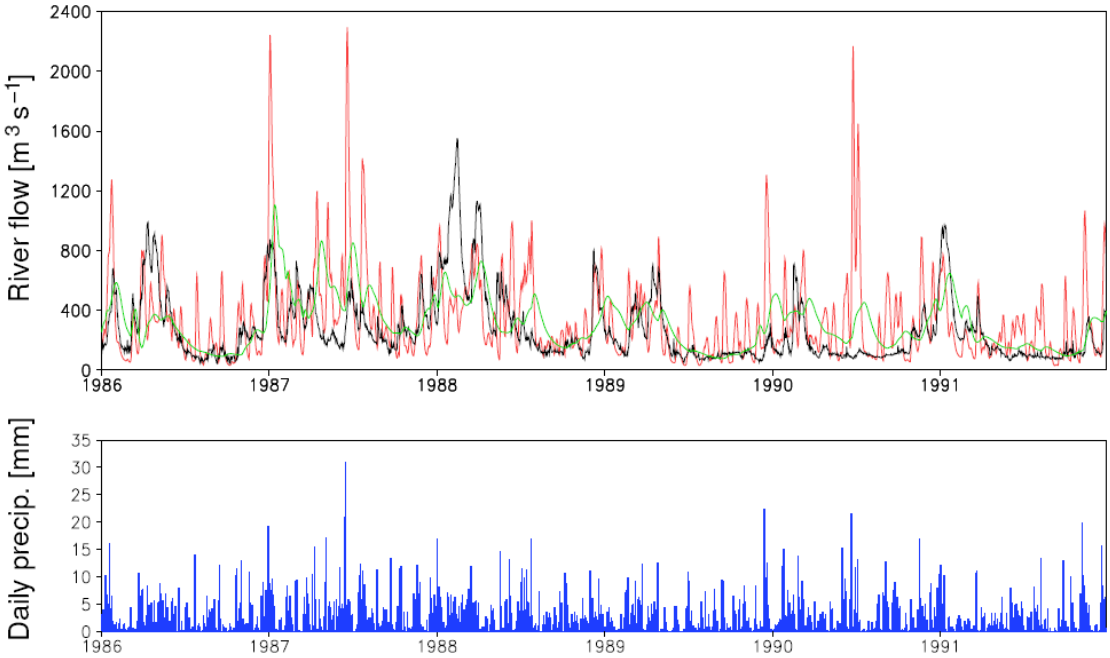

(b) Seine at Troyes

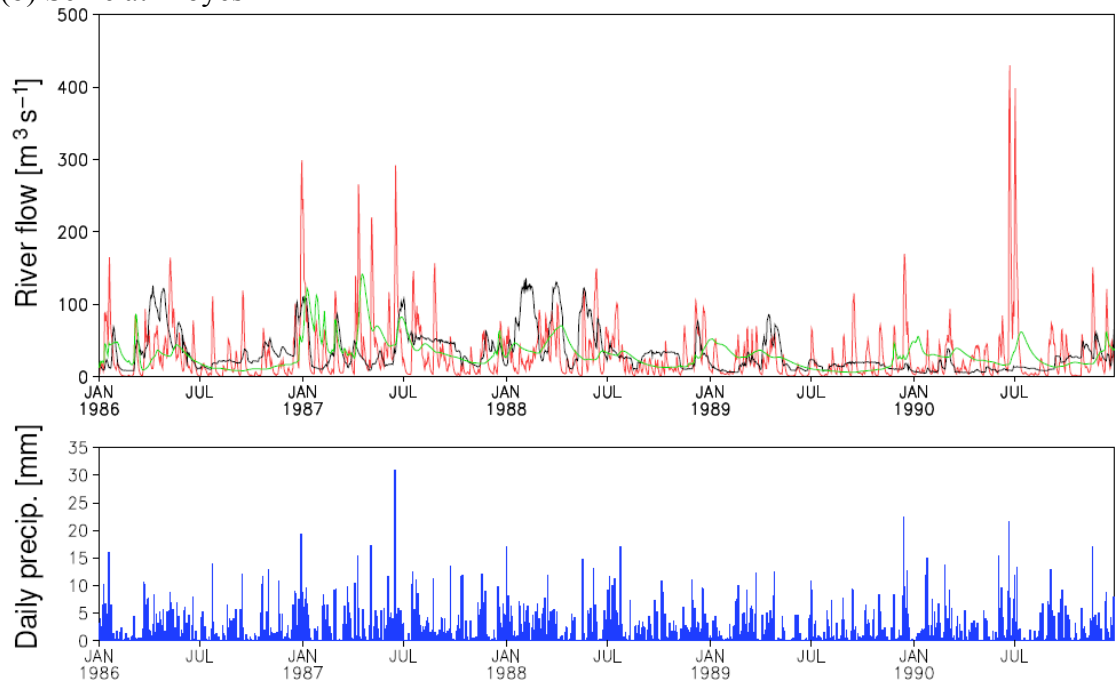

Figure 13. Flow hydrographs for selected European catchments: modelled river flow (red), subsurface flow (green) and observed river flow (black). Lower plots indicate catchment daily precipitation.

(c) Loire at Montjean

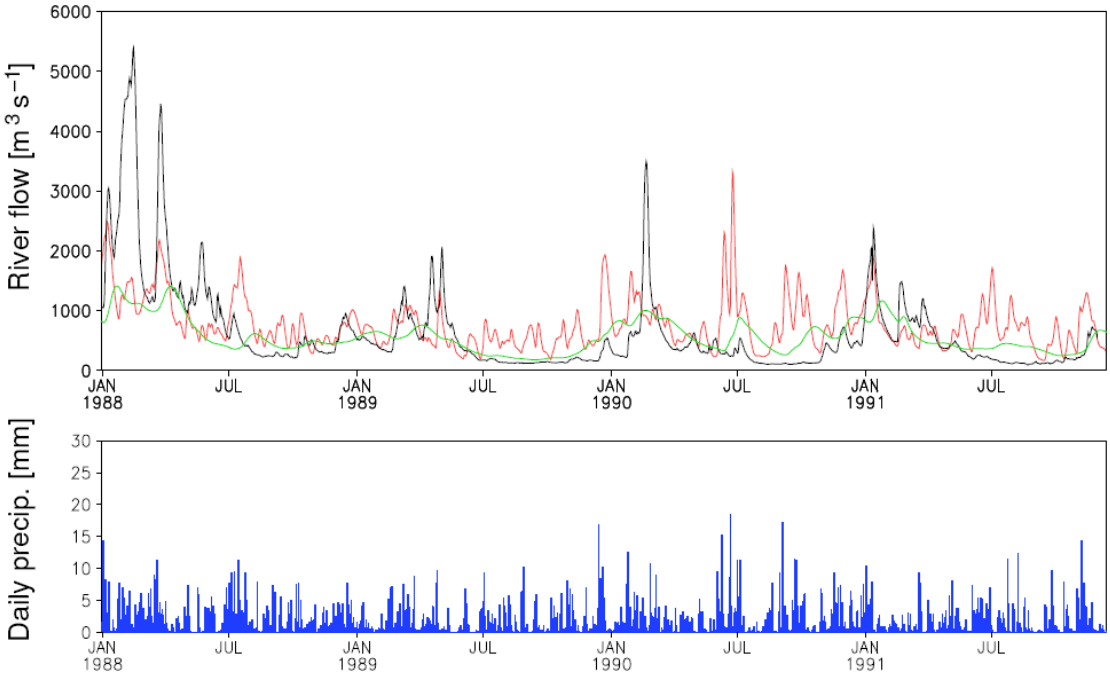

(d) Loire at Orleans

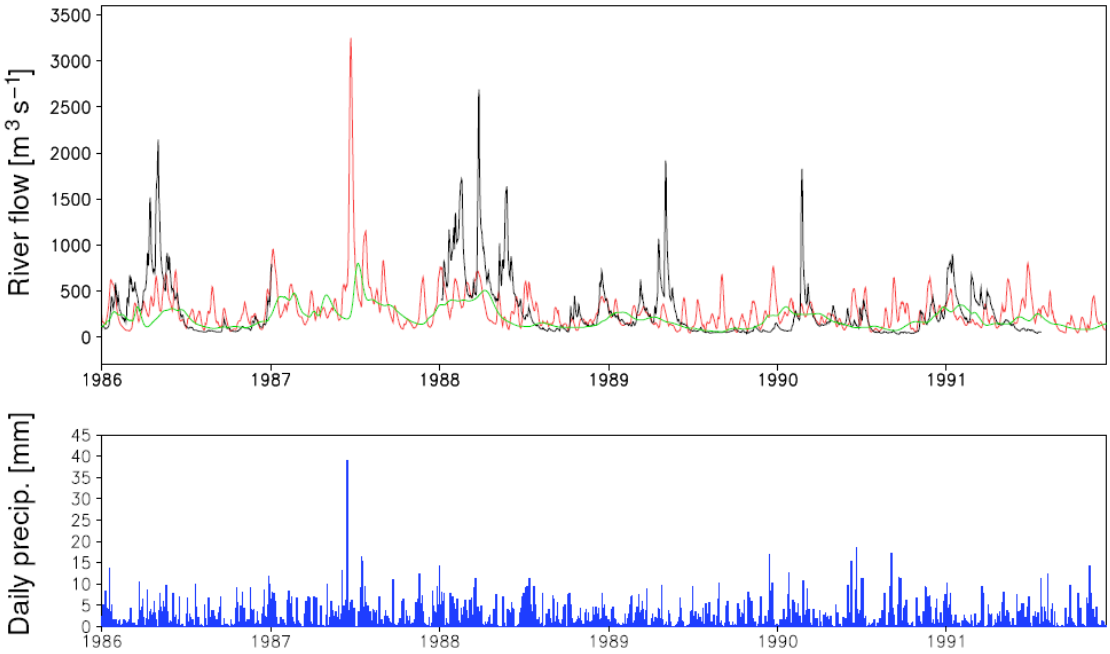

Figure 13. (continued) Flow hydrographs for selected European catchments: modelled river flow (red), subsurface flow (green) and observed river flow (black). Lower plots indicate catchment daily precipitation.

(e) Loire at Chadrac

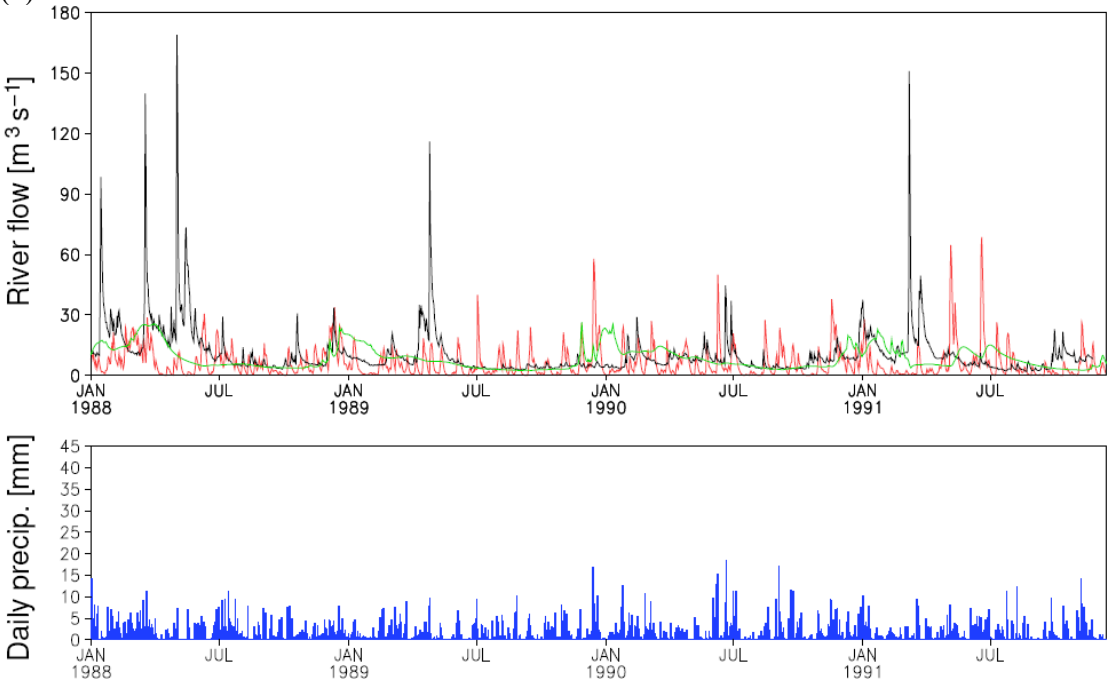

(f) Elbe at Decin

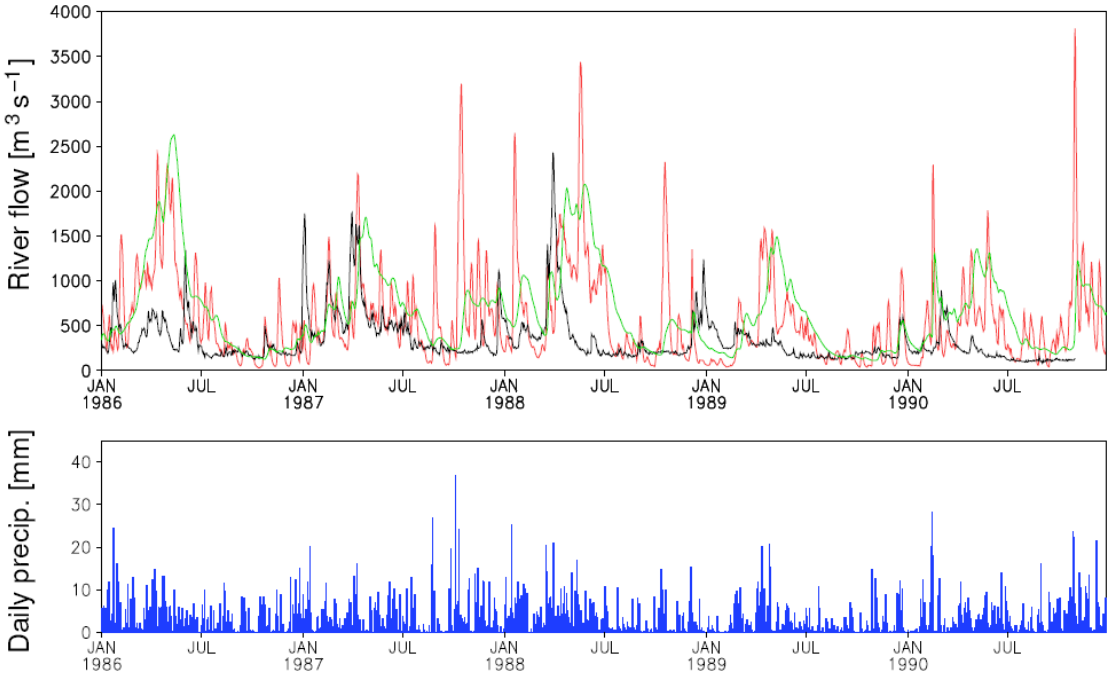

Figure 13 (continued): Flow hydrographs for selected European catchments: modelled river flow (red), subsurface flow (green) and observed river flow (black). Lower plots indicate catchment daily precipitation.

(g) Maas at Lith

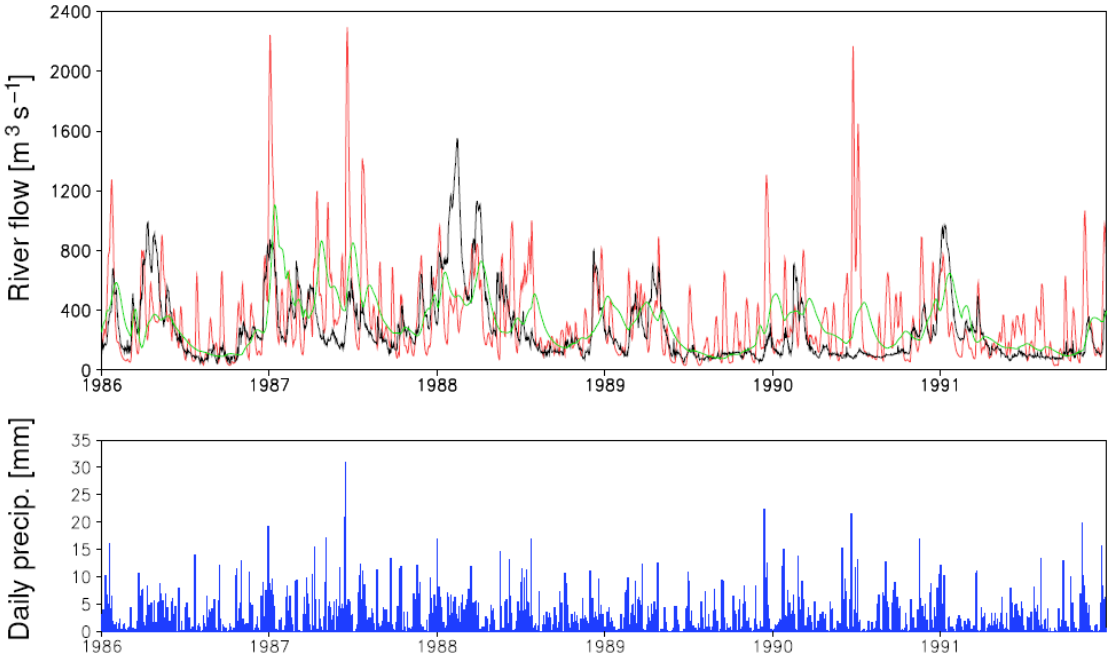

Figure 13 (continued): Flow hydrographs for selected European catchments: modelled river flow (red), subsurface flow (green) and observed river flow (black). Lower plots indicate catchment daily precipitation.

Recommendations for future work at the European scale (continued)

- *Exploration of different runoff production schemes*

Jules–PDM provides options for running the model with different components to represent soil hydrology and runoff production. Possibilities that have yet to be explored include using van Genuchten's model of soil hydrology (instead of the Brooks–Corey/Clapp–Hornberger scheme used in the present work), and using TOPMODEL as an alternative runoff-production scheme (in which case the model is referred to as Jules–LSH). Further work is necessary before these schemes can be used to their full potential.

- *Addition of spatially-varying soil depth*

A further change to the runoff-production scheme may be possible to correct for the fact that the model produces flood hydrographs that are too peaky in some regions yet too delayed in others. The Rhine, for example, exhibits a delayed response to precipitation, whereas the results for the Seine are too flashy. It is thought that the differing topography in each region may exert a control on hydrograph form through its relation to soil depth. Incorporating parametric topographic information into a refinement of the runoff-production scheme in Jules–PDM may allow the shape of flood hydrograph to be determined jointly by the topography and the preset runoff-production and flow-routing parameters.

3.2 UK application of MOSES-G2G

3.2.1 Introduction

For the UK application MOSES-G2G is configured to run on the UK National Grid grid, with MOSES run at a 5km resolution (as in the Nimrod application, Smith *et al.*, 2005), while G2G routing is undertaken at a 1km resolution. MOSES is best run at an hourly time-step, but for stability the G2G needs to be run at a 15 minute time-step. Model performance is assessed at a daily time-step in line with the daily flow records used in this study. The flow-routing model can be assessed with reference to daily flow observations at 25 locations across the UK The flow data are managed by the National River Flow Archive, at CEH Wallingford, with the data originating from the UK Environment Agency. The 25 catchments, listed in Table 6, display a wide range of attributes, ranging from fast upland catchments (e.g. Taw, Dee) to large baseflow dominated regions (e.g. Thames, Lt. Ouse). Columns 4 and 5 present values for the true and DTM-derived area (the figure in brackets) for each catchment, together with the percentage error in catchment delineation. The mean percentage error is 5.6%, which is significantly better the value of 10.5% previously achieved though the use of hand-corrected flow–paths derived from Hydro1k DTM. The use of the NSA method, as described in Section 2.5, is clearly beneficial. A map of the UK showing the catchment boundaries and locations is presented in Figure 14.

Table 6. UK catchments used in model assessment.

Catchment	ID	UK Region	Area (DTM area) Km^2	% error in area	Baseflow Fraction (bfi)	Elevation range (m)
1. Mole at Kinnersley Manor	39069	Thames	142 (127)	-10.6	0.39	130
2. Thames at Kingston	39001	Thames	9948 (9954)	0.06	0.64	325
3. Derwent at Buttercrambe	27041	NE	1586 (1576)	-0.63	0.69	444
4. Wharfe at Flint Mill Weir	27002	NE	759 (776)	2.24	0.39	690
5. Colne at Lexden	37005	Anglia	238 (227)	-4.6	0.52	106
6. Mimram at Panshanger Pk	38003	Thames	134 (134)	0	0.94	148
7. Lambourne at Shaw	39019	Thames	234 (247)	1.28	0.97	185
8. Severn at Bewdley	54001	Midlands	4325 (4289)	-0.83	0.53	810
9. Avon at Evesham	54002	Midlands	2210 (2203)	-0.32	0.51	300
10. Lt. Ouse at Abbey Heath	33034	Anglia	688 (695)	1.02	0.8	91
11. Yscir at Pontaryscir	56013	S.Wales	63 (73)	15.9	0.46	313
12. Cynon at Abercynon	57004	S.Wales	106 (68)	-35	0.41	440
13.Tawe at Ynystanglws	59001	S.Wales	228 (261)	16.2	0.36	793
14. Teifi at Glan Teifi	62001	W.Wales	894 (889)	-0.56	0.54	588
15. Lune at Caton	72004	NW	983 (979)	-0.41	0.32	726
16. Leven at Leven Bridge	25005	NE	196 (210)	7.14	0.44	449
17. Trent at Colwick	28009	Midlands	7486 (7573)	0.01	0.64	620
18. Exe at Thorverton	45001	SW	601 (655)	9	0.5	495
19. Taw at Umberleigh	50001	SW	826 (832)	0.73	0.42	590
20. Dee at Manley Hall	67015	N.Wales	1019 (1015)	-0.39	0.52	859
21. Crimple at Burn Bridge	27051	NE	8 (9)	11.1	0.31	135
22. Blackwater at Swallowfield	39007	Thames	355 (363)	2.25	0.67	183
23. Beult at Stile Bridge	40005	Southern	277 (256)	-7.58	0.24	149
24. Frome at Ebley Mill	54027	Midlands	198 (220)	11.1	0.87	237
25. Taff at Pontypridd	57005	S. Wales	455 (462)	1.5	0.47	841

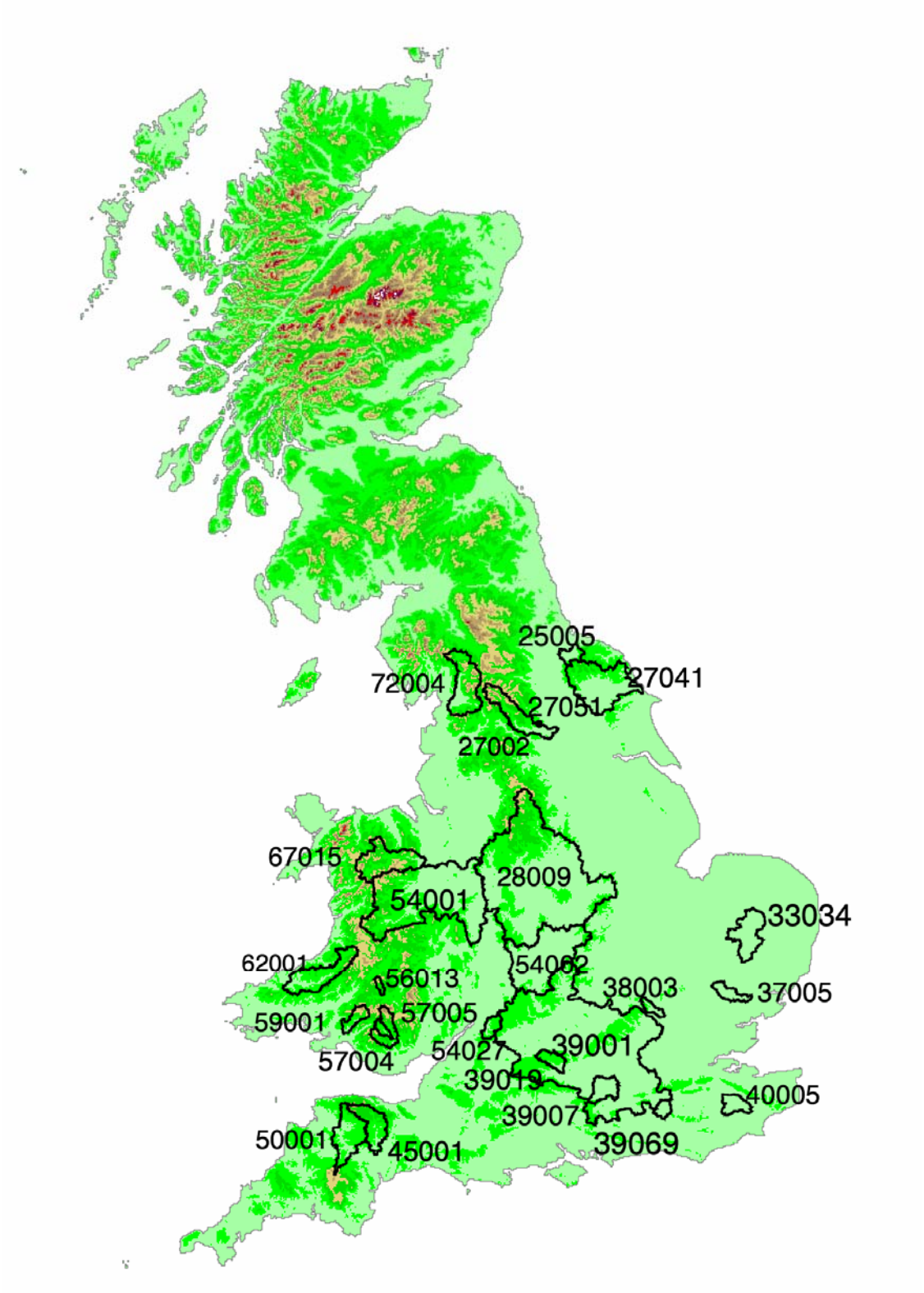

Figure 14. Relief map of Britain showing the location of the 25 study catchments. Catchments are labelled with their ID.

Modelling a domain encompassing all the 25 study catchments using MOSES-G2G is relatively demanding in terms of elapsed processing time, so offline tests have so far been undertaken on a subset. For initial modelling work the UK has been divided into 4 regions covering parts of the North, South Wales, Anglia and the Thames Basin. These regions contain 17 of the 25 study catchments, as shown in the map in Figure 15. The four modelled UK regions are highlighted in pale blue together with their associated catchments. The highlighted areas also indicate simulated river flow on 3 February 1987; the correspondence with nearby rivers is apparent.

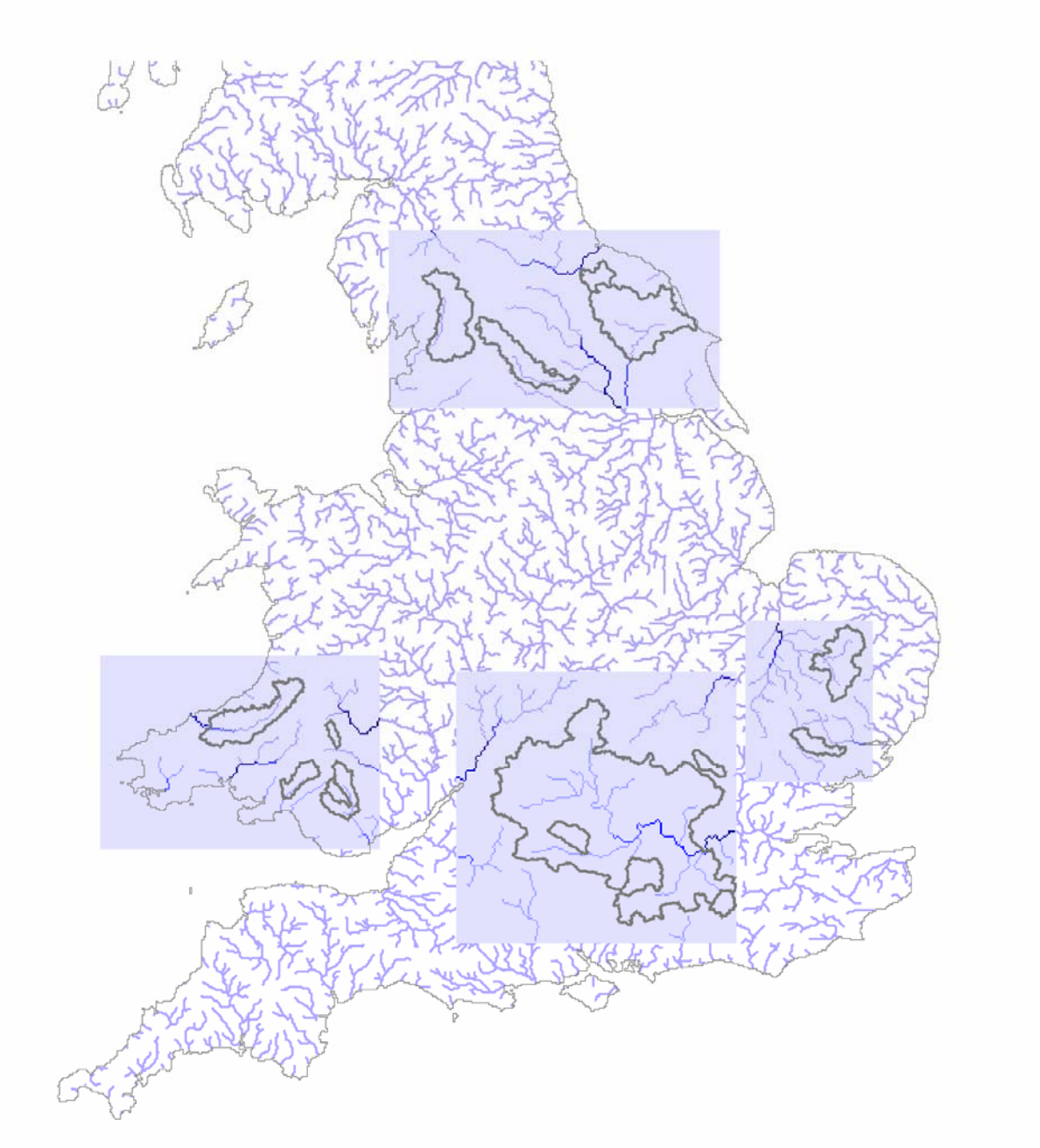

Figure 15. Map showing the four modelled UK regions (highlighted in pale blue) and their associated catchments.

Flow simulation in these catchments using MOSES-G2G has required adjustment of both the G2G routing parameters and selected MOSES parameters which determine runoff. Initial experiments revealed that this calibration was best undertaken using observed 5km gridded raingauge observation obtained from the Met Office in place of hourly RCM rainfall. All other driving data for MOSES (temperature, humidity, wind, radiation used for the potential evaporation calculation) was provided by the RCM. Use of daily observed rainfall data divided into 24 equal hourly values reduced the source of error and enabled calibration of MOSES-G2G to progress.

3.2.2 Comparison of observed and modelled flow hydrographs using observed rainfall data

This analysis uses the best available rainfall data for the G2G routing model. This consists of daily average rainfall provided at a 5km resolution (and as equal hourly values within each day) for the G2G routing model. The G2G produces estimates of flow at an hourly time-step, although it is run at a 15 minute time-step and 'calibrated' using flow observations at a daily time-step.

Following adjustment of G2G routing parameters for a range of catchments, further inspection of simulated flows for the Teifi at Glan Teifi indicated that most flow peaks were underestimated as shown in
Figure 16 16.

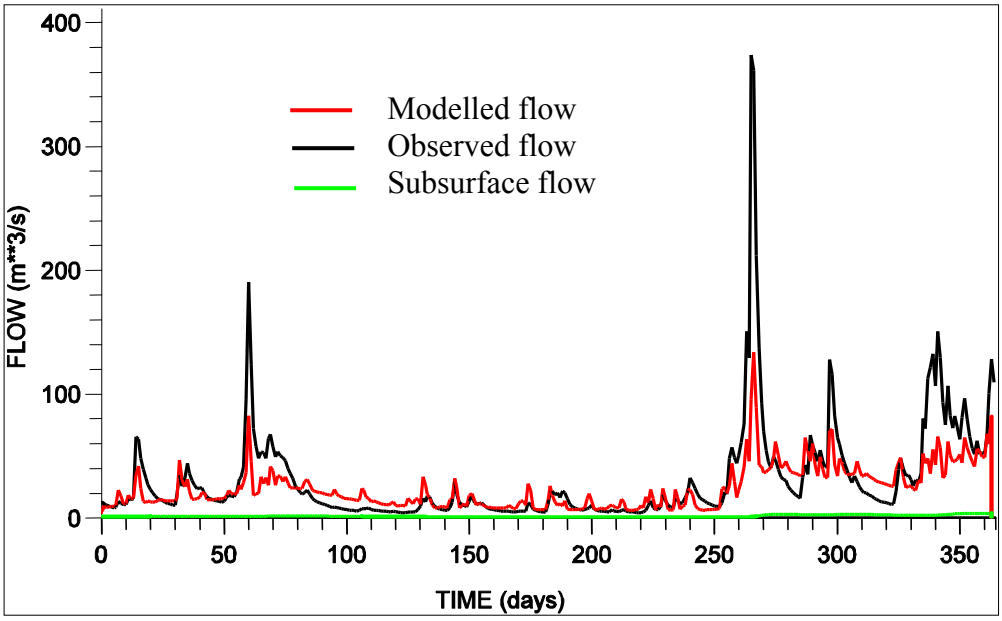

Figure 16. Hydrograph of observed and modelled flow for the Teifi: 25 January 1987 to 24 January 1988.

For this catchment the DTM-derived area is close to the true area (5km^2 error in a 893km^2 catchment), and the baseflow component of flow is small, so the low volume of water in the catchment draining to the river was investigated further. An informal water balance for a grid-cell within the catchment was compared to modelled and observed

flow at the catchment outlet in order to understand the passage of water through MOSES. The water balance is presented in the second column in Table 7.

Table 7. Components of an informal water balance for the Teifi at Glan Teifi for the period 25 January 1987 to 25 January 1988.

Components of the water balance	Standard MOSES with 3m soil layer (10^7 m^3)	MOSES (3m) with reduced canopy (10^7 m^3)	MOSES with 1m soil layer (10^7 m^3)	MOSES with reduced canopy *and* 1m soil layer (10^7 m^3)
Values for a single grid-cell:				
Rainfall	109	109	109	109
Canopy evaporation	-28	-22	-29	-22
Canopy throughfall	80	87	80	87
Soil Evaporation	-17	-17	-16	-17
Runoff	58	63	63	69
Increase in soil moisture store	5	7	1	1
Catchment values:				
Modelled flow	81	86	88	94
Observed flow	96	96	96	96

Note that values for a single grid-cell within the catchment are converted to approximate catchment values by multiplying by the catchment area. This explains why the values of grid-cell runoff and river flow are different.

It is apparent that wet canopy evaporation results in a significant loss of water from MOSES even in winter months, leading to reduction in runoff and simulated river flow. The standard canopy heights in MOSES are shown in Table 8. The values for C3 and C4 grass seem large for the UK, particularly in the winter and an experimental set of adjusted canopy heights for the UK has been used to explore the effect of canopy height on runoff, as shown in column three of Table 8. The values for effective vegetation height used in MORECS are presented for comparison where applicable (Hough and Jones, 1997). The range of values indicates seasonal variation.

Table 8. Canopy heights for the five Plant Functional Types in MOSES.

	Canopy height (m)		
Plant Functional Type	Standard MOSES/Jules	Adjusted height	MORECS effective height
Broadleaf tree	25	10	2-10
Needleleaf tree	20	10	10
C4 grass	1	0.1	0.08-0.8 (for wheat)
C3 grass	1	0.1	0.15
Shrub	2	0.75	n/a

Column three in Table 7 shows the effect on the water balance of reducing the canopy height in this way. Canopy evaporation has been reduced by 20%, leading to an increase

in water entering the soil, and the modelled flow in the catchment has increased. However, the increase in runoff (and flow) is not as dramatic as might be expected because the additional water entering the soil is effectively being stored while it passes through the 3m soil column. The fourth column in Table 7 shows the effect of reducing the depth of the soil column from three to one metre in order to increase both surface runoff and the responsiveness of sub-surface flow. This change has also increased runoff for the specific grid-cell examined here, and modelled river flow has increased further. Reducing the depth of the soil stores has the effect of reducing the time taken for drainage from the soil to contribute to subsurface flow, and increasing the response of the catchment to rainfall. The final column shows the effect of both reducing the canopy height *and* the soil column depth. Implementing both changes has increased runoff-production the most, and improved the accuracy of flow simulation. The water reclaimed through reducing the canopy evaporation is no longer being stored in the soil column, and has further increased runoff and flow.

Figure 17 shows the effect that these changes to MOSES have had on the flow hydrographs. Reducing canopy height alone has not resulted in any improvement in model performance in terms of flows, but combined with a shorter soil column, has lead to improved simulation of flow peaks.

(a) Standard MOSES

(b) MOSES with reduced canopy height

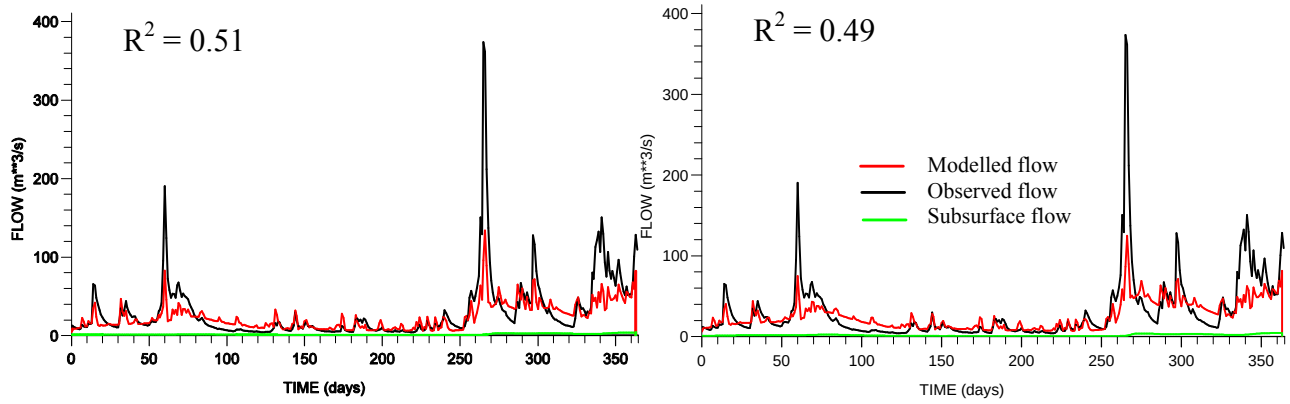

(c) MOSES with reduced soil depth

(d) MOSES with reduced canopy *and* soil depth

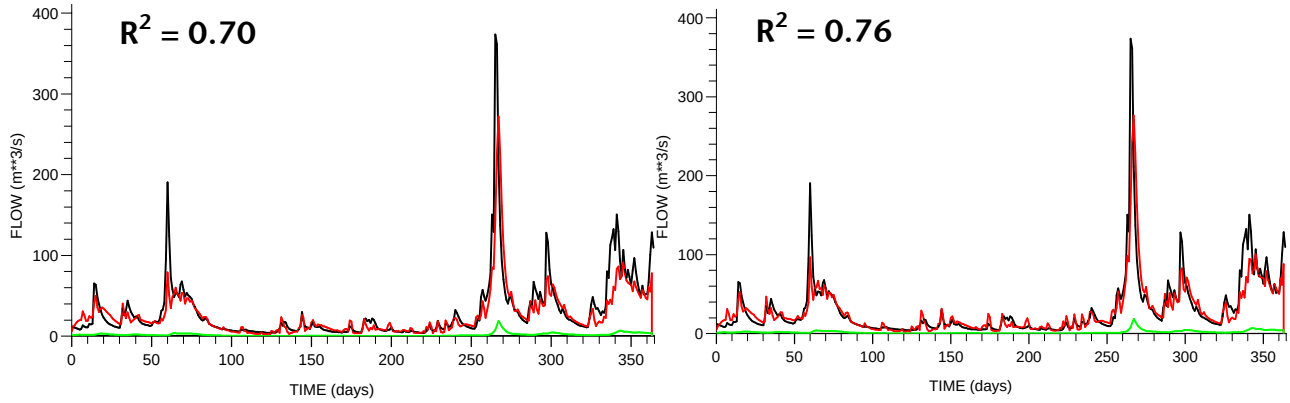

Figure 17. Hydrograph of observed and modelled flow for the Teifi at Glan Teifi for the period 25 January 1987 to 24 January 1988.

G2G model performance over a range of UK catchments is presented in Table 9 in terms of R^2 goodness-of-fit. The three model variants are as follows:

1. Standard MOSES, which has the default canopy height, a 3m soil layer, and PDM applied to the top 1m of soil.
2. MOSES, with a reduced canopy height, a 3m soil layer, and PDM applied to the top 1m of soil.
3. MOSES, with a reduced canopy height, a 1m soil layer, and PDM applied to the top 0.35m of soil

G2G model parameters are the same for each MOSES variant.

Best model performance of the three variants in Table 9 has been highlighted in bold for each catchment. The variant of MOSES with reduced canopy and reduced (1m) soil layer tends to perform better on the majority of catchments, but tends to exacerbate the already poor model performance in baseflow-dominated catchments such as the Mimram and the Lambourne in the Thames Basin. A range of hydrographs is presented in Figure 18

Table 9. R^2 values for model performance using raingauge rainfall observations.

Catchment	ID	UK Region	% error in area	1. Standard MOSES	2. MOSES with reduced canopy	3. MOSES with reduced canopy and reduced (1m) soil layer
1. Mole at Kinnersley Manor	39069	Thames	-10.6	0.26		**0.39**
2. Thames at Kingston	39001	Thames	0.06	**0.07**		-0.31
3. Derwent at Buttercrambe	27041	NE	-0.63	0.37	**0.38**	**0.38**
4. Wharfe at Flint Mill Weir	27002	NE	2.24	0.46	**0.47**	0.44
5. Colne at Lexden	37005	Anglia	-4.6	0.47		**0.53**
6. Mimram at Panshanger Pk	38003	Thames	0	**-148**		-207
7. Lambourne at Shaw	39019	Thames	1.28	**-20.1**		-29
10. Lt. Ouse at Abbey Heath	33034	Anglia	1.02	**-3.97**		-5.48
11. Yscir at Pontaryscir	56013	S.Wales	15.9	0.42	0.43	**0.62**
12. Cynon at Abercynon	57004	S.Wales	-35	0.27	0.27	**0.43**
13.Tawe at Ynystanglws	59001	S.Wales	16.2	0.35	0.37	**0.46**
14. Teifi at Glan Teifi	62001	W.Wales	-0.56	0.51	0.49	**0.76**
15. Lune at Caton	72004	NW	-0.41	0.46	0.47	**0.52**
16. Leven at Leven Bridge	25005	NE	7.14	0.49	0.50	**0.52**
21. Crimple at Burn Bridge	27051	NE	11.1	0.24	0.27	**0.33**
22. Blackwater at Swallowfield	39007	Thames	2.25	**-0.24**		-0.79
25. Taff at Pontypridd	57005	S. Wales	1.5	0.55	0.56	**0.65**

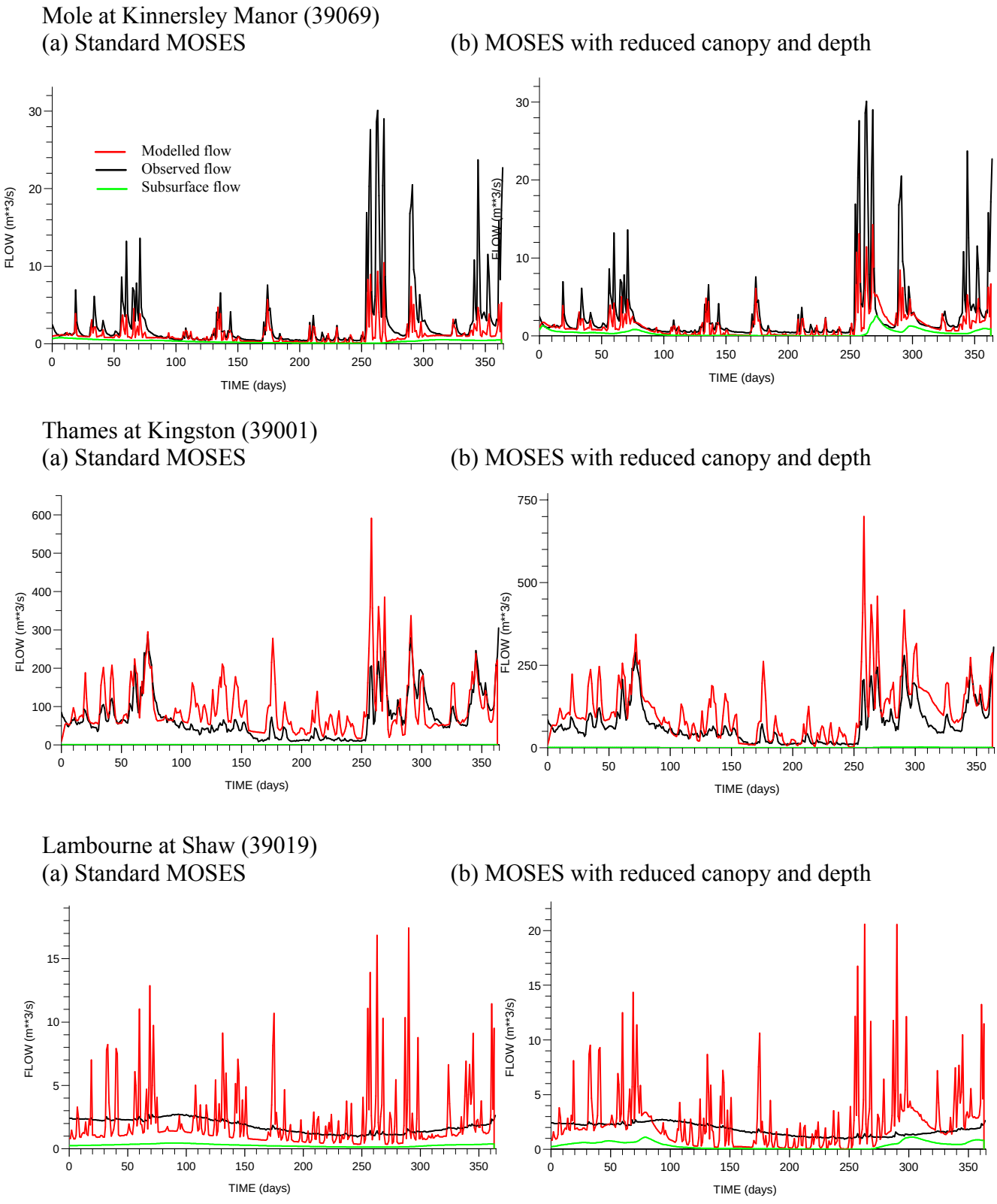

Figure 18. Hydrographs comparing observed and modelled flow using MOSES-G2G for three catchments in the Thames Basin (25 January 1987 to 24 January 1988).

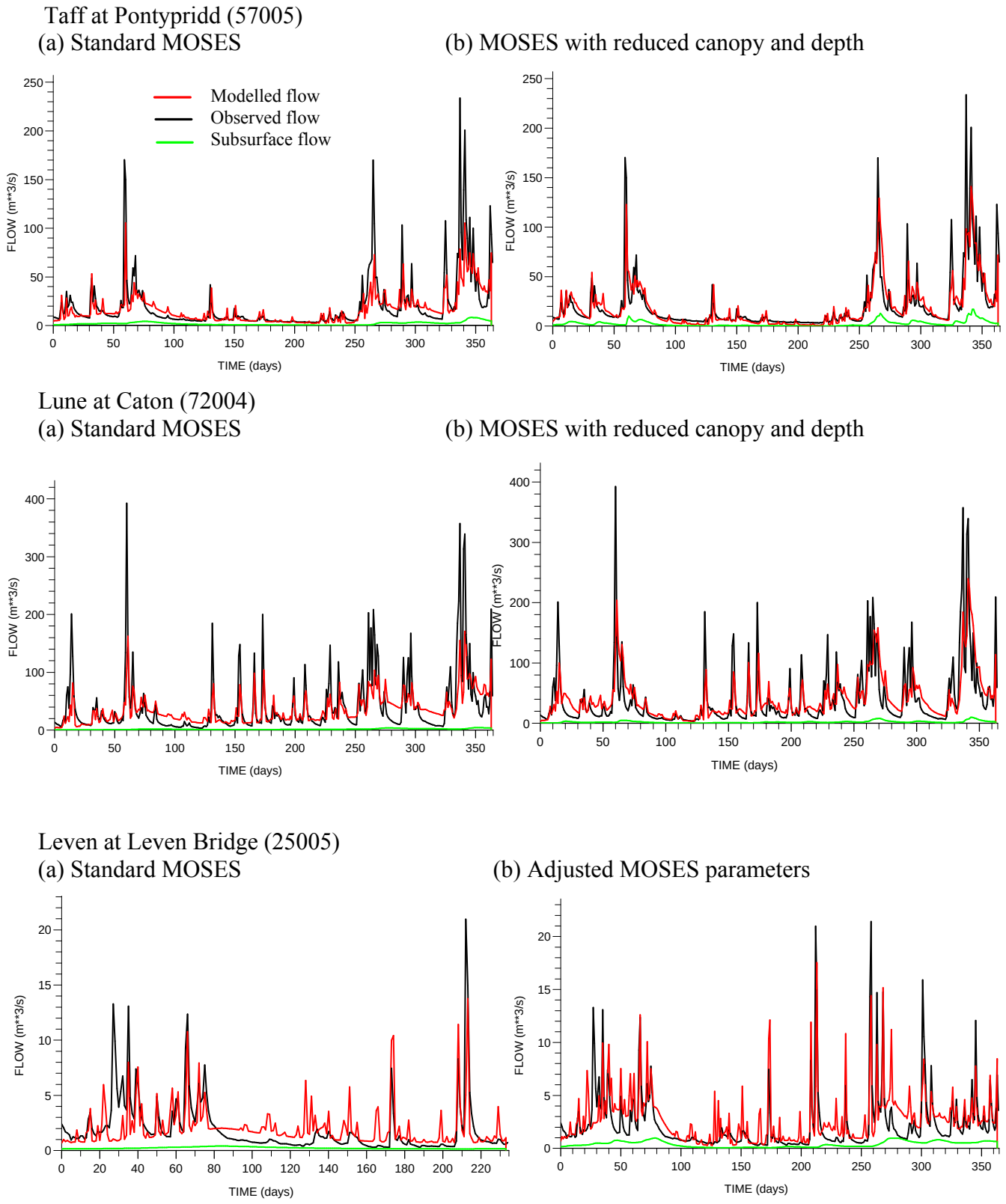

Figure 18 (continued). Hydrographs comparing observed and modelled flow using MOSES-G2G for three UK upland catchments (25 January 1987 to 24 January 1988).

3.2.2 Discussion of model performance

The results of this initial analysis indicate that MOSES-G2G performs best on responsive catchments without a significant groundwater component to the flow. Table 6 identifies catchments with a high groundwater component using the baseflow index, bfi, which is an index reflecting the ratio of baseflow to total streamflow. Catchments with a high baseflow index, such as the Mimram, the Lambourne and the Little Ouse, were particularly poorly modelled by all variants of MOSES. The analysis of modelled river flow arising from the Nimrod implementation of MOSES-G2G also indicated that baseflow-dominated catchments yielded poorer results (Bell and Moore, 2004). They concluded that this was due to overestimation of immediate surface runoff/flow arising from rainfall input to the catchment. The alternative MOSES formulation, LSH, models the height of the water table and its relation to local topography and may prove beneficial, particularly for groundwater dominated catchments. So far, only the PDM runoff production scheme has been invoked in the new combined model MOSES-G2G, but assessment of LSH with MOSES-G2G is planned.

In contrast to the Jules/MOSES-G2G flow simulation results presented here, the Nimrod implementation of MOSES-G2G did not indicate any obvious problems with underestimation of flow peaks arising from excessive canopy evaporation. The Nimrod implementation of MOSES differs from standard MOSES in that it includes some time variation of vegetation physiological characteristics such as Leaf Area Index (LAI), canopy height and root depth. Standard MOSES (and Jules) contains the option of using the TRIFFID global vegetation model (Cox, 2001), but this has not been invoked within Nimrod MOSES or Jules/MOSES-G2G. Instead, Nimrod MOSES has an additional vegetation type, "crop", whose physiological characteristics vary throughout the year in accordance to those assumed in MORECS for spring barley (Hough and Jones, 1997). The LAI of broad-leaf trees is also assumed to vary throughout the year, but all other vegetation types (grass, shrub and needle-leaf treas) are assumed to have a constant value of LAI, root depth and canopy height, again matching those in MOSES (Smith *et al.*, 2004). (The new 2km implementation of Nimrod-MOSES will have the LAI of all vegetation types determined by regular MODIS satellite observations. Root depth and canopy height of crops will be estimated based on the satellite-observed LAI.). Further investigation of vegetation models in MOSES is required, but it may prove beneficial to consider implementation of a simple time-varying vegetation module in the Jules/MOSES-G2G.

The improvement in MOSES-G2G results arising from the use of a truncated soil column (reduced from 3m to 1m) was particularly evident in the more upland Welsh catchments, where soils are generally more shallow than in other parts of Britain. A spatially varying value for soil column depth and PDM-depth in MOSES-G2G is being considered.

Discussions with the Jules team have indicated that if Jules is given a "spin-up" period, then the water stored within the MOSES soil column will stabilise and storage within the soil column will be less influential on runoff and flow simulation.

3.2.3 Comparison of observed and modelled flow hydrographs using ERA-driven RCM rainfall data

At the UK scale initial tests on MOSES-G2G have used RCM variables to drive the evapo-transpiration component of MOSES, with 5km daily gridded raingauge observations providing the rainfall input. This section provides a preliminary assessment of how use of ERA-40 driven 25km RCM rainfall affects MOSES-G2G model performance. The catchment used in the comparison is the Teifi at Glan Teifi, for which reasonably good estimates of river flow were obtained using gridded raingauge observations. Table 10 presents R^2 model performance comparing observed and modelled river flow from MOSES-G2G for the period 25 January 1987 to 24 January 1988 using two sources of rainfall estimate.

Table 10. R^2 model performance comparing observed and modelled river flow for the Teifi

		Source of rainfall	
Catchment	**ID**	**Raingauge**	**RCM**
Teifi at Glan Teifi	62001	0.76	0.45

The reduction in performance from the use of RCM rainfall in place of observations is to be expected. Figure 19 shows the effect of rainfall source on flow hydrographs for the Teifi catchment. The main flow peak of the year (day 270) has been underestimated using RCM rainfall, while the later winter peaks have been slightly overestimated. The timing of the large-scale rainfall as modelled by the RCM appears to be reasonably accurate.

Further work will assess MOSES-G2G performance using RCM rainfall for a range of catchments across England and Wales.

(a) Raingauge rainfall (b) RCM rainfall

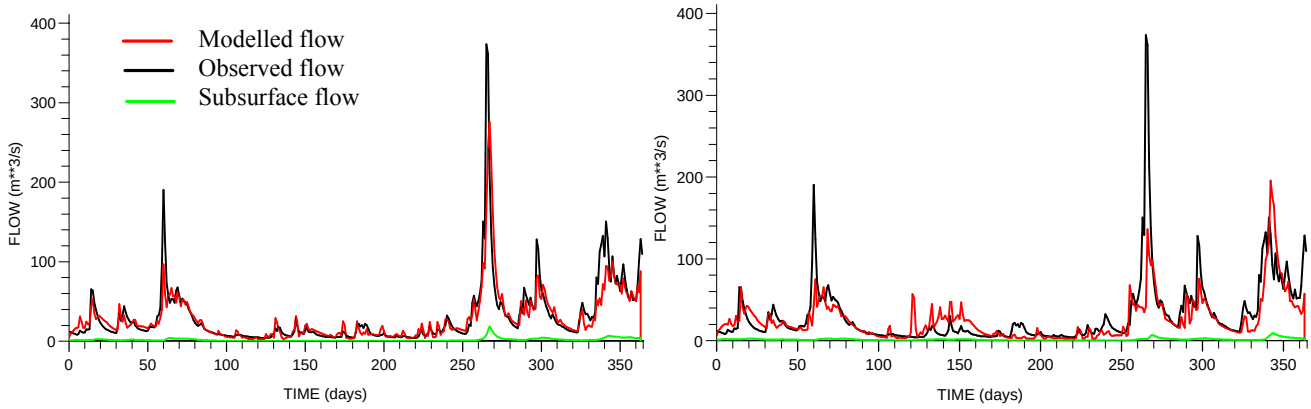

Figure 19. Model hydrographs comparing observed and modelled flow using two sources of rainfall estimate for a year from 25 January 1987: Teifi catchment (62001).

SUMMARY AND FURTHER WORK

An initial system to predict changes in flooding for the UK and Europe has already been developed. This system provides a grid-based methodology for translating RCM meteorological variables, such as rainfall and potential evaporation, into estimates of river flow and fluvial input to the sea. The new model, the Grid-to-Grid model or 'G2G', has already been tested off-line from the RCM, and evaluated for individual catchments in the UK alongside a catchment-based hydrological model, the parameter-generalised PDM.

Within the RCM the Grid-to-Grid flow routing model functions to route the gridded runoff estimates produced by the MOSES-PDM land-surface scheme. However, because recent versions of MOSES have not yet been used in RCM experiments, an interim runoff-production scheme was initially used to allow development of the routing model to be progressed. It has now been possible to run the MOSES-PDM scheme off-line to generate runoff, as a replacement for the interim runoff-production scheme. This has been achieved by developing a standalone version of the MOSES in the form of Joint UK Land Exchange Scheme (Jules) coupled with the G2G routing model.

The new coupled model is currently being evaluated at two scales (a) on the North West European RCM grid, with both MOSES and the G2G run at a 25km resolution, and (b) for the UK, where MOSES is being run at a 5km resolution with 1km G2G routing.

a) At the European scale, the model predicts daily river flows with an average error of 30% over the 17 year period where observations are available, but with substantially higher errors in some catchments (up to 67%) where anthropogenic abstractions of water may significantly alter the water balance. The exact nature of flood hydrographs is less consistently reproduced, primarily as a result of differences in catchment hydrological characteristics that are not resolved in the model at its current spatial scale. Suggestions for further work to achieve more realistic flood hydrographs include improving the model's treatment of soil hydrology and exploring different methods of runoff production.
b) At the UK scale the initial assessment of model performance indicates that MOSES-G2G performs best on responsive catchments without a significant groundwater component to the flow. Tests also indicate the importance of correctly estimating evaporation from the vegetation canopy. It may prove beneficial to consider implementation of a simple time-varying vegetation module in the Jules/MOSES-G2G. The improvement in MOSES-G2G results arising from the use of a less deep soil column (reduced from 3m to 1m) was particularly evident in the more upland Welsh catchments, where soils are generally more shallow than in other parts of Britain. A spatially varying parameter for soil column depth in MOSES-G2G is being considered.

An assessment of model performance at the two spatial scales may provide insight into different aspects of area-wide flow modelling. The larger European catchments are likely to exhibit greater spatial variation in soil and topography, and will perhaps require particular attention to be paid to the effect of spatial variability on runoff-production and routing over long distances. At the UK scale, catchments tend to be smaller, often quickly responding, while still varying considerably in soils and topography. The detailed spatial and observational datasets currently available for the

UK enable a more detailed analysis of model performance to take place, which should prove beneficial to modelling at both spatial scales.

New flow directions have been developed for the G2G at both spatial scales, and have lead to improved accuracy in catchment delineation, thereby reducing errors in modelled river flow arising from incorrect estimation of the area draining to a river.

Previous work has compared the use of ERA-15–driven RCM and observed rainfall as input to hydrological models for simulating river flows. The availability this year of ERA-40-driven RCM data, for 1961-2001, meant that an extended comparison has been possible using the PDM catchment-based hydrological model, for a period including the Autumn 2000 floods in the UK. This analysis is presented in Kay (2006).

The process-based nature of the hydrological models employed here, and used in conjunction with RCM output, will also facilitate investigation into model quality and uncertainty. It should be possible to determine whether the underlying assumptions of a hydrological model are reliable under climate change, and therefore whether the model response to different scenarios can be trusted. This year, the influence of model structure and calibration on the uncertainty in the impact of climate change on flooding has been analysed. A draft report has been produced and a final version will be released in March 2006.

REFERENCES

Bell, V.A., Davies, H. N., Dadson, S. J., Kay, A.L. and Clark, D. B., 2005. River Flow Modelling for Regional Climate Models: Progress Report to the Met Office (Hadley Centre). CEH Wallingford, 38pp.

Bell, V.A., Jones R.G. and Moore R.J., 2003. *Development of a flow routing model coupled to a Regional Climate Model for Europe: Preliminary formulation and results*. Report to the Met Office Hadley Centre, 42pp.

Bell, V.A., Kay, A.L., Jones, R.G. and Moore, R.J., 2004a. Simulation of observed river flows for 1960-2000. *Report to the UK Department for Environment, Food and Rural Affairs, Milestone 03/04 15.06.03,* Met Office Hadley Centre, January 2004, 39pp.

Bell, V.A., Kay, A.L., Jones, R.G. and Moore, R.J., 2004b. *Flow Routing for Regional Climate Models: UK application*. Report to the Met Office Hadley Centre, CEH Wallingford, 125pp.

Bell, V.A. and Moore, R.J., 1998. A grid-based distributed flood forecasting model for use with weather radar data: Part 1: Formulation. *Hydrology and Earth System Sciences*, **2(2-3),** 265-281.

Bell V.A. and Moore R.J., 2004c. *A flow routing and flood inundation facility for Nimrod/CMetS.* Report to the Met Office, CEH Wallingford, 56pp.

Bell, V.A., Kay, A.L., Jones, R.G. and Moore, R.J., 2006. Development of a high resolution grid-based river flow model for use with regional climate model output. *Hydrology and Earth System Sciences*, (in press).

Blyth, E., 2002. Modelling soil moisture for a grassland and woodland site in south-east England. *Hydrol. Earth System Sci*., **6(1)**, 39-47.

Clapp, R. and G. Hornberger, 1978. Empirical equations for some soil hydraulic properties. *Water Resour. Res.,* **14**, 601-604.

Cox, P.M., Betts, R.A., Bunton C.B., Essery, R.M., Rowntree, P.R. and Smith, J.,1999. The impact of new land surface physics on the GCM simulation of climate and climate sensitivity. *Climate Dynamics*, **15,** 183-203.

Cox, P.M. 2001. *Description of the "TRIFFID" Dynamic Global Vegetation Model*. Hadley Centre Technical Note 24. Hadley Centre, Met Office, Exeter, UK, 16pp.

Davies, H. N. and Bell, V. A., 2005. Investigation of new methods for improving DTM-derived river networks. Report to the Met Office (Hadley Centre), CEH Wallingford, 11pp.

Fekete, B. M., Vorosmarty, C. J. and Lammers, R. B., 2001. Scaling gridded river networks for macroscale hydrology: Development, analysis and control of error. *Water Resources Research*, **37(7),** 1955-1967.

Gedney, N. and Cox, P.M., 2003. The sensitivity of global climate model simulations to the representation of soil moisture heterogeneity. *Journal of Hydrometeorology*, **4(6),** 1265-1275.

Hough, M.N. and Jones R.J.A., 1997. The United Kingdom Meteorological Office rainfall and evaporation calculation system: MORECS version 2.0 - and overview. *Hydrology and Earth System Science*, **1**, 227-239.

Kay, A.L., 2006. Catchment modelling with data from an RCM driven by ERA-40 boundary conditions. *Report to the Met Office Hadley Centre, CEH-Wallingford*, 27pp.

Kay, A.L., Reynard, N.S. and Jones, R.G., 2006a. RCM rainfall for UK flood frequency estimation. I. Method and validation. *Journal of Hydrology*, **318**, 151-162.

Kay, A.L., Jones, R.G. and Reynard, N.S., 2006b. RCM rainfall for UK flood frequency estimation. II. Climate change results. *Journal of Hydrology*, **318**, 163-172.

Kay, A.L., Bell, V.A., Jones, R.G. and Moore, R.J., 2004. Assessment of the Autumn 2000 floods in the context of the precipitation record from 1958 to present. *Report to the UK Department for Environment, Food and Rural Affairs, Milestone 03/04 15.07.03,* Met Office Hadley Centre, March 2004, 14pp.

Kay, A.L., 2003. Estimation of UK flood frequencies using RCM rainfall: A further investigation. *Report to the UK Department for Environment, Food and Rural Affairs, Hadley Centre Annex15a,* CEH Wallingford, March 2003, 48pp.

Moore, R.J., 1985. The probability-distributed principle and runoff production at point and basin scales. *Hydrol. Sci. J.*, **30(2)**, 273-297.

Moore, R.J., 1999. Real-time flood forecasting systems: Perspectives and prospects. In: R. Casale and C. Margottini (eds.), *Floods and landslides: Integrated Risk Assessment*, Chapter 11, 147-189, Springer.

Morris D.G. and Flavin R.W., 1990. A Digital Terrain Model for Hydrology. *Proc 4th International Symposium on Spatial Data Handling. Zurich*, 1; 250-262.

Olivera F. and Raina, R. 2003. Development of large scale gridded river networks from vector stream data. Journal of the American Water Resources Association. October, 1235-1248.

Olivera, F., Lear M. S., Famiglietta, J. S. and Asante, K., 2002. Extracting low-resolution river networks from high-resolution digital elevation models. *Water Resources Research,* **38(11),** 1-8.

Reed, S., 2003. Deriving Flow Directions for Coarse Resolution (1 - 4 km) gridded hydrologic modelling. *Water Resources Research*, **39(9),** 1238-1248.

Smith, R.N.B., Blyth, E.M., Finch J.W., Goodchild, S., Hall, R.L. and Madry, S., 2004. Soil state and surface hydrology diagnosis based on MOSES in the Met Office Nimrod

nowcasting system. *Forecasting Research Technical Report No. 428*. Met Office, Exeter, UK, 35pp.

U.S. Geological Survey 1998. *HYDRO 1K: Elevation derivative database*, http://edcwww.cr.usgs.gov/landdaac/gtopo30/hydro/index.html, USGS EROS data Centre, Sioux Falls, S.D.

Part 2: Modelling recent flow history in selected UK catchments

INTRODUCTION

Following a number of flood events in recent years, there has been increasing speculation about whether such events are a consequence of climate change and whether flooding will thus increase in magnitude and frequency in the future. This project is investigating the use of outputs from Regional Climate Models (RCMs) to drive hydrological models, simulating river flows either on a catchment scale (Kay *et al.* 2003, Kay 2003) or on a grid (Bell *et al.* 2003, 2004). Using RCM data from Current and Future time-slices can thus help to address the issue of the potential impact of climate change on flooding. However, an important part of this work is an investigation of the validity of using RCM outputs in this way, particularly in terms of rainfall series generated by the RCM. This validation has been approached by the use of re-analysis data to drive the RCM.

Re-analysis data

European re-analysis (ERA) data are produced by the European Centre for Medium-range Weather Forecasting (ECMWF), from re-analysis runs of their global model. Climate observations are used in the re-analyses, so use of ERA data to drive the RCM at its boundaries (rather than nesting it in a Global Climate Model) means that the simulated (large-scale) rainfall from the ERA-driven RCM should fit more closely (time-wise) with observed rainfall for the same period. This enables a comparison of the use of RCM data and observed data as input to hydrological models.

An initial comparison used ERA-15 data for the UK, available for the 15 years 1979-1993. The results of this were promising (Kay 2003, Bell *et al.* 2004). However, the more recent availability of ERA-40 data, for 1961-2001, meant that an extended validation was possible, including for the Autumn/Winter 2000 floods in the UK. Although the ERA-40 data are available for 1961 onwards, they have currently only been used to drive the RCM for 1985 onwards as this is the period concurrent with the observed data for the majority of the study catchments. Thus the subject of this report is the use of data from an RCM (PRECIS) driven with ERA-40 data for the period 1985-2001.

Report focus

Two different hydrological models are currently being applied within this project. These are

- a gridded model, the Grid-to-Grid (or G2G) (Bell *et al.* 2003, 2004, 2005, 2006), which is being developed for use within the Hadley Centre Regional Climate Model (RCM), as well as for offline work covering Europe (25 km grid) or the UK (1 km grid), and

- the catchment PDM (Kay *et al.* 2003, Kay 2003, Kay *et al.* 2006a,b), which is being used solely offline and helping to validate the G2G model (Bell *et al.* 2004).

This report is solely concerned with the latter of these two models, the catchment PDM, which is described briefly below. The focus is on estimation of flood frequency (Section 2), but there is some discussion of flow simulation, particularly for the period of the Autumn/Winter 2000 floods (Section 3). Conclusions are given in Section 4. A later report will describe the use of the re-analysis data with the gridded model.

The catchment PDM

The PDM (Probability Distributed Model) of Moore (1985, 1999) is a catchment model typical of the relatively simple model structures that nevertheless can be applied effectively across the UK. It is based on conceptual stores, and attempts to represent non-linearity in the transformation from rainfall to runoff by using a probability distribution of soil moisture storage. This determines the time-varying proportion of the catchment that contributes to runoff, through either 'fast' or 'slow' pathways.

In order to be able to apply the model for any catchment in the UK, where calibration data may be unavailable, it is necessary to be able to estimate model parameters from catchment properties. A prototype generalisation of the PDM was achieved in previous research for Defra (Calver *et al.* 2001), where it was found that using simpler model structures (with fewer parameters) held an advantage for generalisation. This generalisation was applied in initial work using the PDM for this project (Kay *et al.* 2003, Kay 2003). Here, more use will be made of calibrated parameter sets. The calibrations were based on the full length of data available for each catchment, which is more than that used here in a small number of cases.

The model as configured for this project requires input time-series of catchment average rainfall and potential evaporation (PE) at an hourly time-step. These catchment averaged data have to be produced from the gridded RCM data. For PE, simple area-weightings were used (after calculating the grid-box PE using Penman-Monteith). For rainfall, an additional SAAR-weighting was used, to account for the greater spatial variability of rainfall due to topography. See Kay *et al.* (2003) for more detail.

Catchments modelled

Fifteen catchments were modelled previously (Kay *et al.* 2003). An extra catchment has been included here, located in western Scotland (catchment number 90003). This improves the spatial coverage of the set of catchments (Figure 0.1), in particular improving the possibility of indicating rain-shadow effects, and was only recently possible, after a further data collection for another project. Details of the 16 catchments are given in Table 0.1, including the full period of data available for their calibration. The modelling in this report is for the period of overlap between the period of observed data, in the table, with the currently available period of the ERA-40-driven RCM data (1985-2001). This is the whole period 1985-2001 for most catchments, but is slightly truncated at the start for three catchments.

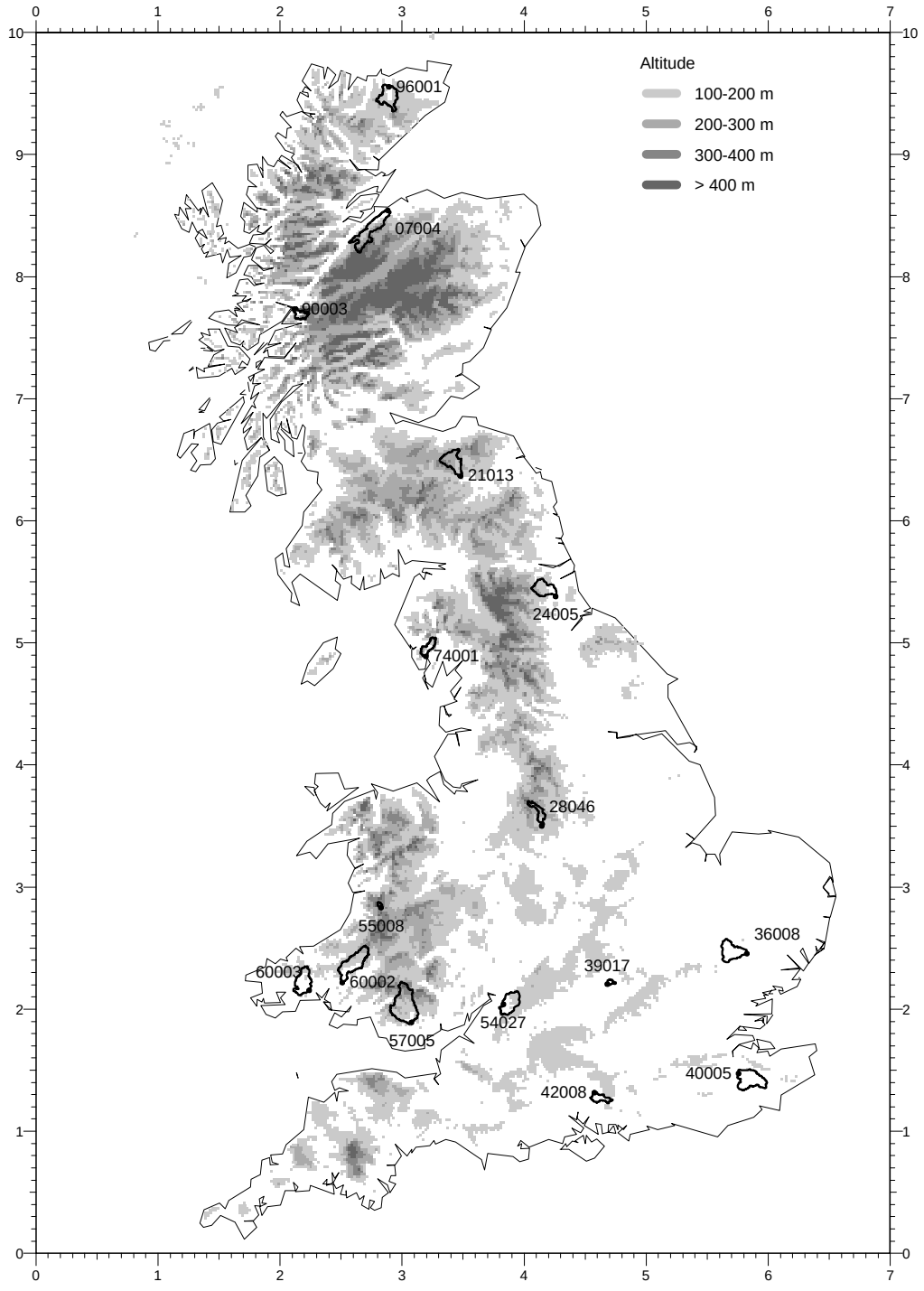

Figure 0.1 Map illustrating the locations and boundaries of the 16 catchments, and the altitude of the surrounding topography.

Table 0.1 Summary of the 16 catchments modelled.

Catchment number	River name	Station name	Period of observed data	Catchment area (km^2)
07004	Nairn	Firhall	1985-2001	313.0
21013	Gala Water	Galashiels	1986-2001	207.0
24005	Browney	Burn Hall	1982-2001	178.5
28046	Dove	Izaak Walton	1985-2001	83.0
36008	Stour	Westmill	1985-2001	224.5
39017	Ray	Grendon Underwood	1987-2001	18.8
40005	Beult	Stile Bridge	1985-2001	277.1
42008	Cheriton Stream	Sewards Bridge	1985-2001	75.1
54027	Frome	Ebley Mill	1985-2001	198.0
55008	Wye	Cefn Brwyn	1969-2001	10.6
57005	Taff	Pontypridd	1985-2001	454.8
60002	Cothi	Felin Mynachdy	1985-2001	297.8
60003	Taf	Clog-y-Fran	1985-2001	217.3
74001	Duddon	Duddon Hall	1985-2001	85.7
90003	Nevis	Claggan	1993-2001	76.8
96001	Halladale	Halladale	1985-2001	204.6

FLOOD FREQUENCY RESULTS

Flood frequency using RCM rainfall

The flood frequency results using all 16 study catchments are presented in Figure 0.1. These show very consistent under-estimation of flood frequency when RCM data are used as input to the rainfall-runoff model, in place of observed data; only one catchment (36008) shows any significant over-estimation when RCM data are used, with 13 catchments showing significant under-estimation.

Note that this work has been undertaken with calibrated parameter values for the rainfall-runoff model, rather than the prototype generalised values used for the original work, in order to demonstrate a truer picture of the effect of rainfall errors without the effect of generalisation errors. The errors using generalised parameter values with the new rainfall inputs are not precisely the same as those presented here for calibrated values, but the direction of the error is the same in every case, and the relative sizes of errors, both between catchments and between return periods, are similar, as shown in Table 0.1.

Table 0.1 Percentage errors in flood peaks simulated using ERA-driven RCM data compared to observed data, at given return periods. Errors using calibrated parameter sets and generalised parameter sets are given.

catchment number	calibrated parameters				generalised parameters			
	Return period (years)				return period (years)			
	2	5	10	20	2	5	10	20
07004	-48.4	-48.9	-49.0	-49.0	-63.4	-65.9	-68.3	-70.7
21013	-31.9	-36.0	-39.0	-42.0	-38.0	-39.9	-40.3	-40.2
24005	-29.2	-30.5	-31.8	-33.3	-36.3	-36.6	-35.8	-34.3
28046	6.7	4.6	2.7	0.6	12.6	9.0	6.0	2.8
36008	25.1	24.9	25.1	25.4	29.1	31.7	33.6	35.3
39017	-20.8	-28.0	-33.9	-39.9	-13.1	-20.8	-27.8	-35.2
40005	-41.9	-42.0	-41.6	-40.8	-27.3	-34.4	-39.7	-44.9
42008	-23.8	-26.3	-28.7	-31.5	-21.4	-22.9	-24.2	-25.5
54027	-14.0	-14.4	-13.3	-11.4	-9.6	-9.5	-8.2	-6.1
55008	-15.8	-17.7	-18.9	-19.8	-18.1	-18.4	-18.3	-18.1
57005	-44.8	-42.0	-39.6	-37.0	-52.5	-50.5	-48.4	-46.0
60002	-20.5	-22.6	-25.0	-27.8	-26.5	-27.2	-26.9	-26.1
60003	-24.2	-23.4	-21.7	-19.2	-24.8	-23.5	-21.7	-19.4
74001	-22.9	-26.3	-29.2	-32.3	-20.3	-27.2	-32.7	-38.0
90003	-23.1	-25.3	-27.0	-28.7	-16.9	-15.8	-15.0	-14.3
96001	-7.8	-7.9	-7.9	-7.9	-16.3	-22.0	-26.8	-31.7

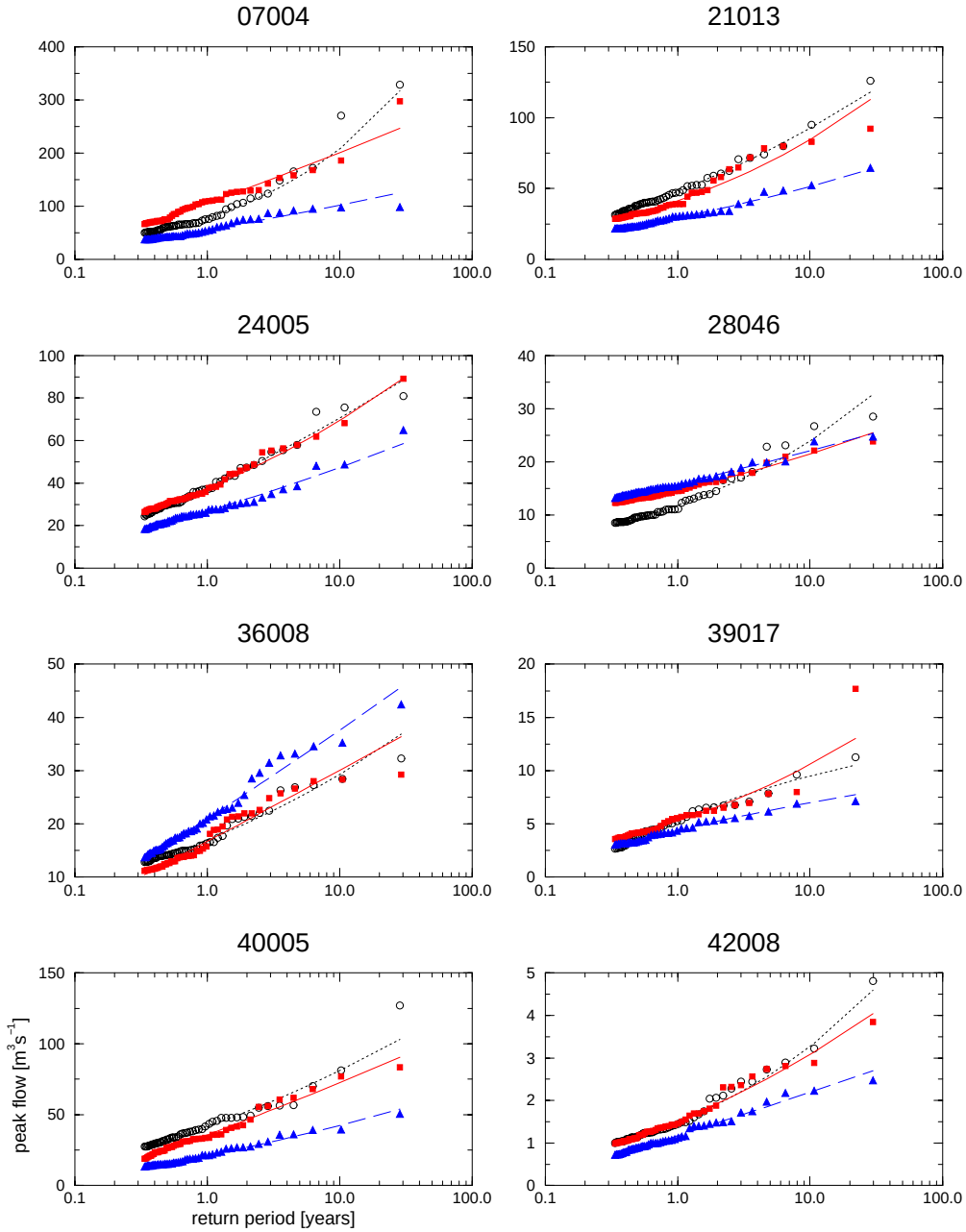

Figure 0.1 Simulated flood frequencies for the study catchments. Results using ERA-40-driven RCM data (blue, filled triangles and dashed line) are compared to those using observed data (red, filled squares and solid line). The flood frequencies derived from observed flows, 1985-2001, (black, open circles and dotted line) are also shown. (Figure continued on following page).

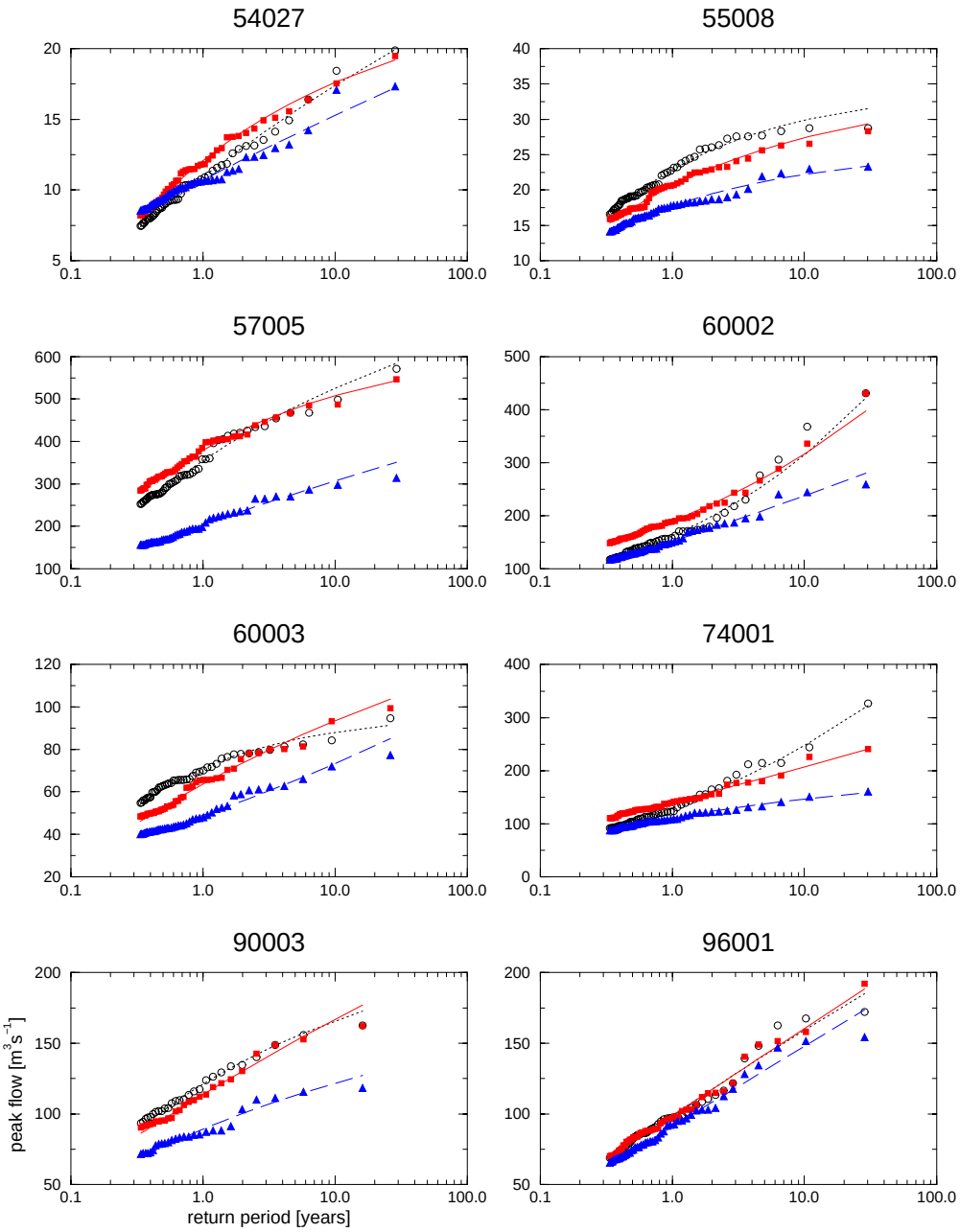

Figure 0.1 (continued).

In the original work, with ERA-15 data (Kay *et al.* 2003), there was more over-estimation of flood frequency with RCM rainfall, particularly in catchments on the western side of the country, with general under-estimation in catchments on the eastern side of the country. This suggested the possibility of an enhanced rain-shadow effect within the RCM. This possibility is not clear here (Figure 0.2), as all of the catchments on the western side of the country show under-estimation.

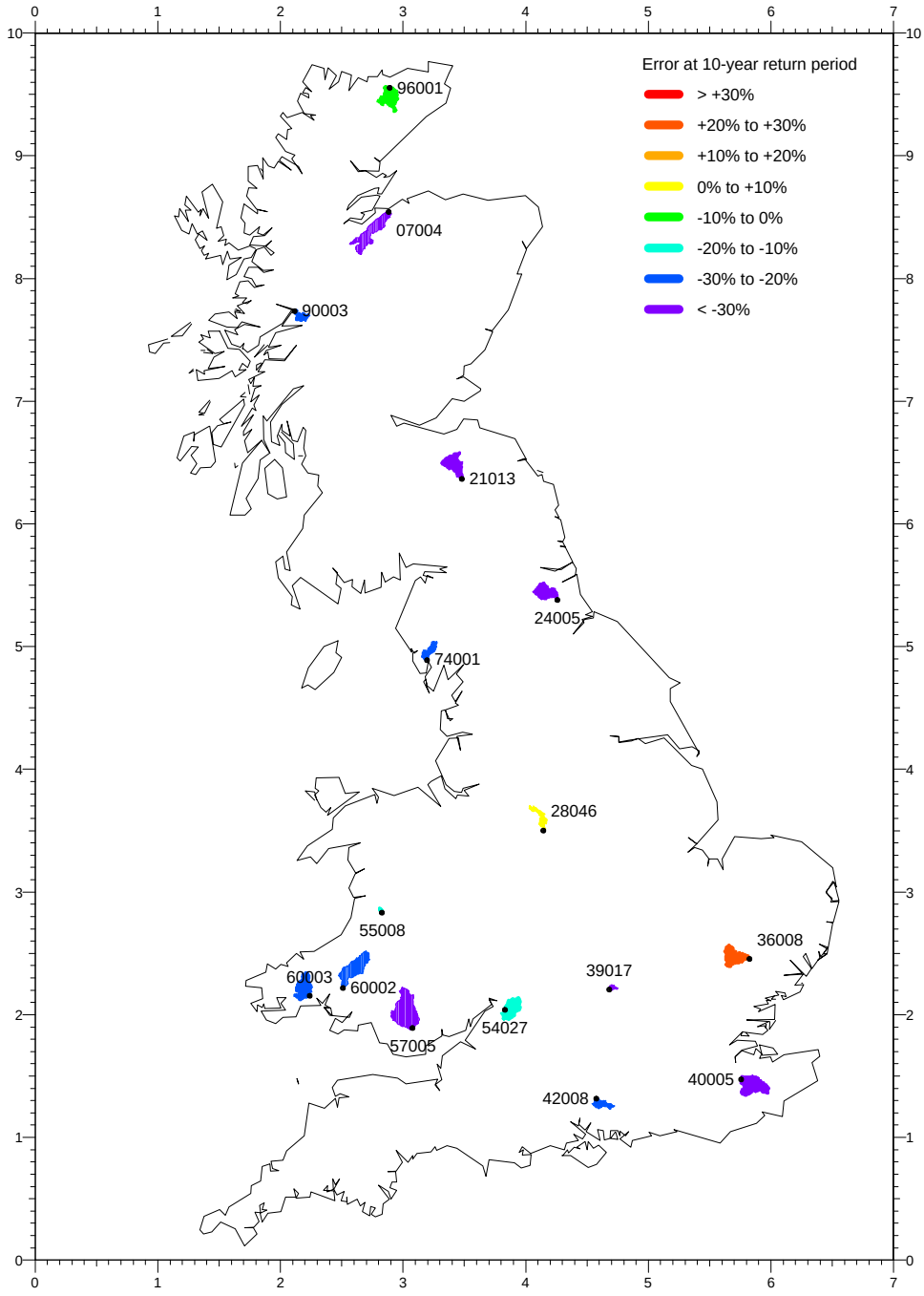

Figure 0.2 Map showing the percentage error in flood frequency at the 10-year return period for each of the study catchments.

Also in the original work, a strong link was shown between errors in flood frequency and errors in annual average rainfall (AAR) (R^2 = 0.86 at the 1-year return period). Although less of a relationship is shown in this case (R^2 = 0.68 at the 1-year return period; Figure 0.3), it still suggests that correcting the error in AAR for each catchment may lead to improvements in simulated flood frequencies. (This is the subject of the next section.) There is also weak evidence of a relationship between catchment area and errors in flood frequency (at least at lower return periods; R^2 = 0.18 at the 1-year return period) or errors in AAR (R^2 = 0.33), as shown in the original work. These relationships have negative gradients, meaning that larger catchments seem more likely to under-estimate AAR and so under-estimate flood frequency. This is probably due to the effect of cumulative errors in rainfall when spatially integrated over catchments.

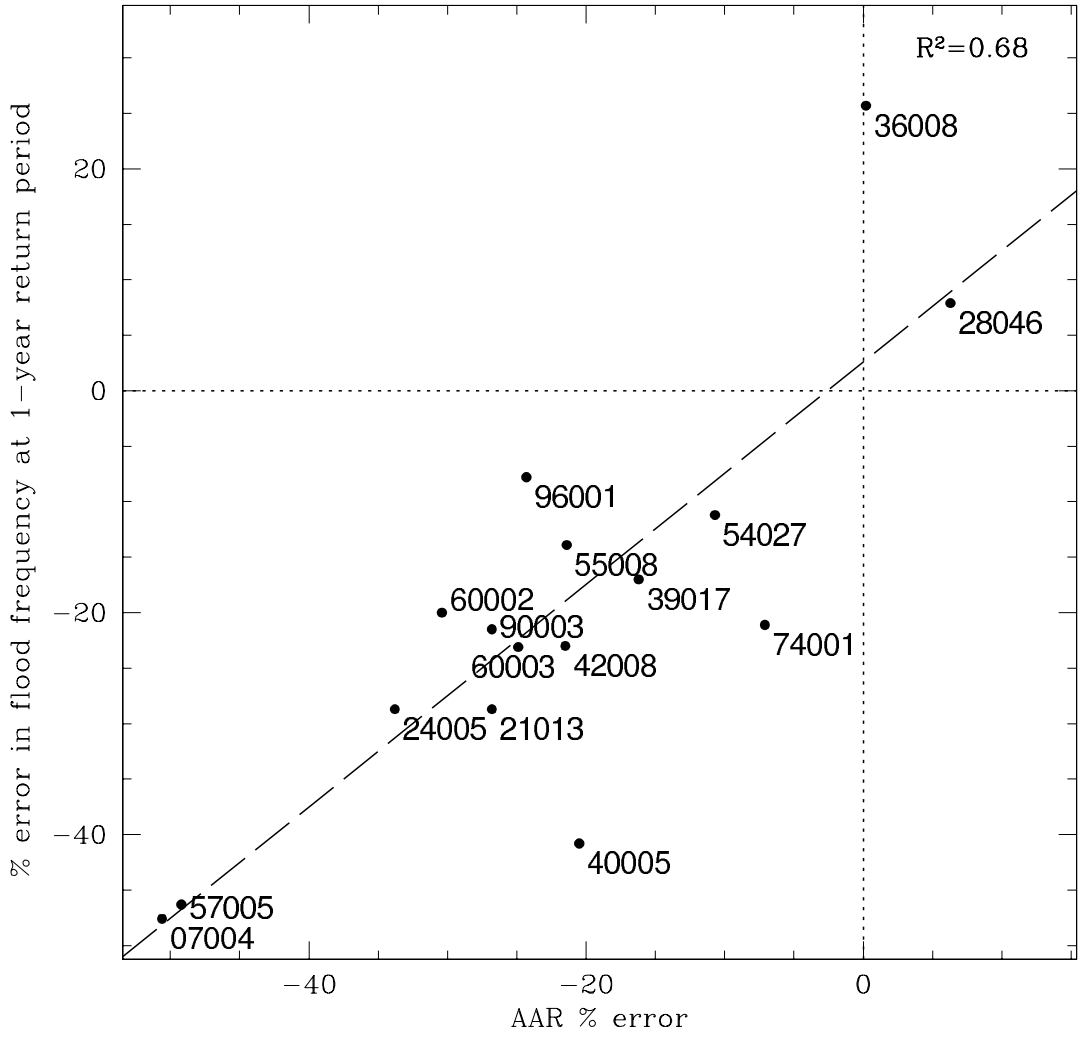

Figure 0.3 Graph showing the relationship between the percentage errors in AAR and the percentage errors in flood frequency at the 1-year return period.

Adjusting RCM rainfall

The errors in catchment AAR from the ERA-driven RCM rainfall data are shown in Table 0.2. It was decided to try correcting for errors in mean rainfall totals by multiplying the time-series of catchment rainfall derived from the RCM data by the ratio observed AAR / RCM AAR for each catchment (last column in Table 0.2). It should be noted that the value of this ratio will depend to some extent on the period over which the AARs are calculated; here the whole period of concurrent observed and RCM data has been used. (The spatial variability of this ratio over Britain is shown in Figure 0.7, based on a dataset of daily rainfall on a 5km grid.) The results using this correction for mean bias are shown in Figure 0.4.

Table 0.2 A comparison of the catchment annual average rainfall (AAR) derived from ERA-driven RCM data to that derived from observed data (1985-2001).

catchment number	catchment $SAAR_{61-90}$ (mm)	observed catchment AAR (mm)	ERA-driven RCM catchment AAR (mm)	AAR % error (RCM to observed)	obs' AAR/ RCM AAR
07004	942	1076	531	-51	2.02
21013	929	990	725	-27	1.37
24005	743	750	497	-34	1.51
28046	1098	1114	1184	6	0.94
36008	589	618	619	0	1.00
39017	622	652	546	-16	1.19
40005	691	722	574	-21	1.26
42008	885	939	737	-22	1.27
54027	827	873	780	-11	1.12
55008	2458	2602	2045	-21	1.27
57005	1832	1997	1015	-49	1.97
60002	1551	1726	1202	-30	1.44
60003	1420	1438	1080	-25	1.33
74001	2265	2285	2122	-7	1.08
90003	2913	2870	2099	-27	1.37
96001	1096	1118	846	-24	1.32

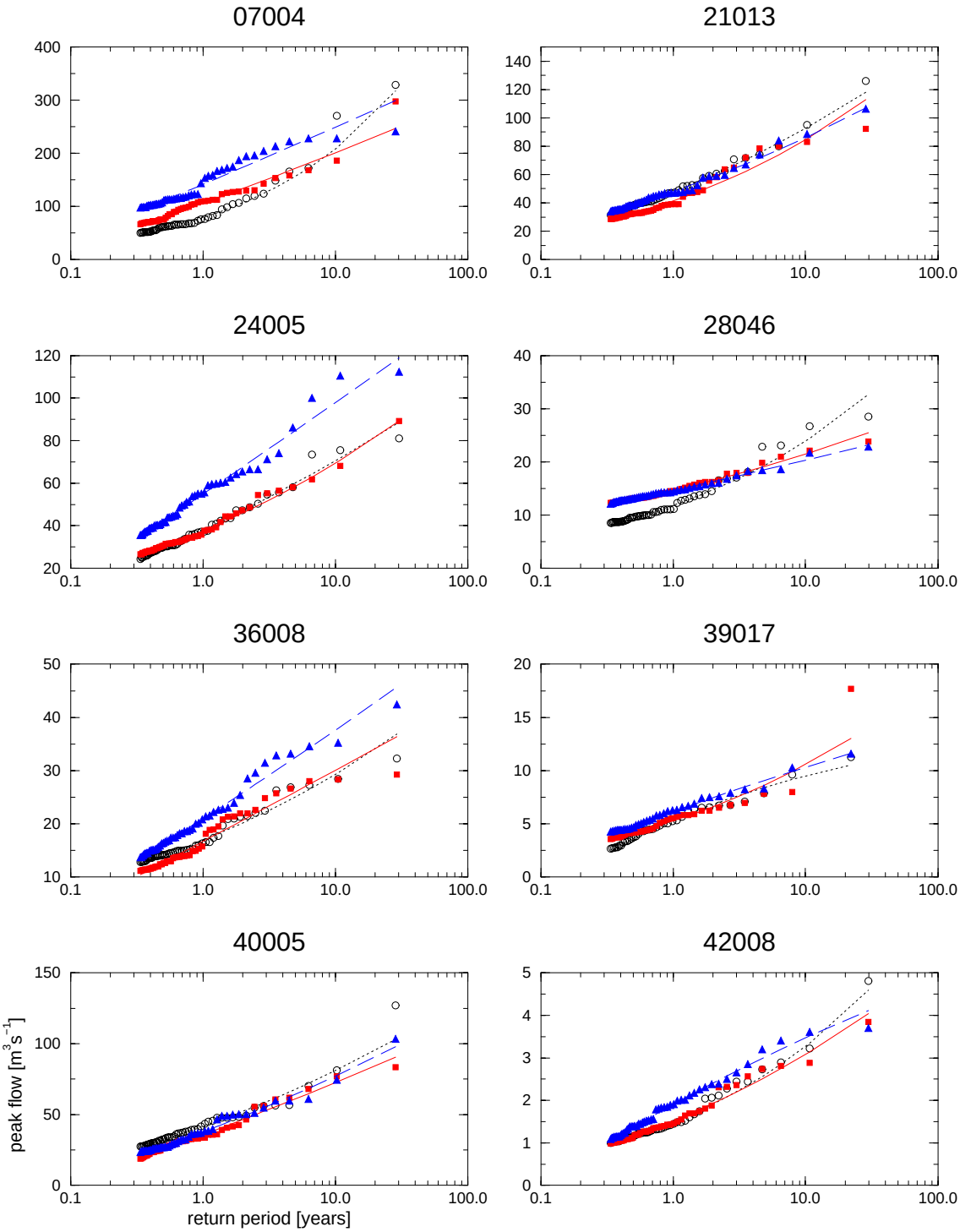

Figure 0.4 Simulated flood frequencies for the study catchments, after correction for mean bias in RCM rainfall. Results using adjusted ERA-40-driven RCM data (blue, filled triangles and dashed line) are compared to those using observed data (red, filled squares and solid line). The flood frequencies derived from observed flows, 1985-2001, (black, open circles and dotted line) are also shown. (Figure continued on following page).

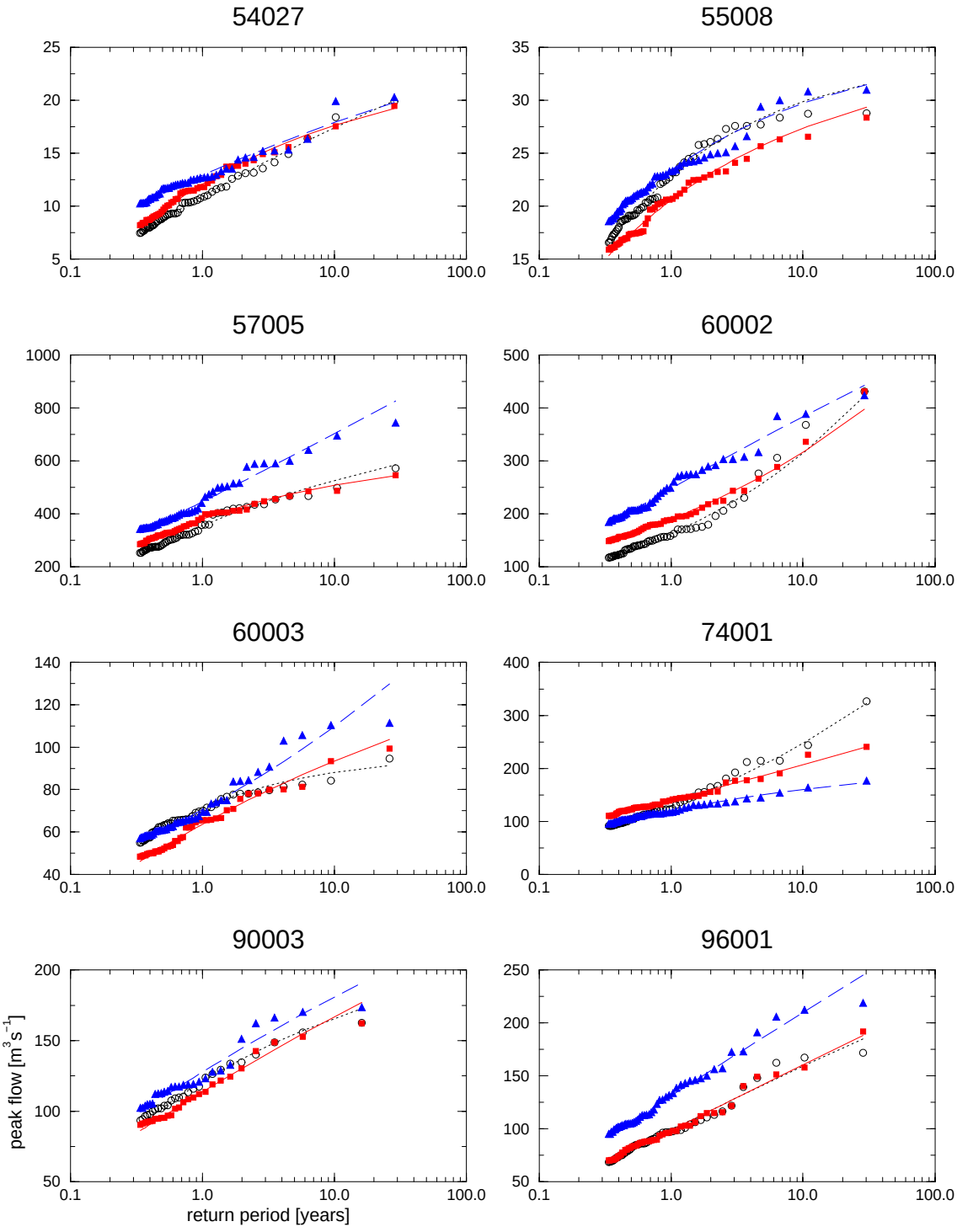

Figure 0.4 (continued).

Applying this simple catchment-specific correction factor to rainfall time-series has led to a significant improvement in simulated flood frequencies for many catchments (Table 0.3 and Figure 0.5), but has made the performance worse for a small number, including those for which performance was acceptable with the original rainfall time-series (28046 and 96001). For some catchments, a significant under-estimation has been turned into a lesser (but sometimes still significant) over-estimation (e.g. 07004, 40005, 42008, 54027, 55008, 90003) while for others there is an improvement at some return periods but a deterioration at other return periods (e.g. 28046, 57005, 60002).

Table 0.3 Percentage errors in flood peaks simulated using original and adjusted ERA-driven RCM data, at given return periods.

catchment number	original rainfall				adjusted rainfall			
	return period (years)				return period (years)			
	2	5	10	20	2	5	10	20
07004	-48.4	-48.9	-49.0	-49.0	29.6	26.1	24.1	22.3
21013	-31.9	-36.0	-39.0	-42.0	12.0	6.2	1.7	-2.7
24005	-29.2	-30.5	-31.8	-33.3	47.1	44.8	41.1	36.5
28046	6.7	4.6	2.7	0.6	-1.2	-3.4	-5.4	-7.6
36008	25.1	24.9	25.1	25.4	25.1	24.9	25.1	25.4
39017	-20.8	-28.0	-33.9	-39.9	12.9	4.8	-2.2	-9.5
40005	-41.9	-42.0	-41.6	-40.8	4.9	5.2	6.0	7.3
42008	-23.8	-26.3	-28.7	-31.5	24.5	18.7	12.6	5.9
54027	-14.0	-14.4	-13.3	-11.4	2.9	1.3	1.5	2.4
55008	-15.8	-17.7	-18.9	-19.8	11.5	9.5	8.5	7.6
57005	-44.8	-42.0	-39.6	-37.0	22.0	30.5	38.3	47.0
60002	-20.5	-22.6	-25.0	-27.8	30.5	26.3	21.2	15.0
60003	-24.2	-23.4	-21.7	-19.2	10.2	13.1	17.2	22.7
74001	-22.9	-26.3	-29.2	-32.3	-15.9	-19.5	-22.7	-26.0
90003	-23.1	-25.3	-27.0	-28.7	11.0	9.4	8.4	7.5
96001	-7.8	-7.9	-7.9	-7.9	32.0	31.3	30.8	30.4

A potentially interesting effect of adjusting the RCM rainfall has been to change the relationship between catchment area and flood frequency errors. Whereas, with the original RCM rainfall data, larger catchments were more likely to under-estimate flood frequency (at least at lower return periods), with the adjusted data they are more likely to over-estimate flood frequency (especially at higher return periods; $R^2 = 0.35$ at the 10-year return period, $R^2 = 0.44$ at the 20-year return period). It is not clear why the adjustment has had this effect.

Remaining errors, after adjustment for mean bias, probably indicate differences in the temporal distribution of the RCM rainfall; applying a single factor to correct for errors in annual average rainfall has the effect of increasing (or decreasing) the totals of all rainfall events in the same way, at all times of year, whereas the deficiency (or excess) could be mainly in certain types of event or at certain times of year.

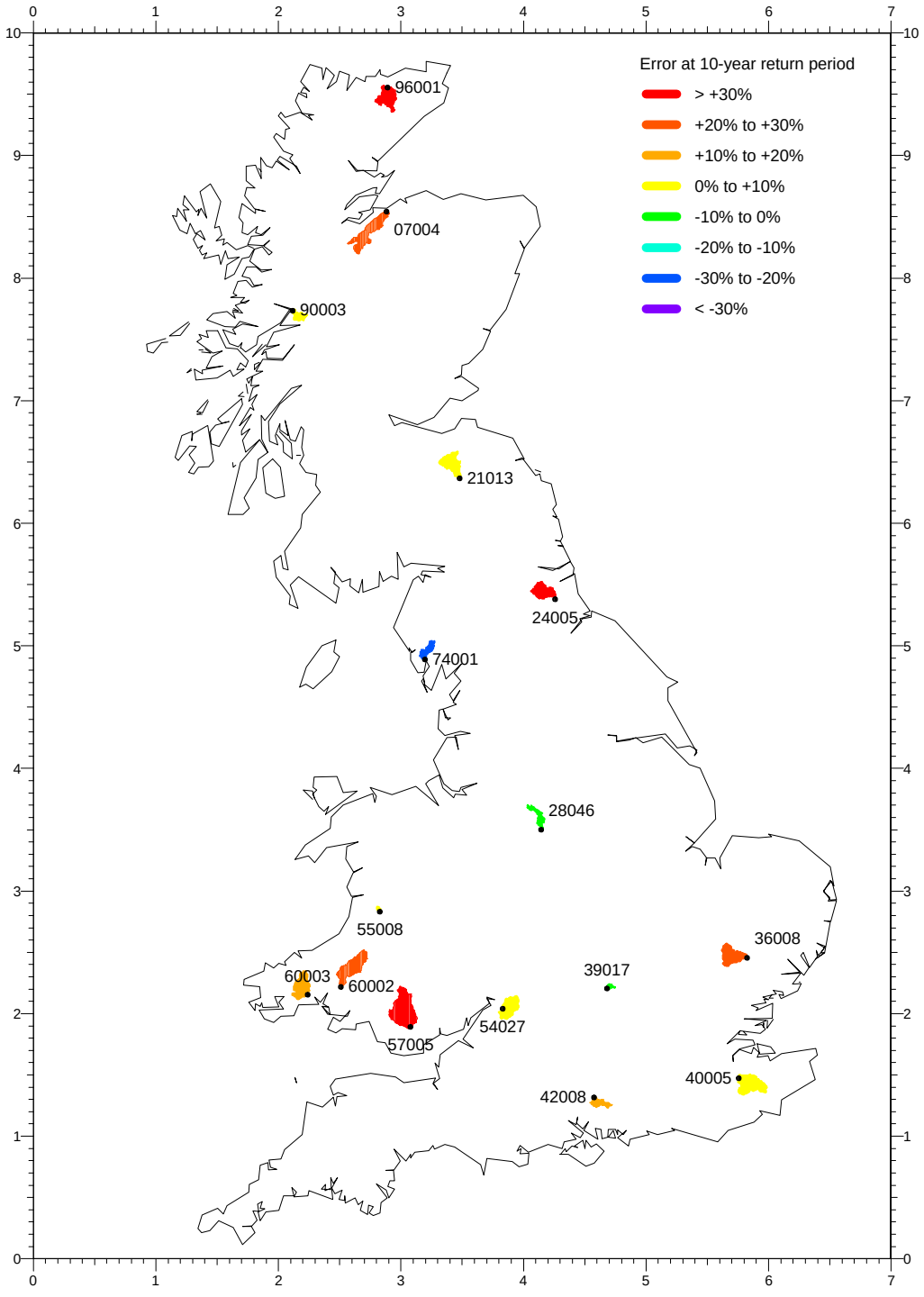

Figure 0.5 Map showing the percentage error in flood frequency at the 10-year return period for each of the study catchments, after correction for mean bias in RCM rainfall.

An example of the differential errors in rainfall by month is shown in Figure 0.6, for catchment 60002. In this case, after the adjustment for mean bias, the RCM rainfall is over-estimated in January-March and under-estimated in July-October. Other catchments also show monthly differences, but with no totally consistent pattern of months with over- or under-estimation.

Spatial differences between annual and seasonal errors over Britain are shown in Figure 0.7 and Figure 0.8, expressed as the ratio observed rainfall / RCM rainfall. The annual pattern looks very similar to the pattern for the winter season (December-February), but seemingly small differences in these ratios are probably important. The most obvious case of this is catchment 36008, for which the annual adjustment factor is 1.0 and so there was no improvement in the over-estimation of flood frequency for this catchment when the factor was applied. However, the winter factor for catchment 36008 is below 1.0, so applying this to the whole time-series, instead of the annual factor, may lead to an improvement in flood frequency estimation, given that winter is generally the main flood season for catchments in Britain (Bayliss and Jones, 1993). This would also have the effect of reducing the already low summer rainfall totals for the catchment though, so there may be a case for applying seasonal factors, which could reflect differing errors for different types of rainfall. Although this has not been pursued further here, the seasonal factors for the study catchments are given in Table 0.4 to demonstrate their variability. Spring has the lowest factor for all but two catchments (and is very close to the lowest value even for those two), but the highest factor can occur in any of the other three seasons, depending on the catchment.

Table 0.4 Comparison of annual and seasonal adjustment factors for RCM rainfall.

catchment number	annual	winter	spring	summer	autumn
07004	2.02	2.78	1.66	1.63	2.25
21013	1.37	1.51	1.15	1.30	1.50
24005	1.51	1.78	1.30	1.36	1.68
28046	0.94	0.93	0.83	0.98	1.03
36008	1.00	0.88	0.86	1.19	1.08
39017	1.19	1.15	1.05	1.27	1.31
40005	1.26	1.21	1.04	1.31	1.46
42008	1.27	1.25	1.11	1.37	1.37
54027	1.12	1.08	0.98	1.23	1.21
55008	1.27	1.12	1.14	1.48	1.48
57005	1.97	1.92	1.68	2.16	2.16
60002	1.44	1.30	1.28	1.66	1.60
60003	1.33	1.30	1.12	1.43	1.50
74001	1.08	0.98	0.98	1.11	1.26
90003	1.37	1.26	1.16	1.64	1.58
96001	1.32	1.51	1.10	1.11	1.57

The yearly variation in monthly rainfall totals (e.g. Figure 0.6), after correction for mean bias, is generally quite good, especially in the winter months. This is not

surprising, due to the higher proportion of convective rather than frontal rainfall in the summer months and the lower capability of the RCM to simulate small-scale, convective rainfall than large-scale, frontal rainfall, as the triggering of convective storms is very complex.

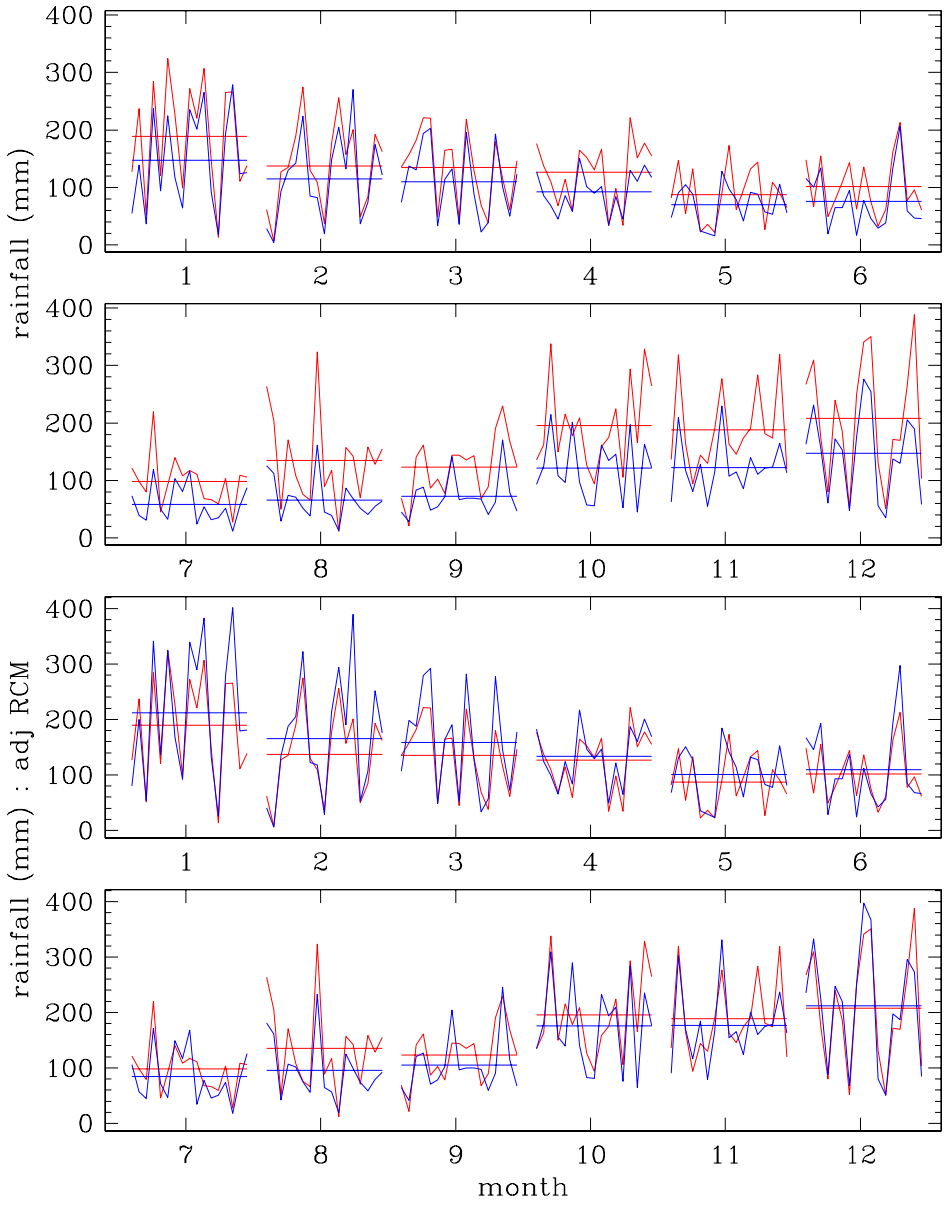

Figure 0.6 Plots of errors in ERA-driven RCM rainfall (blue) compared to observed rainfall (red) for catchment 60002. The horizontal lines indicate the mean monthly totals over the period, with the year-to-year variation superimposed on them. The top two graphs are for the unadjusted RCM-derived rainfall, while the bottom two are with the correction factor for mean bias in RCM rainfall.

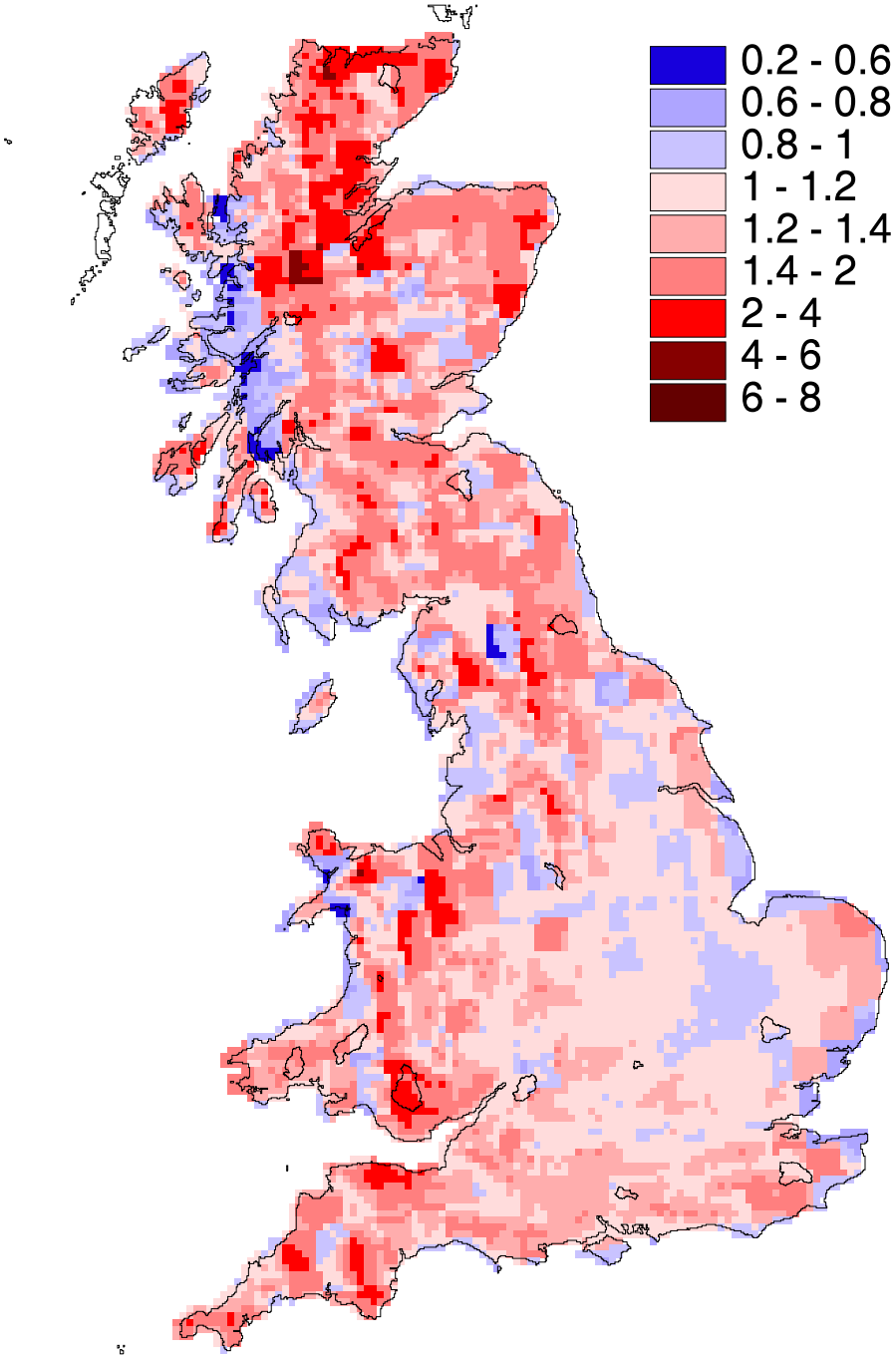

Figure 0.7 Map showing the spatial distribution of the (annual average) ratio of observed rain / ERA-40 RCM rain, for 1985-2001. This has been calculated using 5km daily observed rainfall data, with the RCM data taken from the 25km RCM grid box which covers the 5km observed grid box (i.e. no SAAR downscaling from 25km grid to 5km grid).

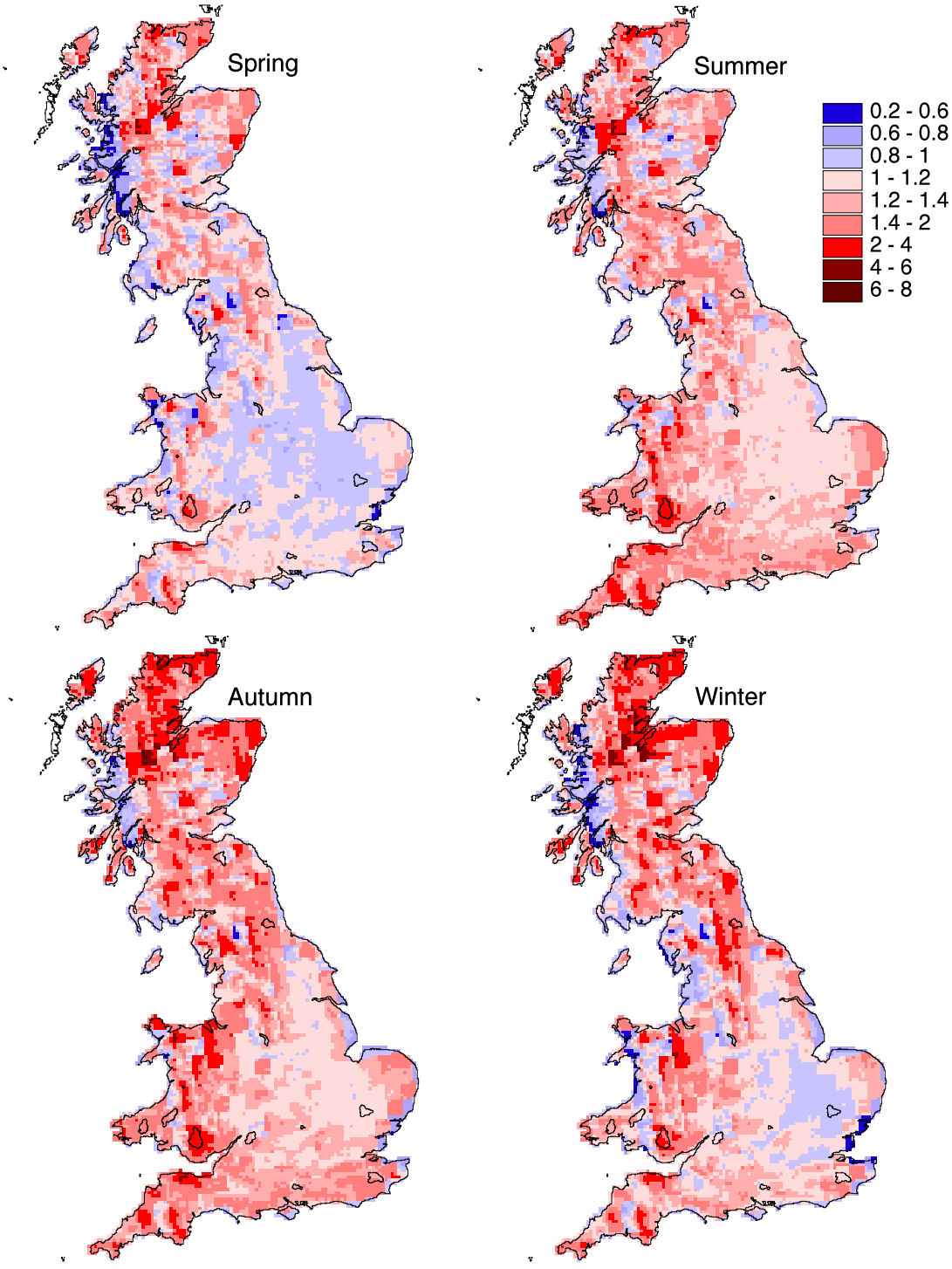

Figure 0.8 Map as Figure 0.7 but showing the seasonal variation in the spatial distribution of the ratio of observed rain / ERA-40 RCM rain, for 1985-2001.

AUTUMN/WINTER 2000 FLOODS

The general under-estimation of flood flows simulated using ERA-driven RCM data shows up in the hydrographs covering the period of the Autumn/Winter 2000 floods, as shown in Figure 0.1 for four of the study catchments more severely affected in this period. Correction for mean bias does improve the simulation of the peaks to some extent (Figure 0.2). However there are still problems, particularly for catchment 40005 (the Beult at Stile Bridge, in South East England) where the simulation with ERA-driven RCM data does not pick up the main flood peak at all.

An analysis of peak rankings (Table 0.1) indicates that, even after adjusting the RCM rainfall for mean bias, the simulations are under-estimating the Autumn/Winter 2000 peak more than some other peaks for many catchments. That is, the peak using RCM rainfall data is frequently ranked lower than that using observed rainfall data or from observed flows. This suggests that there could be a specific difficulty simulating events of the type that caused the Autumn/Winter 2000 flooding.

Table 0.1 Approximate ranks of the maximum flood peak occurring during Oct-Dec 2000, compared to the full period of simulation, from observed flows and from those simulated using observed rainfall, ERA-driven RCM rainfall, and adjusted ERA-driven RCM rainfall. (Rank 1 indicates the highest peak in the full period).

catchment number	observed	simulated - obs' rain	simulated - RCM rain	simulated - adj' RCM rain
07004	6	21	21	32
21013	2	1	31	32
24005	3	1	18	21
28046	3	1	18	20
36008	5	3	1	1
39017	13	2	4	3
40005	1	2	3	2
42008	1	1	3	1
54027	1	1	10	10
55008	30	5	11	14
57005	4	7	2	3
60002	5	6	12	13
60003	4	1	8	8
74001	12	31	51	51
90003	13	24	27	27
96001	18	7	30	30

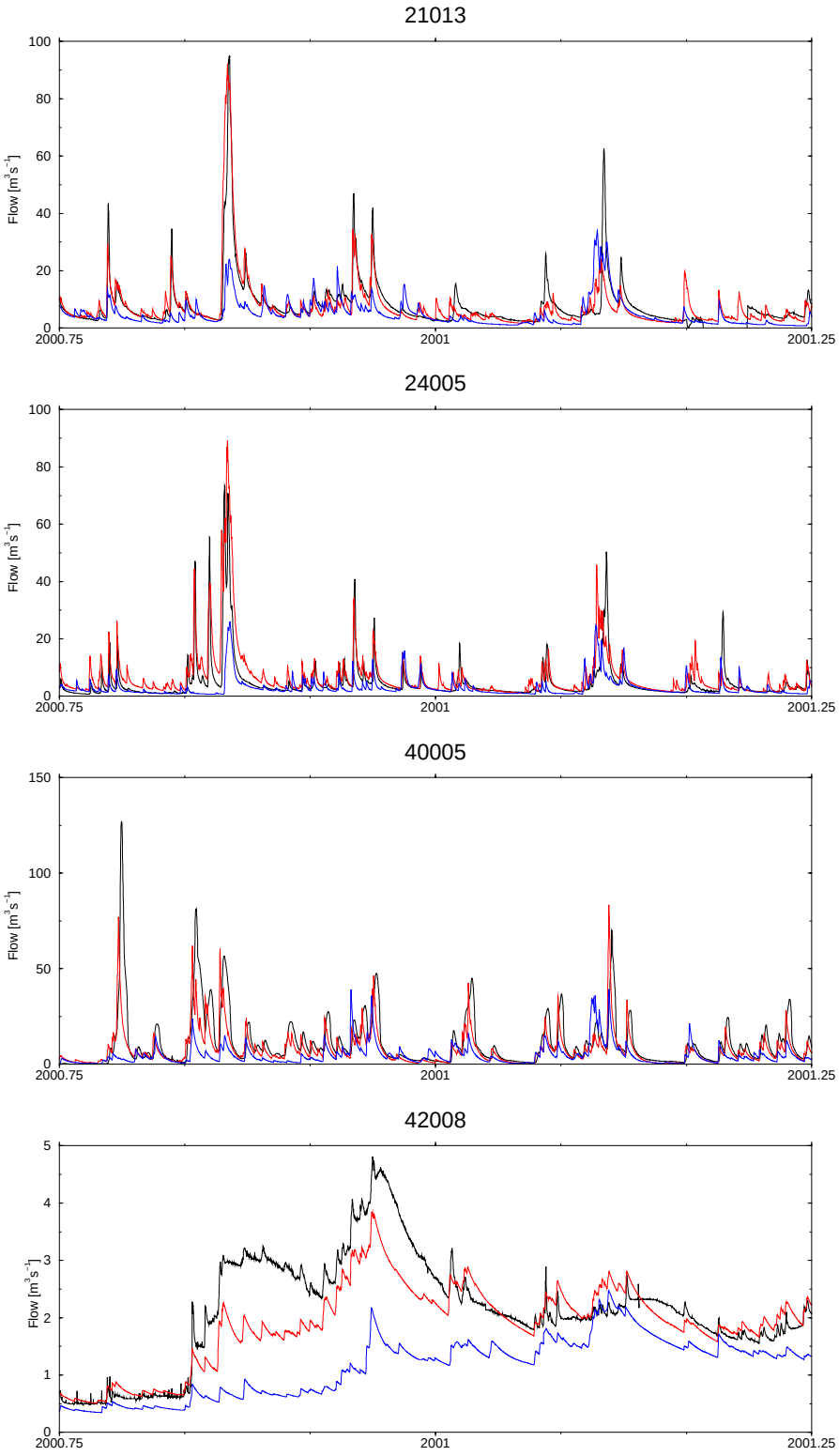

Figure 0.1 Hydrographs for the period 1st October 2000 to 31st March 2001, for four catchments, comparing flows simulated with ERA-driven RCM data (blue) to those simulated with observed data (red) and observed flows (black).

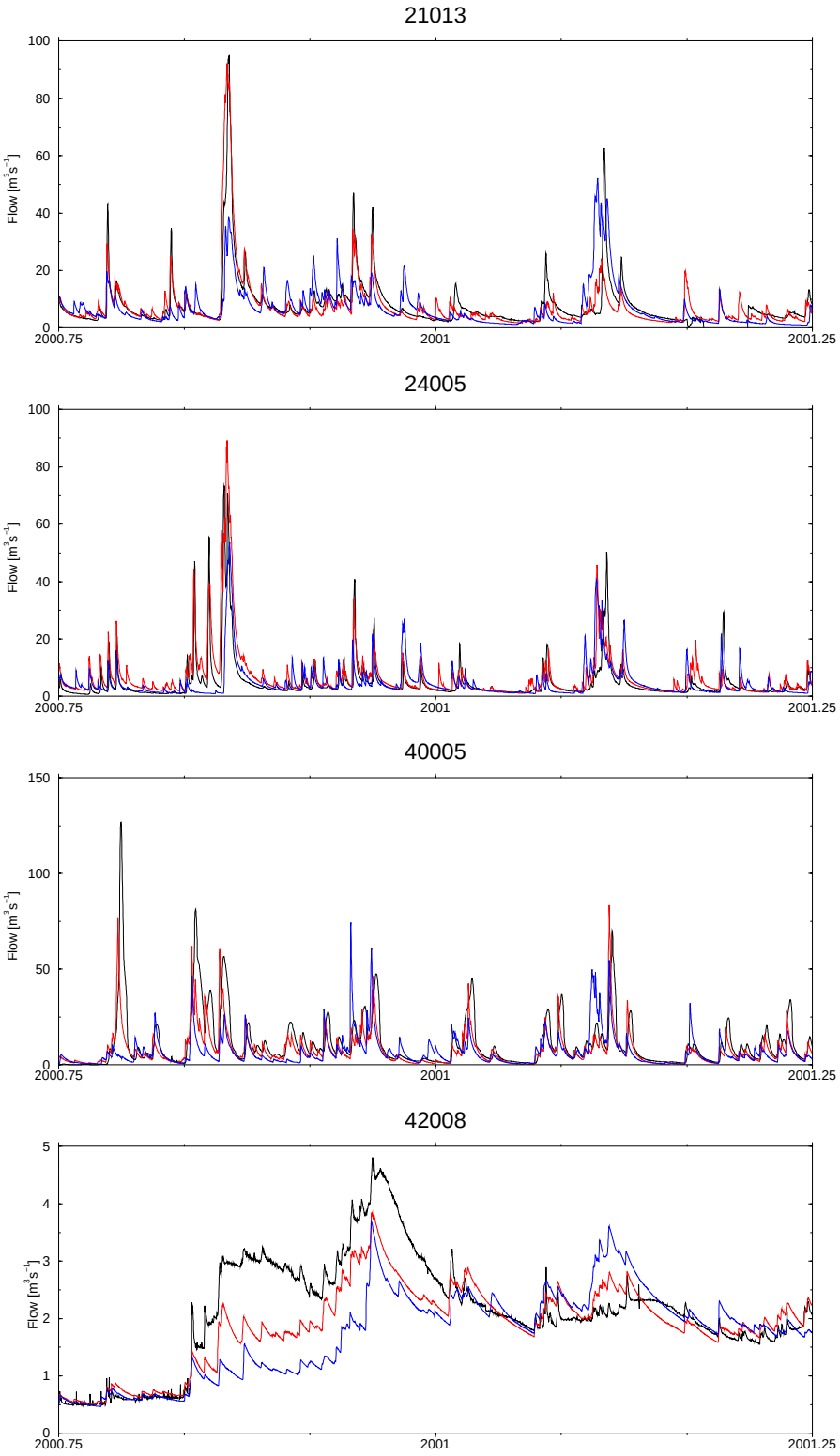

Figure 0.2 Hydrographs for the period 1st October 2000 to 31st March 2001, for four catchments, comparing flows simulated with ERA-driven RCM data (after adjustment for mean bias) (blue) to those simulated with observed data (red) and observed flows (black).

a) 24005

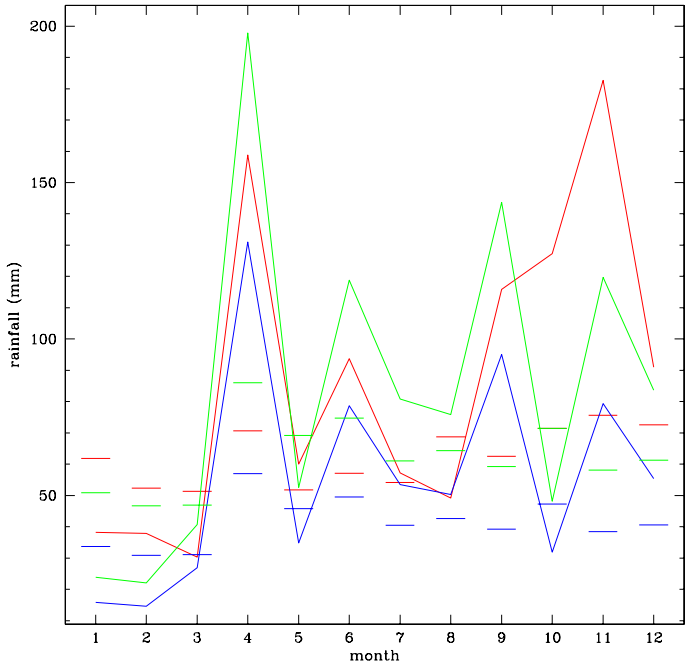

b) 40005

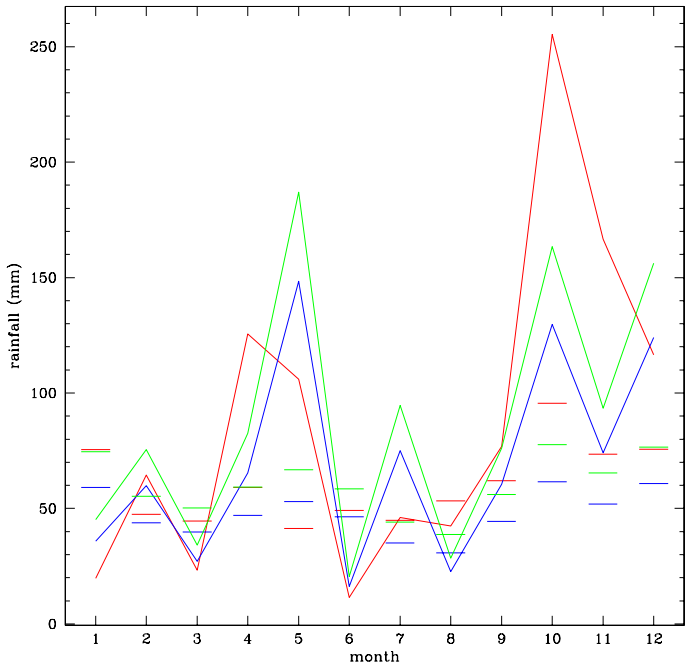

Figure 0.3 Graphs of monthly rainfall totals in the year 2000 (solid lines), from observed rainfall (red), ERA-driven RCM rainfall (blue) and adjusted ERA-driven RCM rainfall (green), for two catchments. The bars indicate the mean monthly totals over the full simulation period, and demonstrate the high totals in Autumn 2000 by comparison.

The most unusual feature of the rainfall in October and November 2000 was its sustained nature, with modestly high daily rainfall totals continuing over the course of two whole months. This helps to explain the difficulty in simulating the flooding during that period using rainfall from the RCM, as modest daily rainfall deficiencies will be aggregated into significant deficiencies in stored water (and flows) compared to actual conditions, leading to a reduced reaction to subsequent high rainfall. In contrast, a flooding event that is caused by a single, isolated high rainfall event is less likely to have large inaccuracies in antecedent conditions, and is less affected by those inaccuracies. Examples of the high observed monthly rainfall totals and RCM rainfall deficits in October and November 2000 are shown in Figure 0.3 for two catchments.

DISCUSSION AND CONCLUSIONS

This report tested the use of ERA-driven RCM data to derive inputs for catchment rainfall-runoff models, for 16 catchments across the UK. The results, in terms of flood frequency estimation over the period ~1985-2001, showed general under-estimation of flood frequency which was relatively consistent with under-estimation in annual average rainfall. The fact that the under-estimation tended to be worse for larger catchments is probably explained by the cumulative effects of spatial integration of rainfall errors over the catchment.

Performance was improved significantly by the application of catchment-specific correction factors for errors in mean annual rainfall. However, this also meant that larger catchments were now more likely to have their flood frequency over-estimated. The reason for this is unclear, although remaining errors are likely to be due to problems with the temporal distribution of rainfall. It could be that seasonal correction factors are required.

The general under-estimation of flows was particularly evident in the flood peaks of Autumn/Winter 2000, even after the application of the correction factor. This is probably because of the sustained nature of the rainfall that caused those floods.

Future development of the RCM will hopefully lead to improved rainfall estimation, annually, seasonally and spatially, in particular through a reduction in grid scale to ~12km for the UK. This will not only mean that there is less averaging of rainfall across grid boxes, but the better representation of topography could lead to better modelling of rainfall in general, as should the better representation of the dynamical processes involved. A comparison of the results here (using an ~25km RCM grid with ERA-40 boundary conditions) with future results using rainfall from an ERA-40 driven RCM on a finer grid will be interesting.

REFERENCES

Bayliss, A.C. and Jones, R.C. 1993. *Peaks-over-threshold flood database: Summary statistics and seasonality.* IH Report No. 121, Institute of Hydrology, Wallingford.

Bell, V.A., Davies, H.N., Dadson, S.J., Kay, A.L. and Clark, D.B. (2005). River flow modelling for Regional Climate Models: Progress report to March 2005. *Report to Met Office Hadley Centre, Annex15a,* CEH Wallingford, April 2005, 37pp.

Bell, V.A., Kay, A.L., Jones, R.G. and Moore, R.J. (2004). Flow Routing for Regional Climate Models: UK application. *Report to the Met Office Hadley Centre*, CEH-Wallingford, April 2004, 125pp.

Bell, V.A., Kay, A.L., Jones, R.G. and Moore, R.J. (2006). *Development of a high resolution grid-based river flow model for use with regional climate model output*. Hydrology and Earth System Sciences, in press.

Bell, V.A., Moore, R.M. and Jones, R.G. (2003). Development of a flow routing model coupled to a Regional Climate Model for Europe: Preliminary formulation and results. *Report to the UK Department for Environment, Food and Rural Affairs, Hadley Centre Annex15a,* CEH-Wallingford, March 2003, 42pp.

Calver, A., Lamb, R., Kay, A.L. and Crewett, J. 2001. *The continuous simulation method for river flood frequency estimation.* DEFRA Project FD0404 Final Report, CEH Wallingford.

Kay, A.L. (2003). Estimation of UK flood frequencies using RCM rainfall: A further investigation. *Report to the UK Department for Environment, Food and Rural Affairs, Hadley Centre Annex15a,* CEH-Wallingford, March 2003, 48pp.

Kay, A.L., Bell, V.A., Moore, R.J. and Jones, R.G. (2003). Estimation of UK flood frequencies using RCM rainfall: An initial investigation. *Report to the UK Department for Environment, Food and Rural Affairs, Hadley Centre Annex15a,* CEH-Wallingford, January 2003, 30pp.

Kay, A.L., Jones, R.G. and Reynard, N.S. (2006a). RCM rainfall for UK flood frequency estimation. II. Climate change results. *Journal of Hydrology*, **318**, 151-162.

Kay, A.L., Reynard, N.S. and Jones, R.G. (2006b). RCM rainfall for UK flood frequency estimation. I. Method and validation. *Journal of Hydrology*, **318**, 163-172.

Moore, R.J. 1985. *The probability-distributed principle and runoff production at point and basin scales.* Hydrological Sciences Journal, **30**, 273-297.

Moore, R.J. 1999. *Real-time flood forecasting systems: Perspectives and prospects*. In: Floods and landslides: Integrated Risk Assessment, R. Casale and C. Margottini (eds.), Chapter 11, 147-189. Springer.